

1 **Overview: Recent advances on the understanding of the Northern Eurasian environments and of the**  
 2 **urban air quality in China - Pan Eurasian Experiment (PEEX) program perspective**

3  
 4 Hanna K. Lappalainen<sup>1,2</sup>, Tuukka Petäjä<sup>1,2</sup>, Timo Vihma<sup>3</sup>, Jouni Räisänen<sup>1</sup>, Alexander Baklanov<sup>4</sup>, Sergey  
 5 Chalov<sup>5</sup>, Igor Esau<sup>6</sup>, Ekaterina Ezhova<sup>1</sup>, Matti Leppäranta<sup>1</sup>, Dmitry Pozdnyakov<sup>7,46</sup>, Jukka Pumpanen<sup>8</sup>,  
 6 Meinrat O. Andreae<sup>9,42,43</sup>, Mikhail Arshinov<sup>10</sup>, Eija Asmi<sup>3</sup>, Jianhui Bai<sup>11,44</sup>, Igor Bashmachnikov<sup>7</sup>, Boris  
 7 Belan<sup>10</sup>, Federico Bianchi<sup>1</sup>, Boris Biskaborn<sup>12</sup>, Michael Boy<sup>1</sup>, Jaana Bäck<sup>13</sup>, Bin Cheng<sup>3</sup>, Natalia Ye  
 8 Chubarova<sup>5</sup>, Jonathan Duplissy<sup>1,45</sup>, Egor Dyukarev<sup>14</sup>, Konstantinos Eleftheriadis<sup>15</sup>, Martin Forsius<sup>16</sup>, Martin  
 9 Heimann<sup>17</sup>, Sirkku Juhola<sup>20</sup>, Vladimir Konovalov<sup>18</sup>, Igor Konovalov<sup>19</sup>, Pavel Konstantinov<sup>5,33</sup>, Kajar  
 10 Koster<sup>13</sup>, Elena Lapsina<sup>21</sup>, Anna Lintunen<sup>1,13</sup>, Alexander Mahura<sup>1</sup>, Risto Makkonen<sup>3</sup>, Svetlana Malkhazova<sup>5</sup>,  
 11 Ivan Mammarella<sup>1</sup>, Stefano Mammola<sup>22,23</sup>, Stephany Mazon<sup>1</sup>, Outi Meinander<sup>3</sup>, Eugene Mikhailov<sup>24, 25</sup>,  
 12 Victoria Miles<sup>6</sup>, Stanislav Myslenko<sup>5</sup>, Dmitry Orlov<sup>5</sup>, Jean-Daniel Paris<sup>26</sup>, Roberta Pirazzini<sup>3</sup>, Olga  
 13 Popovicheva<sup>27</sup>, Jouni Pulliainen<sup>3</sup>, Kimmo Rautiainen<sup>3</sup>, Torsten Sachs<sup>28</sup>, Vladimir Shevchenko<sup>29</sup>, Andrey  
 14 Skorokhod<sup>30</sup>, Andreas Stohl<sup>31</sup>, Elli Suhonen<sup>1</sup>, Erik S. Thomson<sup>32</sup>, Marina Tsidilina<sup>39</sup>, Veli-Pekka Tynkkynen  
 15 <sup>34</sup>, Petteri Uotila<sup>1</sup>, Aki Virkkula<sup>3</sup>, Nadezhda Voropay<sup>35</sup>, Tobias Wolf<sup>6</sup>, Sayaka Yasunaka<sup>36</sup>, Jiahua Zhang<sup>37</sup>,  
 16 Yubao Qiu<sup>37</sup>, Aijun Ding<sup>38</sup>, Huadong Guo<sup>37</sup>, Valery Bondur<sup>39</sup>, Nikolay Kasimov<sup>5</sup>, Sergej Zilitinkevich  
 17 (†)<sup>1,2,3</sup>, Veli-Matti Kerminen<sup>1</sup> and Markku Kulmala<sup>1,2,39,40,41</sup>

18

19 <sup>1</sup> Institute for Atmospheric and Earth System Research / Physics, Faculty of Science, University of  
 20 Helsinki, Finland

21 <sup>2</sup> Tyumen State University, Department of Cryosphere, 625003 Tyumen, Russia

22 <sup>3</sup> Finnish Meteorological Institute, 00101 Helsinki, Finland

23 <sup>4</sup> World Meteorological Organization, WMO, Geneva, Switzerland

24 <sup>5</sup> Faculty of Geography, Lomonosov Moscow State University, Lenin Hills, 119991, Moscow, Russia

25 <sup>6</sup> Nansen Environmental and Remote Sensing Center/Bjerknes Centre for Climate Research, Bergen,  
 26 Norway

27 <sup>7</sup> Nansen International Environmental and Remote Sensing Centre”, Nansen Centre, NIERSC, St.  
 28 Petersburg, Russia

29 <sup>8</sup> Department of Environmental and Biological Sciences, PO Box 1627 (Address: Yliopistonranta 1 E), FI-  
 30 70211 Kuopio, Finland

31 <sup>9</sup> Max Planck Institute for Chemistry, Mainz, Germany

32 <sup>10</sup> V.E. Zuev Institute of Atmospheric Optics (IAO) SB RAS, Tomsk, 634055, Russia

33 <sup>11</sup> LAGEO, Institute of Atmospheric Physics, Chinese Academy of Sciences (IAP-CAS), Beijing, 100029,  
 34 PR, China

35 <sup>12</sup> Alfred Wegener Institute, Helmholtz Centre for Polar and Marine Research, Potsdam, Germany

36 <sup>13</sup> Institute for Atmospheric and Earth System Research /Forest Sciences, University of Helsinki, Helsinki,  
 37 Finland

- 38 <sup>14</sup> Institute of Monitoring of Climatic and Ecological Systems SB RAS, Tomsk, 634055, Russia; Yugra  
39 State University, Khanty-Mansiysk, 628012, Russia
- 40 <sup>15</sup> ERL, Institute of Nuclear and Radiological Science & Technology, Energy & Safety, NCSR  
41 Demokritos, Attiki, Greece
- 42 <sup>16</sup> Finnish Environment Institute SYKE, Latokartanonkaari 11, 00790 Helsinki, Finland
- 43 <sup>17</sup> Max-Planck-Institute for Biogeochemistry, Jena, Germany
- 44 <sup>18</sup> Institute of Geography RAS, Moscow, Russia
- 45 <sup>19</sup> Institute of Applied Physics, Nizhny Novgorod, Russia
- 46 <sup>20</sup> Faculty of Biological and Environmental Sciences, University of Helsinki, Helsinki, Finland
- 47 <sup>21</sup> Yugra State University, Khanty-Mansiysk, 634012, Russia
- 48 <sup>22</sup> Finnish Museum of Natural History (LUOMUS), University of Helsinki, Helsinki, 00100, Finland
- 49 <sup>23</sup> Molecular Ecology Group (MEG), Water Research Institute (IRSA), National Research Council of Italy  
50 (CNR), Verbania Pallanza, 28922, Italy
- 51 <sup>24</sup> St. Petersburg State University, 7/9 Universitetskaya nab, St. Petersburg, 199034, Russia
- 52 <sup>25</sup> Multiphase Chemistry and Biogeochemistry Departments, Max Planck Institute for Chemistry, 55020  
53 Mainz, Germany
- 54 <sup>26</sup> Laboratoire des Sciences du Climat et de l'Environnement, IPSL CEA-CNRS-UVSQ, 91190 Gif-sur-  
55 Yvette, France
- 56 <sup>27</sup> Institute of Nuclear Physics, Lomonosov Moscow State University, Moscow, Russia
- 57 <sup>28</sup> GFZ German Research Centre for Geosciences, Telegrafenberg, Potsdam, Germany
- 58 <sup>29</sup> Shirshov Institute of Oceanology, Russian Academy of Sciences, Moscow, Russia
- 59 <sup>30</sup> A.M. Obukhov Institute of Atmospheric Physics, Moscow, Russia
- 60 <sup>31</sup> Department of Meteorology and Geophysics, University of Vienna, Vienna, Austria
- 61 <sup>32</sup> Department of Chemistry & Molecular Biology, University of Gothenburg, Göteborg, 41296, Sweden
- 62 <sup>33</sup> Peoples' Friendship University of Russia (RUDN), Laboratory of sSart technologies for sustainable  
63 development of urban environment under global changes, Moscow, Russian Federation
- 64 <sup>34</sup> Aleksanteri Institute, University of Helsinki, Helsinki, Finland
- 65 <sup>35</sup> V B Sochava Institute of Geography SB RAS, Irkutsk, 664033, Russia; Institute of Monitoring of  
66 Climatic and Ecological Systems SB RAS, Tomsk, 634055, Russia
- 67 <sup>36</sup> Japan Agency for Marine-Earth Science and Technology (JAMSTEC), Yokosuka, Japan
- 68 <sup>37</sup> Aerospace Information Research Institute, Chinese Academy of Sciences, Beijing, 100094, China
- 69 <sup>38</sup> Joint International Laboratory of Atmospheric and Earth System sciences (JirLATEST), Nanjing  
70 University, Nanjing, China
- 71 <sup>39</sup> Institute for Scientific Research of Aerospace Monitoring "AEROCOSMOS", Moscow, 105064, Russia
- 72 <sup>40</sup> Aerosol and Haze Laboratory, Beijing Advanced Innovation Center for Soft Matter Sciences and  
73 Engineering, Beijing University of Chemical Technology (BUCT), Beijing, China
- 74 <sup>41</sup> Guangzhou Institute of Geography, Guangzhou Academy of Sciences, Guangzhou, China
- 75 <sup>42</sup> Department of Geology and Geophysics, King Saud University, Riyadh, Saudi Arabia

76 <sup>43</sup> Scripps Institution of Oceanography, UCSD, La Jolla, CA, USA

77 <sup>44</sup> Interdisciplinary Scientific and Educational School of M.V.Lomonosov Moscow State

78 University «Future Planet and Global Environmental Change, Russia

79 <sup>45</sup> Helsinki Institute of Physics, University of Helsinki, 00014 Helsinki, Finland

80 <sup>46</sup> St. State Petersburg University (St. Petersburg State University, 7/9 Universitetskaya nab. St. Petersburg,  
81 199034. Russia

82

83 **Corresponding author(s):** Hanna Lappalainen, [hanna.k.lappalainen@helsinki.fi](mailto:hanna.k.lappalainen@helsinki.fi), Veli-Matti Kerminen, [veli-matti.kerminen@helsinki.fi](mailto:veli-matti.kerminen@helsinki.fi)

84

85

86 **Keywords**

87 Grand Challenges, climate change, land-atmosphere interactions and feedbacks, biogeochemical cycles,  
88 Arctic Ocean, Northern Eurasia, China, Arctic marine ecosystem, atmospheric composition, air quality,  
89 Arctic greening, land use change, permafrost, Pan-Eurasian Experiment (PEEX), Global Earth Observatory,  
90 Digital Earth, Silk Road Economic Belt, Arctic societies, energy policy, boreal region, science diplomacy

91

92 **ABSTRACT**

93 The Pan-Eurasian Experiment (PEEX) Science Plan, released in 2015, addressed a need for a holistic system  
94 understanding and outlined the most urgent research needs for the rapidly changing Arctic-boreal region. Air  
95 quality in China, together with the long-range transport of atmospheric pollutants, was also indicated as one  
96 of the most crucial topics of the research agenda. These two geographical regions, the Northern Eurasian  
97 Arctic-boreal region and China, especially the megacities in China, were identified as a “PEEX region”. It  
98 is also important to recognize that the PEEX geographical region is an area where science-based policy  
99 actions would have significant impacts on the global climate. This paper summarizes results obtained during  
100 the last five years in the Northern Eurasian region, together with recent observations on the air quality in the  
101 urban environments in China, in the context of the PEEX program. The main regions of interest are the  
102 Russian Arctic, Northern Eurasian boreal forests (Siberia) and peatlands, and the megacities in China. We  
103 frame our analysis against research themes introduced in the PEEX Science Plan in 2015. We summarize  
104 recent progress towards an enhanced holistic understanding of the land – atmosphere – ocean systems  
105 feedbacks. We conclude that although the scientific knowledge in these regions has increased, the new  
106 results are in many cases insufficient and there are still gaps in our understanding of large-scale climate-  
107 Earth surface interactions and feedbacks. This arises from limitations in research infrastructures, especially  
108 the lack of coordinated, continuous and comprehensive in situ observations of the study region as well as  
109 integrative data analyses, hindering a comprehensive system analysis. The fast-changing environment and  
110 ecosystem changes driven by climate change, socio-economic activities like the China Silk Road Initiative,  
111 and the global trends like urbanization further complicate such analyses. We recognize new topics with an  
112 increasing importance in the near future, especially “the enhancing biological sequestration capacity of  
113 greenhouse gases into forests and soils to mitigate the climate change” and the “socio-economic  
114 development to tackle air quality issues”.

115	
116	Contents
117	Table of contents
118	ABSTRACT
119	1. INTRODUCTION
120	2. RESULTS
121	2.1. LAND ECOSYSTEMS
122	2.1.1 Changing land ecosystem processes (Q1)
123	<i>High-latitude photosynthetic productivity</i>
124	<i>Vegetation changes</i>
125	<i>New methodologies determining Earth surface characteristics</i>
126	2.1.2 Thawing permafrost (Q2)
127	<i>Observations of ground temperature evolution</i>
128	<i>Changing GHG fluxes and VOCs due to permafrost thaw</i>
129	2.1.3 Ecosystem structural change (Q3)
130	<i>Changes in microbial activity</i>
131	<i>Effects of forest fires on soils</i>
132	2.2. ATMOSPHERIC SYSTEM
133	2.2.1 Atmospheric composition and chemistry (Q4)
134	<i>Boreal forests carbon balance</i>
135	<i>Arctic methane (CH<sub>4</sub>) balance</i>
136	<i>Northern Eurasian carbon monoxide (CO)</i>
137	<i>Northern Eurasian Ozone (O<sub>3</sub>)</i>
138	<i>Sources and properties of atmospheric aerosols in boreal and Arctic environments</i>
139	<i>Black carbon and dust in the atmosphere and snow</i>
140	<i>Methodological and model developments related to atmospheric chemistry and physics</i>
141	2.2.2 Urban air quality and megacities (Q5)
142	<i>Air quality in China – recent observations</i>
143	2.2.3 Weather and atmospheric circulation (Q6)
144	<i>Cold and warm episodes</i>
145	<i>Cyclone density dynamics and atmosphere-ocean interaction</i>
146	<i>Circulation effect on temperature</i>
147	<i>Cloudiness in Arctic</i>
148	<i>Boundary layer dynamics and urban heat islands</i>
149	2.3 ARCTIC-BOREAL AQUATIC SYSTEM
150	2.3.1 Changing water systems, snow, sea ice and ocean sediments (Q7)
151	<i>Sea ice and thermodynamics with atmospheric and ocean dynamics</i>
152	<i>Snow depth/mass and sea ice thickness</i>

153	<i>Ocean floor and Sediments: composition and fluxes</i>
154	2.3.2 Marine ecology (Q8)
155	<i>Living marine organisms weaken or even subdue CO<sub>2</sub> accumulation</i>
156	<i>Organic carbon in lakes</i>
157	<i>Lake ice cover</i>
158	<i>Lake Baikal and Selenga River delta</i>
159	<i>Asian water lakes</i>
160	2.4 SOCIETY
161	2.4.1. Anthropogenic impact (Q10)
162	<i>Mitigation</i>
163	2.4.2 Environmental impact (Q11)
164	<i>Reindeer (Rangifer tarandus L.) grazing and ground vegetation structure and biomass</i>
165	2.4.3 Natural hazards (Q12)
166	<i>Naturally-determined diseases</i>
167	<i>UV variations</i>
168	3. SYNTHESIS AND FUTURE PROSPECTS
169	3.1 Future research needs from the system perspectives
170	3.2 Feedback mechanisms under changing climate, cryosphere conditions and urbanization
171	3.3 Climate scenarios for the Arctic-boreal region
172	ACKNOWLEDGEMENTS
173	REFERENCES
174	
175	

176

## 177 1. INTRODUCTION

178 Earth system is facing major challenges, including climate change, biodiversity loss, ocean acidification,  
179 epidemics and energy demand on a global scale (Ripple et al., 2017). These “Grand Challenges” are highly  
180 connected and interlinked. This creates a need for an approach of a multidisciplinary scientific program,  
181 which could deliver science-based messages to fast-tracked policy making (Kulmala et al., 2015). The recent  
182 estimates based on observed atmospheric concentrations of CO<sub>2</sub>  
183 ([ftp://aftp.cmdl.noaa.gov/products/trends/co2/co2\\_mm\\_mlo.txt](ftp://aftp.cmdl.noaa.gov/products/trends/co2/co2_mm_mlo.txt)) and business-as-usual scenario show that  
184 humankind should find solutions to answer the Grand Challenges (IPCC, 2021). Deep understanding of the  
185 feedbacks and interactions between the land, atmosphere and ocean domains, and accounting for social  
186 aspects in the regions of substantial changes, are needed for effective technical solutions, mitigation and  
187 adaption policy actions. The northern regions (> 45°N), together with the arctic coastal zone and Siberian  
188 region in Russia, are among the most critical areas for the global climate (Smith 2011; Kulmala et al., 2015;  
189 Kasimov et al., 2015).

190

191 The idea of the Pan-Eurasian Experiment (PEEX) ([www.atm.helsinki.fi/peex](http://www.atm.helsinki.fi/peex)), originating from a group of  
192 Finnish and Russian scientists and research organizations in 2012, is a bottom-up research and capacity  
193 building program concentrating on the sustainable development of the Arctic-boreal regions of the Northern  
194 Eurasia under changing climate and socio-economic megatrends (Kulmala et al., 2015, Lappalainen et al.,  
195 2016). The program was laid on four interconnected parts, namely research agenda, research infrastructures,  
196 capacity building and societal impacts (Lappalainen et al., 2014; Kulmala et al., 2016a, Lappalainen et al.,  
197 2017, Kulmala 2018). In addition to a strong involvement of the Russian partners, the PEEX China  
198 collaboration was established in 2013. China has a strong economic interest in Arctic regions (Tillman et al.  
199 2018). Furthermore, China is already facing extensive environmental and air pollution challenges and has  
200 major interests toward finding technical solutions for environmental monitoring of the Silk Road Economic  
201 Belt Program (SREB) initiated by the President XI Jinping in 2013 (Kulmala 2018, Lappalainen et al., 2018,  
202 Dave and Kobayashi, 2018). The PEEX program is an umbrella for several bilateral scientific projects and  
203 activities in Russia (e.g. Chalov et al., 2015, 2018; Esau et al., 2016; Alekseychik et al., 2017; Bobylev et  
204 al., 2018; Malkhazova et al., 2018; Kukkonen et al., 2020; Ezhova et al., 2018b; Ziltinkevich et al., 2019;  
205 Petäjä et al., 2020 submitted; ; Bondur et al, 2019 a,b,c,d,e,f; Yuanhuizi He et al, 2020), whereas in China  
206 the primary focus is on the development of atmospheric in-situ stations and advanced air quality monitoring  
207 in megacity environments (e.g. Ding et al., 2016 b; Yao et al., 2018; Ying et al., 2020; Wang et al., 2020).  
208 Furthermore, PEEX is closely collaborating with the Digital Belt and Road (DBAR) Program coordinated by  
209 the Institute for Digital Earth and Remote Sensing (RADI). The PEEX collaboration with DBAR is driven by  
210 a need for a novel in-situ station network and ground-based data as a complementary information for the  
211 remote sensing in the Silk Road economic region. Long-term development of a “Station Measuring the

212 Earth Surface and Atmosphere Relations” (SMEAR) concept could provide baselines for this (Hari et al.  
213 2016; Kulmala 2015, Kulmala 2018; Lappalainen et al., 2018).

214

215 The PEEEX program is motivated by the need for obtaining scientific information that combines research in  
216 the Arctic and boreal environments, and for understanding large-scale feedbacks and interactions operating  
217 in land-atmosphere-ocean systems (Kulmala et al., 2004; Kulmala et al., 2016a; Vihma et al., 2019) and  
218 large-scale weather impacts related to the Arctic amplification (e.g. Coumou et al., 2014; Vihma et al.,  
219 2020). One of the scientific backbones of PEEEX is the previously coordinated research frameworks and their  
220 synthesis. For example, the latest comprehensive overview on the interactions between the atmosphere,  
221 cryosphere and ecosystems at northern high latitudes was performed by the Nordic Center of Excellence in  
222 “Cryosphere-atmosphere interactions in a changing Arctic climate“, CRAICC) community (Boy et al.,  
223 2019). The PEEEX program can upscale the CRAICC results into a wider geographical context.

224

225 Climate change, as a main driver of environmental changes in the Northern Eurasian Arctic-boreal region  
226 and China, sets environmental boundaries for the future socio-economic activities of these regions in general.  
227 The harsh climate of this region puts a pressure on the ecosystems and living conditions of the local people  
228 (e.g. IPCC, 2019). PEEEX introduced fifteen large-scale research questions, which would help us to fill the  
229 key gaps in our holistic understanding of land-atmosphere interactions and their connections to societies  
230 living in the northern Eurasian region (Kulmala et al., 2015; Lappalainen et al., 2018). This approach also  
231 sets the framework of the current paper. Here we introduce the recent research progress in the large-scale  
232 scientific themes relevant to the PEEEX region. The PEEEX study region consists of the Northern Eurasian  
233 Arctic and boreal (taiga) environments, thus the major geographical part of the environments is located in the  
234 Russian territory. China was added to the study area in 2013 as it was seen as locally and globally  
235 consequential region for climate change, air quality and long-term transport of atmospheric pollutants  
236 (Kulmala et al., 2015 a,b; Lappalainen et al., 2016, 2018).

237 Here we introduce the scientific results from PEEEX scientific output, review the main results from PEEEX  
238 scientific papers and present an analysis of the key gaps in the current scientific understanding. We use the  
239 PEEEX research agenda structure (Kulmala et al. 2016, Lappalainen et al. 2018) as a reference and mirror new  
240 rising themes and results against this plan. For the literature material, we used the following sources for  
241 demonstrating the results: (i) individual inputs sent by the PEEEX research community, (ii) contents of the  
242 scientific papers published in Atmospheric Chemistry and Physics (ACP) PEEEX special issue in 2016-2019  
243 ([www.atmos-chem-phys.net/special\\_issue395.html](http://www.atmos-chem-phys.net/special_issue395.html)) and (iii) scientific outputs from PEEEX-labeled projects  
244 ([www.atm.helsinki.fi/peex/index.php/projects](http://www.atm.helsinki.fi/peex/index.php/projects)) and other relevant results reported by the PEEEX partners. For  
245 the individual input, we asked the PEEEX research community to identify the main published papers in peer  
246 reviewed journals for each question out of their own work and to connect the work with one of the 15  
247 science questions introduced in the PEEEX science plan. Based on the abstracts we listed “addressed research  
248 themes” over last 5 years per PEEEX key topical areas (Table 1), which we review in more detail in section 2.

249 The results are first discussed with a holistic approach and then we categorize the advances through a set of  
250 identified feedbacks and interactions within the Arctic boreal environment. We follow up with a discussion  
251 on the need for a future research infrastructure to be able to provide relevant data and underline the future  
252 socio-economics development of the region setting the boundaries for proposed new science-based concepts  
253 and technical solutions.

## 254 **2. RESULTS**

255 In the PEEEX Science Plan, we indicated four main thematic research domains: the land system, the  
256 atmospheric system, the water system and the society with 15 thematic research areas and related large-scale  
257 research questions (Q) presented in Table 1 (Lappalainen et al., 2015), also indicated in the structure of the  
258 “Table of Contents”. This is the framework we re-visited and utilized in the synthesis of new results of the  
259 PEEEX community brought together in this paper. Furthermore, we synthesized the results and discuss their  
260 contribution to the large - scale feedbacks and interactions in the Arctic context in the sections below.

261

### 262 2.1. LAND ECOSYSTEMS

263

#### 264 2.1.1 Changing land ecosystem processes (Q1)

265

##### 266 *High-latitude photosynthetic productivity*

267

268 High-latitude terrestrial ecosystems are crucial to the global climate system and its regulation by vegetation.  
269 These ecosystems are typically temperature limited, and thus also considered especially sensitive to climate  
270 warming. Better understanding of an inter-annual and seasonal dynamics and resilience of the photosynthetic  
271 activity of forest vegetation as a whole is needed for the quantification of photosynthesis, or gross primary  
272 production (GPP), and for analyzing the carbon balance of the boreal forests. The carbon sink and source  
273 dynamics of the boreal forests have been intensively studied during the last five years at the SMEAR  
274 (Stations Measuring Atmosphere Ecosystem Relations) II station in Finland (Hari and Kulmala 2005; Hari et  
275 al., 2009). Recent results show that the Norway spruce and Scots pine ecosystems are rather resilient to a  
276 short-term weather variability (Matkala et al., 2020). Overall, the analyses by Kulmala et al. (2019) and  
277 Matkala et al. (2020) on subarctic Scots pine and Norway spruce stands at the northern timberline in Finland  
278 serve as examples of the canopy scale dynamics, showing that these ecosystems are generally weak carbon  
279 sinks but have a clear annual variation. Kulmala et al. (2019) observed that there is a difference between tree  
280 canopy photosynthesis compared to forest floor photosynthesis which starts to increase after the snowmelt.  
281 Thus, the models for photosynthesis should also address the snow cover period in order to better capture the  
282 seasonal dynamics of photosynthesis of the Northern forests (Kulmala et al., 2019).

283

284 The abundance of tree species, stand biomass, increasing tree growth and coverage of broadleaf species may  
285 also affect biogenic volatile organic compound (BVOC) emissions from the forest floor and impact the total



286 BVOC emissions from northern soils. At least the stand type has been shown to affect BVOCs fluxes from  
287 the forest floor in a hemi boreal-boreal region (Mäki et al., 2019). As a whole, BVOCs emitted by boreal  
288 evergreen trees are connected to the photosynthetic activity with a strong seasonality and have a crucial role  
289 in atmospheric aerosol formation processes over the boreal forest zone. BVOC emissions have low rates  
290 during photosynthetically inactive winter and increasing rates towards summer (Aalto et al., 2015). High  
291 emission peaks caused by enhanced monoterpene synthesis were found in spring periods simultaneously with  
292 the photosynthetic spring recovery (Aalto et al., 2015). This suggests that monoterpene emissions may have  
293 a protective functional role for the foliage during the spring recovery state, and that these emission peaks  
294 may contribute to atmospheric chemistry in the boreal forest in springtime. Vanhatalo et al. (2018) studied  
295 the interplay between needle monoterpene synthase activities, its endogenous storage pools and needle  
296 emissions in two consecutive years at a boreal forest in Finland. They found no direct correlation between  
297 monoterpene emissions and enzyme activity or the storage pool size. Monoterpene synthase activity of  
298 needles was different depending on seasonality and needle ontogenesis. However, the pool of stored  
299 monoterpenes did not change with the needle age (Vanhatalo et al., 2018). Also, clear annual patterns of  
300 primary biological aerosol particles have been measured from a boreal forest, with late spring and autumn  
301 being the seasons of a dominant occurrence. Increased levels of free amino acids and bacteria were observed  
302 during the pollen season in the SMEAR II station in Finland, whereas the highest levels for fungi were  
303 observed in autumn (Helin et al., 2017).

304  
305 Extensive measurements of Scots pine photosynthesis and modelling resulted in optimized predictions of the  
306 daily behavior and annual patterns of photosynthesis in a subarctic forest (Hari et al., 2017). The study  
307 connected theoretically the fundamental concepts affecting photosynthesis with the main environmental  
308 drivers (air temperature and light), and the theory gained strong support through empirical testing.  
309 Understanding stomatal regulation is fundamental in predicting the impact of changing environmental  
310 conditions on photosynthetic productivity. Lintunen et al. (2020) showed that the canopy conductance and  
311 soil-to-leaf hydraulic conductance are strongly coupled, and that both soil temperature and soil water content  
312 influence the canopy conductance through changes in the belowground hydraulic conductance. In particular,  
313 the finding that the soil temperature strongly influences the belowground hydraulic conductance in mature,  
314 boreal trees may help to better understand tree behavior and photosynthetic productivity in cold  
315 environments. The plant photosynthetic rate is concurrently limited by stomatal and non-stomatal limitations,  
316 and recent modelling (Hölttä et al., 2017) and empirical (Salmon et al., 2020) studies suggest that stomatal  
317 and non-stomatal controls are coordinated to maximize leaf photosynthesis, i.e. non-stomatal limitations to  
318 photosynthesis increase with a decreasing leaf water potential and/or increasing leaf sugar concentration.  
319 This new approach allows including the effects of non-stomatal limitations in models of tree gas-exchange  
320 (Fig. 1).

321  
322 Due to climate warming, it seems that trees in high-latitudes have been progressively decreasing their  
323 regional growth coherence in the last decades (Shestakova et al., 2019). Shestakova et al. (2019) showed

324 results that unequivocally linked a substantial decrease in the temporal coherence of forest productivity in  
325 boreal ecosystems to a less temperature-limited growth that is concurrent with regional warming trends. This  
326 emerging pattern points, for example, to an increasing dependence of the carbon balance on local drivers  
327 and the role of forests as carbon sinks in the northern Ural region.

328

329 Vegetation gross primary production (GPP) is the largest CO<sub>2</sub> flux of the carbon cycle in terrestrial  
330 ecosystems and impacts all of the carbon cycle variables (Beer et al., 2010). Ecosystem models usually  
331 overestimate GPP under drought and during spring, late fall and winter (Ma et al., 2015). Several new  
332 methodological improvements for a better quantification and scaling of GPP have been reported (Zhang et  
333 al., 2018; Pulliainen et al., 2017; Kooijmans et al., 2019). The GPP, measuring photosynthesis, is crucially  
334 important for the global carbon cycle and its accurate estimation is essential for ecosystem monitoring and  
335 simulation. Pulliainen et al. (2017) introduced a new proxy indicator for spring recovery from *in situ* flux  
336 data on CO<sub>2</sub> exchange. This made it possible to quantify the relation between spring recovery and carbon  
337 uptake, and to assess changes in the springtime carbon exchange, demonstrating a major increase in the CO<sub>2</sub>  
338 sink. Zhang et al. (2018) introduced a new water-stress factor that effectively mitigates the overestimation of  
339 GPP under drought conditions, while Bai et al. (2018 a,b) developed a method for quantifying the  
340 evapotranspiration of crops by using a remote sensing-based two-leaf canopy conductance model. These  
341 methods can provide novel insights into the quantification of GPP under different conditions and, in general,  
342 into the impacts of biosphere-atmosphere relations on a larger scale.

343

344 Methods for satellite-based remote sensing of photosynthesis have been developed recently based on solar-  
345 induced chlorophyll fluorescence signal, such as the OCO-2 product that has an improved spatial resolution,  
346 data acquisition and retrieval precision, as compared with earlier satellite missions with solar-induced  
347 chlorophyll fluorescence (SIF) capability, which allows for validation of the data directly against ground and  
348 airborne measurements (Sun et al., 2017). Interpretation of the solar-induced chlorophyll fluorescence signal  
349 has also been improved by many *in situ* studies. For example, Liu et al. (2019a, 2019b) simulated SIF in  
350 realistic 3D birch stand reconstructed from terrestrial laser scanning data and found a large contribution of  
351 the understory layer to the remote sensing signal.

352

### 353 *Vegetation changes*

354

355 The normalized difference vegetation index (NDVI) is used for detecting large-scale changes in vegetation  
356 productivity. In the past decades, these changes include an increasing NDVI, called “greening”, taking place  
357 in the tundra regions and a decreasing NDVI, called “browning”, in the Northern forest regions (Miles and  
358 Esau, 2016). A deeper analysis behind these changes are needed. For example, in Northern West Siberia only  
359 18% of the total area had statistically significant changes in productivity either towards greening or  
360 browning, and having these opposite trends for different species within the same bioclimatic zone. The  
361 observed complexity of the patterns and trends in the vegetation productivity underlines the need for new

362 studies on how forest types and different species are responding to climate and environmental changes in the  
363 Northern environments (Miles and Esau, 2016). Also understanding the variations in small-scale plant  
364 communities, seasonality and biogeochemical properties are needed for modeling the functioning of the  
365 arctic tundra in global carbon cycling. Also the rapid development of the leaf area index (LAI, leaf area per  
366 ground area,  $\text{m}^2 \text{m}^{-2}$ ) during the short growing season and the yearly climatic variation address the  
367 importance of optimal timing of the satellite data images when it is compared with the field verification data  
368 in the Arctic region (Juutinen et al., 2017).

369

370 Bondur and Vorobyev (2015) analyzed the vegetation indices and complex spectral transformations derived  
371 from processed long-term satellite data (1973-2013) for areas around the cities of Arkhangelsk and  
372 Zapolyarny (Murmansk oblast). They demonstrated that these areas are subject to a peak anthropogenic  
373 impact associated with specific industrial facilities, leading to changes in landscapes and depletion of natural  
374 ecosystems, consequently leading to the decline in the quality of life and health conditions (Bondur and  
375 Vorobyev, 2015). Region-wide changes in the vegetation cover and changes in and around several urbanized  
376 areas in Siberia reveal robust indications of an accelerated greening near the older urban areas. Many  
377 Siberian cities have turned greener while their surroundings have been dominated by wider browning. The  
378 observed urban greening could be associated not only with a special tending of within-city green areas but  
379 also with urban heat islands and succession of more productive shrub and tree species growing on warmer  
380 sandy soils (Koronatova and Milyaeva 2011, Sizov and Lobotrosova 2016). Tundra and forest-tundra biomes  
381 are sensitive to mean summer temperatures, which increases production and greening. Taiga biomes are  
382 sensitive to precipitation and soil moisture with increased production in wet summer (Miles et al., 2019).

383

#### 384 *New methodologies determining Earth surface characteristics*

385

386 Earth surface characteristics are fundamental knowledge to the understanding and quantification land-  
387 atmosphere processes. The methods for determining Earth surface characteristics from satellites are  
388 improving. As an example, a method for recognition of the Earth surface types according to space images  
389 using an object-oriented classification was developed. The classification relies on Markov stochastic  
390 segmentation for object extraction and supervised classification of the objects (Gurchenkov et al., 2017).  
391 Furthermore, a prototype algorithm for hemispheric scale detection of autumn soil freezing using space-  
392 borne L-band passive microwave observations was developed (Rautiainen et al., 2016) and is currently an  
393 operative soil freeze and thaw product that delivers freely available data (<ftp://litdb.fmi.fi/outgoing/SMOS-FTService/>). The CryoGrid 3 land surface model provides improved descriptions of possible pathways of ice-  
394 wedge polygon evolution and describes better the complex processes affecting ice-rich permafrost  
395 landscapes (Nitzbon et al., 2019). In addition, there are new observations for validating satellite observations  
396 and permafrost models. Boike et al. (2016) introduced a new, 16-year permafrost and meteorology data set  
397 from the Samoylov Island Arctic research site, north-eastern Siberia. Terentieva et al. (2016) introduced  
398

399 maps used as a baseline for validation of coarse-resolution land cover products and wetland data sets at high  
 400 latitudes. Other examples of available data for the model validation are “BC emissions from agricultural  
 401 burns and grass fires in Siberia” by Konovalov et al. (2018) and permafrost records at the Lena River delta”  
 402 by Boike et al. (2016).

403

404 Tundra ecosystems are under pressure and intensifying permafrost thawing, plant growth and ecosystem  
 405 carbon exchange under the changing climate. The heterogeneity of Arctic landscapes is an extra challenge  
 406 for environmental monitoring. For example, remote sensing methods are not able to capture variations in  
 407 moss biomass, which is dominating the plant biomass and controlling soil properties in the Arctic. The  
 408 general accuracy of landscape level predictions in the land cover type (LCT) is good, but the spatial  
 409 extrapolation of the vegetation and soil properties relevant for the regional ecosystem and global climate  
 410 models still needs to be improved (Mikola et al., 2018). Furthermore, for the future, we need to have a land  
 411 characterization, in order to perform quantification and assessment of the ecosystem services at different  
 412 scales using integrative techniques and integrated field observations together with remote sensing and  
 413 modelling at the landscape scale (Burkhard et al., 2009, Fu and Forsius, 2015). At smaller scales, the isotopic  
 414 composition of carbon and oxygen in peat can be used for the climate reconstruction (Granath et al., 2018).

415

#### 416 2.1.2 Thawing permafrost (Q2)

417

##### 418 *Observations of ground temperature evolution*

419

420 Permafrost regions of the Northern Eurasia are warming along with the climate (IPCC, 2019). During the  
 421 Global Terrestrial Network for Permafrost reference decade, 2007 - 2016, the temperature at the depth of  
 422 zero annual amplitude increased by  $0.39 \pm 0.15$  °C in the continuous permafrost zone and by  $0.20 \pm 0.10$  °C  
 423 in the discontinuous permafrost zone. At the same time, the mountain permafrost warmed by  $0.19 \pm 0.05$  °C.  
 424 The global average of the permafrost temperature increased by  $0.29 \pm 0.12$  °C (Biskaborn et al., 2019). The  
 425 observed trend in the continuous permafrost zone follows the air temperature trend in the Northern  
 426 Hemisphere.

427

428 The changes in the permafrost region affect climate, hydrology and ecology from local to global scales  
 429 (Arnell et al., 2010; Hinzman et al., 2005). Several local studies focused on differences introduced by  
 430 vegetation, soil and hydrological characteristics at the same site (Göckede et al., 2017, 2019). Göckede et al.  
 431 (2017, 2019) presented findings on shifts in energy fluxes from paired ecosystem observations in northeast  
 432 Siberia comprising a drained and a corresponding control site. Drainage disturbance triggered a suite of  
 433 secondary shifts in ecosystem properties, including alterations in vegetation community structure, which in  
 434 turn influenced changes in snow cover dynamics and surface energy budget. First, the drainage reduced heat  
 435 transfer into deeper soil layers, which may have led to shallower thaw depths. Second, the vegetation change  
 436 due to the drainage led to an albedo increase, which decreased the total energy income, or net radiation, into

437 the system. Third, the drainage reduced water content available for evapotranspiration, which resulted in a  
438 reduced latent heat flux and increased sensible heat flux, transferring more energy back to the atmosphere.  
439 The reported affects led to surface and permafrost cooling (Göckede et al., 2019).

440

441 Kukkonen et al. (2020) compared temperature data from several shallow boreholes in the Nadym region,  
442 Siberia, and predicted permafrost evolution for different climate scenarios. The Nadym area represents a  
443 typical site located in the discontinuous permafrost zone. Kukkonen et al. (2020) found that the permafrost  
444 thawed most rapidly in low-porosity soils, whereas high-porosity soils in the top layer (e.g., peatland)  
445 retarded thawing considerably. Similarly, the depth of a seasonally frozen layer and the temperature regime  
446 of peat soils in the oligotrophic bog in the southern taiga zone of Western Siberia showed significant  
447 differences between the sites with high and low levels of bog waters (Kiselev et al., 2019). Both Kukkonen et  
448 al. (2020) and Kiselev et al. (2019) results are in line with previous conclusions on the importance of  
449 volumetric water content and unfrozen water content for soil thermal properties governing heat transfer and  
450 phase change processes (Romanovsky and Osterkamp, 2000). Locally, the sites with a thin snow cover (e.g.,  
451 hill tops) demonstrated a higher resistance to the thawing (Williams and Smith, 1989; Kukkonen et al.,  
452 2020). To follow-up on the development of permafrost thaw in different soil types require continuous and  
453 comprehensive observations during the coming decades.

454

455 *Changing GHG fluxes and VOCs due to permafrost thaw*

456

457 Biogenic GHG emissions are strongly connected with permafrost conditions and changes in other related  
458 environmental conditions, such as soil temperature and moisture conditions. Here we discuss recent results  
459 on the observed emissions from these permafrost perspectives and, later in section 2.2.1, address the  
460 connections between GHG fluxes and the other environmental factors, like deforestation and forest fires.

461

462 During the permafrost thaw, even small changes in the soil carbon cycle can turn a terrestrial ecosystem from  
463 a sink into a source (Schuur et al., 2008). Based on regional *in situ* observations of CO<sub>2</sub> fluxes, Natali et al.  
464 (2019) estimated a winter-time carbon loss of 1 662 TgC per year, which is more than predicted by the  
465 process models estimates. Furthermore, Natalie et al. (2019) found that even if the soil CO<sub>2</sub> loss were  
466 enhanced due to winter warming, the growing season might start earlier and onset the carbon uptake under  
467 warming climate conditions. For a better understanding of these connections and both spatial and temporal  
468 dynamics of the Arctic carbon cycle, we need more observations from permafrost ecosystems. Additional  
469 flux measurements are urgently needed to understand the variation between the current measurements and,  
470 especially extended measurements on the CH<sub>4</sub> emissions to better quantify their role in the carbon balance.  
471 For example, a new data assimilation system estimates an Arctic carbon sink of -67 g C m<sup>-2</sup> yr<sup>-1</sup>, but this  
472 value is associated with very high uncertainties. Furthermore, these estimates do not include methane, which  
473 is even more difficult to evaluate (López-Blanco et al., 2019). Based on the field flux measurements, the  
474 Carbon Cycle Report 2018 (Schuur et al., 2018) estimated that the Eurasian boreal wetland is a source of 14

475 Tg CH<sub>4</sub> per year. On the other hand, Kirschke et al. (2013) estimations, based on atmospheric  
476 measurements, ended up to the value of 9 Tg CH<sub>4</sub> per year. Locally, methane fluxes measured in 2005-2013  
477 showed significant year-to-year variations. Interestingly, the observed variability in North America,  
478 specifically in the Hudson Bay lowlands, appears to have been driven partly by the soil temperature, while in  
479 the Western Siberian lowlands the variability was dependent on the soil moisture (Thompson et al., 2017).  
480 The comparison of high-resolution modelling of atmospheric CH<sub>4</sub> to CH<sub>4</sub> observations already in 2012 from  
481 the East Siberian Arctic Shelf (ESAS), a potentially large CH<sub>4</sub> source, confirms that methane releases are  
482 highly variable and inhomogeneous (Berchet et al., 2016).

483  
484 Long-term flux measurements provide insight into the carbon sink - source dynamics. The flux  
485 measurements from the moist tussock tundra in the north-eastern Siberia indicated that drainage influences  
486 the carbon cycle and that the tundra is changing to a weaker CO<sub>2</sub> sink and CH<sub>4</sub> source. Another relevant  
487 observation was that the time outside the growing season influences the carbon balance of ecosystem  
488 processes, especially during the zero-curtain period (Kittler et al. 2017). This is in line with similar studies in  
489 Alaska (Commane et al., 2017; Euskirchen et al., 2017). Therefore, the autumn temperature was identified as  
490 a major driving factor describing the differences between the annual GHG fluxes. Notably, however, the  
491 seasonal amplitudes of CO<sub>2</sub> concentrations in Siberia were found to be significantly higher than those in the  
492 North American continent, likely due to the more intense biological activity here (Timokhina et al., 2015a).  
493 A recent study showed that the Siberian carbon cycle is a major contributor to the Northern Hemisphere  
494 amplitude of CO<sub>2</sub> variation (Lin et al., 2020).

495  
496 Observations from non-permafrost sites may give us a clue on the future dynamics of fluxes, as the  
497 permafrost is thawing. The chamber measurements of CH<sub>4</sub> and CO<sub>2</sub> fluxes from a non-permafrost site in the  
498 Siberian peatland in August, 2015, showed that the highest values of methane fluxes were obtained in burnt  
499 wet birch forest and the lowest ones in seasonally waterlogged forests (Glagolev et al., 2018). The fluxes can  
500 vary even between different sites of a bog, as measured by Dyukarev et al. (2019). The net ecosystem  
501 exchange (NEE), ecosystem respiration (ER) and gross primary production (GPP), based on the measured  
502 CO<sub>2</sub> fluxes at a ridge-hollow complex bog and a model for ridge and hollow sites at oligotrophic bog in  
503 Middle Taiga Zone of West Siberia, showed that a two-year-average NEE at the hollow site was 1.7 times  
504 higher than at the ridge site (Dyukarev et al., 2019). The ecosystem processes are influenced by drying in  
505 tundra ecosystems. Kwon et al. (2019) reported from Alaska that drying in the tundra ecosystems increased  
506 contributions of modern soil carbon to the ecosystem respiration but, at the same time, decreased  
507 contributions of old soil carbon. These changes were attributed mainly to modified soil temperatures at  
508 different soil layers due to the altered thermal properties of organic soils following drainage. Furthermore,  
509 the drainage lowered CH<sub>4</sub> fluxes by a factor of 20 during the growing season, with post drainage changes in  
510 microbial communities, soil temperatures, and plant communities also affecting the flux reduction in an  
511 Arctic wetland ecosystem (Kwon et al., 2017).

512

513 Voigt et al. (2016) reported that, under warming conditions, the vegetated tundra in north-eastern European  
514 Russia shifted from a GHG sink to a source. The positive warming response was dominated by CO<sub>2</sub>;  
515 however, N<sub>2</sub>O emissions were also significant. N<sub>2</sub>O was emitted not only from bare peat, already identified  
516 as a strong source, but also from vast vegetated peat areas not emitting N<sub>2</sub>O under current climate conditions.  
517 These results can be explained by the dynamics between the temperature, nitrogen assimilation by plants and  
518 soil microbial activity, having a strong impact on the future GHG balance in Arctic (Voigt et al., 2016; Gil et  
519 al., 2017). Studying N<sub>2</sub>O emissions from a typical permafrost peatland in Finnish Lapland, it was concluded  
520 that about 25% of the Arctic territory are areas that potentially emit nitrous oxide (Voigt et al., 2017). It  
521 seems that there is positive feedback mechanism between the permafrost thawing and moisture regime.  
522 Predicting the response of soils to climate change or land use is central to understanding and managing N<sub>2</sub>O  
523 emissions. According to recent results, the N<sub>2</sub>O flux can be predicted by models that incorporate soil nitrate  
524 concentration (NO<sub>3</sub><sup>-</sup>), water content and temperature (Pärn et al., 2018).

525

526 In addition to CO<sub>2</sub> and CH<sub>4</sub>, thawing or collapsing of arctic permafrost can release volatile organic  
527 compounds (VOCs). Li et al. (2020a) examined the release of VOCs from thawing permafrost peatland soils  
528 sampled from Finnish Lapland in laboratory. The average VOC fluxes were four times as high as those from  
529 the active layer, and mainly attributed to direct release of old, trapped gases from the permafrost. These  
530 results demonstrate a potential for substantive VOC releases from thawing permafrost and suggests that  
531 future global warming could stimulate VOC emissions from the Arctic permafrost.

532

### 533 2.1.3 Ecosystem structural change (Q3)

534

#### 535 *Changes in microbial activity*

536

537 Climate change is likely to cause an increased appearance of trees on open peatlands, but we do not know  
538 how this vegetation change will influence the below-ground microbiology and composition. Changes along  
539 bog ecotones at three Russian peatland complexes suggest that tree encroachment may reduce the trophic  
540 level of *Testate Amoeba* communities and reduce the contribution of mixotrophic *Testate Amoebae* to  
541 primary production. Thus, it seems that increased tree recruitment on open peatlands will have important  
542 consequences for both microbial biodiversity and microbial-mediated ecosystem processes (Payne et al.,  
543 2016). We also need to understand better the dynamics affecting the bacteria, fungi and other related species  
544 in the ground air layer. Recent studies by Korneykova and Evdokimova (2018) and Korneikova et al. (2018  
545 a, 2018b) showed the influences of anthropogenic sources (Copper-Nickel Plant) and acidic soils in Russian  
546 northern taiga and tundra on the portion of the airborne fungi, and on the structure of algological and  
547 mycological complexes (Korneikova et al., 2018 a, 2018b). New methods were reported on how to improve  
548 soil conditions, developed on all kinds of materials made or exposed by human activity that otherwise would  
549 not occur at the Earth's surface, referred as "Techno sol engineering" (Slukovskaya et al., 2019), and how to

550 monitor climate change impacts on the functional state of bogs by using *Sphagnum* mosses (Preis et al.,  
551 2018).

552

### 553 *Effects of forest fires on soils*

554

555 Forest fires, a significant environmental factor in the Northern Eurasian region, change soil chemical and  
556 physical properties and may influence greenhouse gas fluxes and emissions of BVOCs. Recent results  
557 indicate that a slower post-fire litter decomposition has a clear impact on the recovery of soil organic matter  
558 following forest fires in northern boreal coniferous forests due to accumulated soil organic matter. The soil  
559 recovery is related to slow litter composition and reduced enzymatic and microbial activity (Köster et al.,  
560 2016).

561

562 Post-fire studies on the long-term evolution of the structure and functioning of bacterial communities are  
563 sparse. Sun et al. (2016) showed that the major drivers influencing bacterial community are the soil  
564 temperature, pH and moisture. Furthermore, Köster et al. (2015) analyzed long-term effects of fire on soil  
565 CO<sub>2</sub>, CH<sub>4</sub> and N<sub>2</sub>O fluxes in pine forest stands in the Finnish Lapland, and discussed the role of microbial  
566 bio mass in this context. They did not detect significant effects of fires on CO<sub>2</sub> emissions or N<sub>2</sub>O fluxes, but  
567 there were long-lasting strengthening of the CH<sub>4</sub> sink by the soil. Interestingly, Köster et al. (2018) did not  
568 find a similar kind of long-term effect on the CH<sub>4</sub> sink dynamics in studies carried out in Siberia.

569

570 Forest wildfires also regulate the BVOC emissions from boreal forest floors by changing the ground  
571 vegetation. Total BVOC emissions from a forest floor were found to decrease after a forest fire and then to  
572 increase again along with the succession of forests (Zhang-Turpeinen et al., 2020). For a comparison, Bai et  
573 al. (2017) showed that biomass burning resulted in increased BVOC emission fluxes and ozone  
574 concentration above canopy in a subtropical forest in China.

575

## 576 2.2. ATMOSPHERIC SYSTEM

577

578 Concerning critical atmospheric processes and large-scale climate implications, we concentrate here on  
579 greenhouse gases and aerosol particles over Northern Eurasia and Arctic, urban air quality, and issues related  
580 to the weather and atmospheric circulation. We summarize the recent measurements on the atmospheric  
581 composition relevant to sink and source dynamics in Siberia, on the sources and properties of atmospheric  
582 aerosols in Arctic-boreal environments, including black carbon and dust in the atmosphere and snow, and on  
583 the methodological and model developments related to atmospheric chemistry and physics (Q4, section  
584 2.2.1). Furthermore, we introduce new results and observations on atmospheric pollution in rural, suburban  
585 and mega city environments in China and Russia (Q5, section 2.2.2). We briefly show some recent results  
586 related to synoptic-scale weather in Arctic-boreal regions, focusing on cold and warm episodes, cyclone



587 density and atmosphere-ocean interaction, effects of circulation on temperature and moisture, cloudiness in  
 588 the Arctic, and boundary layer dynamics (Q6, section 2.2.3).

589

590 2.2.1 Atmospheric composition and chemistry (Q4)

591

592 *Boreal forests carbon balance*

593

594 As already discussed in section 2.1.1, boreal forests as a carbon sink and the related role of forestation have  
 595 been under international debate. It seems that early snowmelt increases springtime carbon uptake of the  
 596 boreal forests of Eurasia and North America and shows a major advance in the CO<sub>2</sub> sink (Pulliainen et al.,  
 597 2017). A scenario of a complete global deforestation by Scott et al. (2018), combining radiative forcing to  
 598 CO<sub>2</sub>, surface albedo and short-lived climate forcers (SLCFs), suggests that global deforestation could cause a  
 599 0.8 K warming after 100 years, with SLCFs contributing 8% of the effect. However, deforestation as  
 600 projected by the RCP8.5 scenario leads to zero net radiative forcing from SLCF, primarily due to  
 601 nonlinearities in the aerosol indirect effect. Tuovinen et al. (2019) showed that methane fluxes vary strongly  
 602 with a wind direction in a tundra ecosystem having heterogeneous vegetation. By combining very high-  
 603 spatial-resolution satellite imagery and footprint modelling, they were able to estimate the relation between  
 604 the main land cover types and ecosystem-level measurements. CH<sub>4</sub> emissions originated mainly from wet fen  
 605 and graminoid tundra patches, whereas the areas of bare soil and lichen acted as strong CH<sub>4</sub> sinks (Tuovinen  
 606 et al. 2019. Tsuruta et al. (2017) reported posterior mean global total emissions of 516±51 Tg CH<sub>4</sub> yr<sup>-1</sup> during  
 607 2000-2012, which indicates that these emissions had increased by 18 Tg CH<sub>4</sub> yr<sup>-1</sup> from the period 2001-2006  
 608 to the period 2007-2012. This increase can be explained by increased emissions from the temperate region in  
 609 South America and from the temperate region and tropics in Asia.

610

611 Analysis of the trends and the diurnal, weekly and seasonal cycles of CO<sub>2</sub> and CH<sub>4</sub> mixing ratios derived  
 612 from the long-term data of the “Japan–Russia Siberian Tall Tower Inland Observation Network” showed that  
 613 the frequency of identified events of elevated concentration differs for CO<sub>2</sub> and CH<sub>4</sub> and may reach up to  
 614 20% of days in some months (Belikov et al., 2019). These observations made it possible to reduce  
 615 uncertainties in the biosphere surface CO<sub>2</sub> uptake (Kim et al., 2017). Although the CO<sub>2</sub> uptake in boreal  
 616 Eurasia estimated by Kim et al. (2017) was about 30% lower than that obtained without the assimilation of  
 617 Siberian observation data, Siberia still remains a key contributor to the terrestrial CO<sub>2</sub> sink in the Northern  
 618 Hemisphere.

619

620 There are tendencies of a significant growth or suppression of soil CO<sub>2</sub> fluxes across different types of  
 621 human impacts, such as forest fires, trampling, settlements, reindeer grazing and clearcuts on cryogenic  
 622 ecosystems in Russia (Karelin et al., 2017). For example, Ivanhov et al. (2019) analyzed CO<sub>2</sub> measurements  
 623 during 2010-2017 and reported CO<sub>2</sub> concentration increases of 20 ppm in Tiksi at a coast of Laptev Sea and  
 624 of 15 ppm at the Cape Baranov station. They also detected that wildfires in Siberia can lead to a parallel

625 increase of the CO<sub>2</sub> concentration at the Russian Arctic. Furthermore, the measurements showed that the  
626 atmospheric CO<sub>2</sub> concentration increased on average by 2.0 ppm yr<sup>-1</sup> during 2006-2013 in central Siberia,  
627 with a large inter-annual variations. The highest increase were found in 2010 and 2012 (3.6 and 4.3 ppm yr<sup>-1</sup>,  
628 respectively), when large wildfires released huge amounts of CO<sub>2</sub> in Siberia (Timokhina et al., 2015b).  
629 Repeated wildfires in boreal forests can combust a portion of the thick organic soil layer characteristic for  
630 this ecosystem, and change the forests from a carbon sink into a carbon source (Walker et al., 2019). A study  
631 on a fire chronosequence of the central Siberian permafrost soil showed that soils affected by fires over  
632 decades act as CO<sub>2</sub> sources, and that the CO<sub>2</sub> emissions from these soils increased with an increasing time  
633 since the last fire (Köster et al., 2018). However, there were no similar effects on CH<sub>4</sub> emissions, with soils  
634 acting as a CH<sub>4</sub> sink without any connection to forest fires. In addition to CO<sub>2</sub>, wildfires also release large  
635 amounts of other trace gases and aerosols. Emission factors of several trace gases and aerosols from Siberian  
636 fires measured from the Trans-Siberian railway were reported by Vasileva et al. (2017). The impact of  
637 Siberian fires as elevated aerosol concentrations was at times observed to extend up on the Arctic coast  
638 (Asmi et al., 2016).

639

#### 640 *Arctic methane (CH<sub>4</sub>) balance*

641 Deep understanding on the dynamics of methane emissions in the Arctic is needed for identifying and  
642 quantifying GHG-related feedbacks and global methane cycle (Dean et al., 2018). During the winter,  
643 methane originates mostly from anthropogenic sources, while on smaller scales also emissions from the  
644 oceans, including the Eastern Siberian Arctic Shelf (ESAS), can play an important role. During the warm  
645 season, the balance is dominated by emissions from wetlands and freshwater bodies. Thonat et al. (2017)  
646 employed the CHIMERE model for an assessment of the methane cycle in Arctic. They reported that all  
647 methane sources, except biomass burning, contributed to measurements at six study sites. That study  
648 emphasizes the importance of a joint model-measurements approach for studies of complex phenomena at  
649 large spatial scales. Accounting for OH oxidation and soil uptake, two important sinks of methane, improved  
650 the agreement between observed and modelled methane concentrations (Thonat et al., 2017). Peltola et al.  
651 (2019) up-scaled CH<sub>4</sub> fluxes measured at 25 northern wetland sites and showed three different maps of  
652 wetland distribution with the annual methane emissions varying from 31 to 38 Tg(CH<sub>4</sub>) yr<sup>-1</sup>. (For the monthly  
653 up scaled CH<sub>4</sub> flux data products see [doi.org/10.5281/zenodo.2560163](https://doi.org/10.5281/zenodo.2560163)). Multiple sources, together with  
654 different spatiotemporal dynamics and magnitudes, are influencing the total Arctic CH<sub>4</sub> budget and addresses  
655 the need for the further improved assessments (Peltola et al., 2019; Thonat et al., 2017).

656

#### 657 *Northern Eurasian carbon monoxide (CO)*

658 Analysis of long-term trends in the atmospheric composition in remote Northern Eurasia (1998–2016)  
659 showed that the total column carbon monoxide (CO) amount has been stabilized or increased in summer and  
660 autumn months (Rakitin et al., 2018). The changes in the global photochemical system, especially changes in  
661 the ratio between the sources and sinks of minor atmospheric chemical species, could explain these trends  
662 (Skorokhod et al., 2017). A comparative study (1998–2014) on the atmospheric total column CO amount in

663 background and polluted regions of Eurasia indicated that this amount has decreased remarkably in the  
664 Moscow urban environments ( $3.73\% \pm 0.39\%$  per year) compared to the background regions (0.9–1.7% per  
665 year) (Wang et al., 2018a).

666

#### 667 *Northern Eurasian Ozone ( $O_3$ )*

668 Atmospheric measurements of ozone, its precursors and other pollutants over Siberia are important for the  
669 atmospheric chemistry modelling, satellite product validation and comparisons between Siberia and other  
670 regions of the Northern Hemisphere. Isoprene and monoterpenes together with nitrogen oxides impact  
671 tropospheric  $O_3$  formation and lead to an increase in the daytime ozone-forming potential (OFP) in urban  
672 environments. Bai et al. (2021) showed that  $O_3$  may respond either positively or negatively to isoprene and  
673 monoterpene emissions depending on the level of solar radiation and atmospheric loadings of trace gases and  
674 aerosol particles. It was demonstrated that monoterpenes have a major contribution to tropospheric  $O_3$   
675 formation, especially in cities in Siberia having high atmospheric  $NO_x$  concentration (10–20 ppb) and  
676 daytime temperatures ( $>25\text{ }^\circ\text{C}$ ) (Berezina et al., 2019). In contrast, isoprene is dominating the  $O_3$  formation  
677 and the increasing OFP in the cities in Far East. The isoprene-derived OFP can originate from deciduous  
678 vegetation growing in city environments or nearby regions, or from an anthropogenic isoprene source. The  
679 monoterpene-derived OFP was found to be the lowest in medium-size cities and the highest in small cities  
680 (Berezina et al., 2019). The total contribution of benzene and toluene to photochemical  $O_3$  production was  
681 found to be up to 60–70% in urbanized environments, indicating anthropogenic pollutant sources  
682 (Skorokhod et al., 2017). In addition to atmospheric chemistry, the connection between stratospheric  $O_3$ , UV  
683 radiation and health effects needs to be addressed in the populated urban environments of Siberia. Chubarova  
684 et al. (2019b) estimated that the wintertime  $O_3$  depletion in northern regions of Siberia is not critical, but the  
685 much larger  $O_3$  reductions observed in the early spring can lead to dangerous levels of erythema UV  
686 radiation (see also section 2.4.3 Natural Hazards and UV variation) .

687

#### 688 *Sources and properties of atmospheric aerosols in boreal and Arctic environments*

689

690 Atmospheric new particle formation (NPF) is the largest contributor to the number concentration of aerosol  
691 particles in the global troposphere. During the past couple of decades, NPF has been measured in more than  
692 10 boreal forest sites (Kerminen et al., 2018). The annual frequency of NPF event days varies between about  
693 10 and 30% in the boreal forest zone, being the highest in the western part of this region and lowest in the  
694 northern edge and Siberian part of it. Similar high nucleation frequencies were found at two very remote  
695 sites in boreal North America (Andreae et al., 2019). In contrast, annual NPF event frequencies below 2%  
696 were reported from central Siberia (Wiedensohler et al., 2019). Similarly, in the northern Siberia on the  
697 Arctic coast, NPF events were mainly connected with marine and coastal air masses and rarely observed in  
698 continental air masses (Asmi et al., 2016). Seasonally, NPF tend to be most frequent during spring, even  
699 though high NPF event frequencies can also be observed during summer or autumn. Winter-time NPF is rare  
700 throughout the boreal forest region. In the Arctic, NPF appears to be a major aerosol particle source from

701 spring to summer, after which this source collapses during autumn and is practically absent over the whole  
702 winter (Freud et al., 2017). 20 years of NPF observations in a boreal forest at the SMEAR II station in  
703 Finland show higher frequency of NPF events under clear-sky conditions in comparison to cloudy conditions  
704 (Dada et al. 2017). Also oxidized organic vapors showed a higher concentration during the clear-sky NPF  
705 event days, whereas the condensation sinks and some trace gases had higher concentrations during the  
706 nonevent days.

707

708 The overall importance of atmospheric NPF in boreal and Arctic areas depends on the growth of freshly-  
709 formed particles to cloud condensation nuclei. In the boreal forest environment, both observations and model  
710 simulations indicate that the particle growth is tied strongly with the oxidation products of biogenic volatile  
711 organic compounds originating from forest ecosystems (Paasonen et al., 2018; Östrom et al., 2017). The  
712 important compound group in this respect are monoterpenes, even though also sesquiterpenes were found to  
713 have high secondary organic aerosol yields in boreal forest environments (Hellén et al., 2018). The observed  
714 particle growth rates were found to increase with an increasing particle size and to be highest in summer  
715 (Paasonen et al., 2018). The chemistry of new particle growth in the Arctic atmosphere is not well  
716 characterized, even though available observations suggest that this growth is associated mainly with biogenic  
717 emissions from high-latitude marine areas (Giamarelou et al., 2016; Heintzenberg et al., 2017; Kecorius et  
718 al., 2019).

719

720 Wildfires are an important source of particulate pollutants on a global scale and are affecting both air quality  
721 and climate (Andreae, 2019; Bondur et al., 2020). Satellite observations indicate that the annual burned area  
722 by wildfires in Russia decreased by a factor of 2.6 during 2005–2016 owing to early detection and  
723 suppression of fire sources, whereas in Ukraine the relative size of burned-out areas increased by a factor of  
724 6–9 from 2010–2013 to 2014–2016 (Bondur et al., 2017; 2019d). For Siberia, Ponomarev et al. (2016)  
725 reported strong increases in both number and burned areas based on satellite data, with burned areas  
726 doubling from 2005 to 2016. While biomass burning emissions have been measured widely over Russia  
727 (Bondur, 2016; Bondur and Ginzburg, 2016; Bondur et al., 2019d), there is still a need for further  
728 information on the atmospheric composition of wildfire emissions and related emission ratios from the  
729 Siberian region. Fire experiments provide important information on the emission and aging characteristics of  
730 smoke aerosols (e.g. Kalogridis et al., 2018).

731

732 Luoma et al. (2019) presented a detailed trend analysis for aerosol optical properties at the SMEAR II station  
733 in Finland. They found a statistically significantly decreasing trend for the scattering coefficient, and even a  
734 stronger decreasing trend for the absorption coefficient during 2006 – 2017. These trends are very likely  
735 indicative of decreasing influence of anthropogenic emissions, with the contribution from emissions  
736 containing black carbon decreasing even faster.

737

738 Measurements of carbonaceous aerosols over central Siberia during 2010-2012 showed that in fall and  
739 winter, high concentrations of such aerosols were caused by long-range transport from the cities located in  
740 southern and southwestern regions of Siberia (Mikhailov et al., 2015a). In spring and summer, pollution  
741 levels were high due to regional forest fires and agricultural burning in the Russian-Kazakh region. The  
742 variability of the background concentration of organic aerosols correlated with the air temperature in  
743 summer, implying that biogenic sources dominated the formation of organic particles at that time of the year  
744 (Mikhailov et al., 2015b). Based on a five-year study by Mikhailov et al. (2017), it seems that the  
745 atmospheric pollution originating from the biomass burning and anthropogenic emissions is  
746 significantly affecting the Siberian region. However, in summer precipitation is removing the  
747 pollutants from the air and leading to relatively clean atmospheric conditions in this region.  
748

749 At circumpolar sites over the Arctic, aerosol optical properties were found to vary both seasonally and  
750 spatially (Schmeisser et al., 2018). Arctic haze aerosols in late winter and spring are characterized by  
751 increased concentrations of sulfate, whereas in summer rich organic chemistry seems to be associated with  
752 vegetation, local urban and shipping sources as well as secondary aerosol formation influenced by emissions  
753 from low latitude Siberia (Popovicheva et al., 2019a). In a longer perspective, Arctic observations show large  
754 decreases in both sulfate and black carbon concentrations since the early 1980s (Breider et al., 2017).  
755

756 Observations on the elemental composition of surface aerosols on the coastal Kandalaksha Bay of the White  
757 Sea were indicative of the dominance of biogenic aerosol particles during summer time, with heavy metal  
758 concentrations in aerosols being at Arctic background levels (Starodymova et al., 2016). Increases in Ni and  
759 Cu concentrations were observed in air masses arriving from the western part of the Kola Peninsula  
760 indicative of emissions from the smelters in that region.  
761

#### 762 *Black carbon and dust in the atmosphere and snow*

763

764 Black carbon (BC) is a potentially large contributor to climate forcing in the Arctic region, however, the  
765 assessment of its pollution is hampered by the lack of aerosol studies in Northern Siberia (Popovicheva et al.,  
766 2019). The spatial variability of Arctic BC was studied using a harmonized dataset from six circumpolar  
767 Arctic observatories (Backman et al., 2017). These data suggested a significant spatial and seasonal  
768 variability (Schmeisser et al., 2018), addressing a need for more year-round data. BC observations (Sep 2014  
769 – Sep 2016) at the Hydrometeorological Observatory Tiksi at a coast of the Laptev Sea showed a seasonal  
770 variation, with the highest concentrations (up to 450 ng/m<sup>3</sup>) from January to March and the lowest ones  
771 (about 20 ng/m<sup>3</sup>) in June and September. During winter, stagnant weather and stable atmospheric  
772 stratification resulted in the accumulation of pollution, depending also on the wind direction and air mass  
773 transport (Popovicheva et al., 2019a).  
774

775 For Arctic, important sources of BC include industrial regions of Northern Europe, gas flares of the oil fields  
776 in the North Sea and Siberia, and Siberian biomass burning (Shevchenko et al., 2015; Konovalov et al.,  
777 2018). In 2012, for example, approximately a quarter of the biogenic BC emissions from Siberia after fire  
778 season were transported into the Arctic (Konovalov et al., 2018). Popovicheva et al. (2017a) analyzed the BC  
779 origins over the Russian Arctic seas together with simulated BC concentrations. Concentrations were  
780 observed to be high (100-400 ng m<sup>-3</sup>) over the Kara Strait, Kara Sea and Kola Peninsula, and extremely high  
781 (about 1000 ng m<sup>-3</sup>) over the White Sea. It seems that the gas-flaring emissions from the Yamal-Khanty-  
782 Mansiysk and Nenets-Komi regions affected the measurements made over the Kara Strait (northerly 70 °N)  
783 region, while the Near Arkhangelsk (White Sea) region was connected to the biomass burning in mid-  
784 latitudes. Combustion in Central and Eastern Europe were also identified as important BC sources.

785

786 Atmospheric aging promotes an internal mixing of BC with other aerosol constituents, leading to enhanced  
787 light absorption and radiative forcing. *In situ* observations at Arctic stations demonstrated an absorption  
788 enhancement due to the internal mixing of BC, which is a systematic effect and should be considered for  
789 quantifying the aerosol radiative forcing in this region (Zanatta et al., 2018).

790

791 Regional modelling of the Arctic aerosol pollution showed that long-range transported anthropogenic  
792 emissions and biomass burning are the main contributors to direct aerosol radiative effects in the region  
793 (Marelle et al., 2018). However, a scenario for 2050 indicates that shipping emissions in the Arctic Ocean  
794 could become the main source of surface aerosol and local flaring as a major source of BC, as the flaring  
795 already is a major source of BC in northwestern Russia. Kühn et al. (2020) assessed the effects of different  
796 BC mitigation measures on Arctic climate and showed that reducing BC emissions by the Arctic Council  
797 member states can reduce BC deposition by about 30 % compared to the current situation. A full execution  
798 of recommendation by the Arctic Council member and observer countries could reduce the annual global  
799 premature deaths due to PM by ~9 % by 2030 (Kühn et al. 2020). Evangeliou et al. (2018) estimated the  
800 origin of elemental carbon (EC) in snow and showed that for western Siberia where gas flaring emissions is a  
801 major contributor, the model underestimation was significant. Furthermore, the model was evaluated by  
802 independent BC measurements in snow over the Arctic showed and, again, the model underestimated BC  
803 concentrations, especially in spring.

804

805 Climatically significant cryosphere effects of light-absorbing, high-latitude dust can be similar to the albedo  
806 and melt effects of BC (Peltoniemi et al., 2015; Svensson et al., 2016, 2018; Meinander et al. 2020a, 2020b).  
807 Iceland is the most significant source for European Arctic dust and plays a role in the cryosphere-  
808 atmosphere-biosphere interactions and feedbacks (Boy et al., 2019; Dragosics et al., 2016, Dagsson-  
809 Waldhauserova and Meinander, 2019). Dust storms from technogenic mining industry tailing dumps on the  
810 Kola Peninsula are also an important source of local atmospheric pollution for neighbor cities, e.g., Apatity  
811 and Kirovsk (Amosov et al., 2020). Besides regional-scale dust storms from deserts in Kazakhstan, also  
812 Mongolia and China are significant sources of aerosol pollution for these regions and for the Northern Asia.

813

814 *Methodological and model developments related to atmospheric chemistry and physics*

815

816 Several methods to characterize the atmospheric chemistry were introduced or improved. Motivated by the  
817 ability of atmospheric ion measurements to identify new particle formation (NPF) events in the atmosphere  
818 (Leino et al., 2016), a new classification method for atmospheric NPF was developed (Dada et al., 2018).  
819 The new method uses both ion and aerosol particle number concentration measurements in the size ranges of  
820 2-4 nm and 7-25 nm, respectively, is complementary to the traditional event analysis, and can also be used as  
821 an automatic way of determining new particle formation events from large data sets. Zaidan et al. (2018b)  
822 used a mutual information approach for a variety of simultaneously monitored ambient variables, including  
823 trace gas and aerosol particle concentrations and several meteorological variables, in order to identify key  
824 factors contributing to atmospheric NPF. This method can be used in the atmospheric studies also to discover  
825 other interesting phenomena and relevant variables. The NPF is directly observed by monitoring the time  
826 evolution of ambient aerosol particle size distributions. A new machine learning-based approach, a Bayesian  
827 neural network (BNN) classifier, points out the potential of these methods and suggest further exploration in  
828 this direction (Zaidan et al., 2018a).

829

830 The condensation sink, being proportional to the surface area of an aerosol population, is one of the major  
831 parameters controlling NPF. A simple model for the time evolution of the condensation sink in the  
832 atmosphere for intermediate Knudsen numbers was developed to describe the coupled dynamics of the  
833 condensing vapor and the condensation sink (Ezhova et al., 2018a). The model gives reasonable predictions  
834 of condensation sink dynamics during periods of particle growth by condensation in the atmosphere. A new  
835 empirical relation between the atmospheric cloud condensation nuclei (CCN) concentration and aerosol  
836 optical properties was derived (Shen et al., 2019), making it possible to estimate CCN concentrations at sites  
837 with continuous observations of aerosol optical properties.

838

839 Empirical models of solar radiation were developed and used for calibrations of solar radiometers (Bai,  
840 2019). This method can be used to calibrate all kinds of solar radiometers. A solar radiation model combined  
841 with ceilometer and pyranometer measurements was used to classify clouds at SMEAR II (Ylivinkka et al.,  
842 2020) It opens new possibilities for studies of aerosol-cloud interactions.

843

844 Che et al. (2016) made an inter-comparison of three satellite (AATSR Level 2) aerosol optical depth (AOD)  
845 products (SU, ADV and ORAC) over China. The SU algorithm performs very well over sites with different  
846 surface conditions in mainland China from March to October, but slightly underestimates AOD over barren  
847 or sparsely vegetated surfaces in western China. The ADV product has the same precision and error  
848 distribution as the SU product. The main limits of the ADV algorithm are underestimation and applicability.  
849 The ORAC algorithm has the ability to retrieve AOD at different ranges, including high values of AOD, but

850 its stability decreases significantly with an increasing AOD, especially when  $AOD > 1.0$  (see also section  
851 2.2.2 Urban air quality and megacities).

852

853 One of the major problems for both interpretation of satellite data and applications of empirical models of  
854 solar radiation is related to elevated aerosol layers in the atmosphere. It was demonstrated that their origin  
855 can be attributed at a higher confidence when back trajectories are combined with lidar and radiosonde  
856 profiles (Nikandrova et al., 2018).

857

858 Black carbon measurement methods have progressed. A representative value for the multiple scattering  
859 enhancement factor, a fundamental quantity correcting atmospheric black carbon measurement using an  
860 aethalometer, was derived for the first time in the Arctic environment (Backman et al., 2017). By analyzing  
861 BC measurements made with an Aethalometer in Nanjing, Virkkula et al. (2015) showed that the  
862 compensation parameter of a widely-used data processing method depends both on single-scattering albedo  
863 and backscatter fraction of the aerosol (see also section 2.2.2 Urban air quality and megacities). The  
864 multiple-scattering correction factor of quartz filters and the effect of filtering particles mixed in snow was  
865 estimated by Svensson et al. (2019) who applied the method for analyzing light absorption and BC in snow  
866 samples taken from the Finnish Lapland and the Indian Himalayas.

867

868 Measurement of atmospheric sub-10 nm particle number concentrations has been of substantial interest  
869 recently. A new high flow differential mobility particle sizer (HF-DMPS) was built, calibrated and operated  
870 in field conditions for one month (Kangasluoma et al. 2018). The counting uncertainties of the HFDMPs  
871 were reduced by about 50% as compared to the traditional DMPS. The HFDMPs detected about two times  
872 more particles than the DMPS in the size range of 3–10 nm. Below 3 nm, the HF-DMPS is currently limited  
873 by the inability of diethylene glycol to condense on biogenic particles. For collecting BVOC samples, a  
874 novel collection method offering portability and improved selectivity and capacity was developed. A solid-  
875 phase microextraction (SPME) Arrow sampling (Barreira et al. 2018) can be used for static and dynamic  
876 collection of BVOCs in the field conditions. A significant improvement on sampling capacity was observed  
877 with the new SPME Arrow system over SPME fibers. A fully automated online dynamic in-tube extraction  
878 (ITEX)–gas chromatography/mass spectrometry (GC/MS) method was introduced for continuous and  
879 quantitative monitoring of volatile organic compounds in air (Lan et al. 2019). The stability and suitability of  
880 the developed system was validated with a measurement campaign, and the ITEX method provided 2–3  
881 magnitudes lower quantitation limits than established methods. Parshintsev et al. (2015) introduced a new,  
882 fast analysis method for the desorption atmospheric pressure photoionization high-resolution (Orbitrap) mass  
883 spectrometry (DAPPI-HRMS). The DAPPI results agreed with the aerosol particle number measured with an  
884 established method and was found to detect different compounds and giving complementary information  
885 about the aerosol samples.

886



887 Fragmentation of molecular clusters inside mass spectrometers is a significant uncertainty-source in many  
888 chemical applications. A novel model, capable of quantitatively predicting the extent of fragmentation of  
889 sulfuric acid clusters was developed (Passananti et al. 2019). The fragmentation cannot be described in terms  
890 of rate constants under equilibrium conditions, because clusters accelerate under electric fields (Zapadinsky  
891 et al. 2019). A model describing an energy transfer to the cluster internal modes caused by collisions with  
892 residual carrier gas molecules was developed. The model can be used to interpret experimental  
893 measurements done with atmospheric pressure interface mass spectrometers.

894

895 Recently, a new atmospheric observation site equipped with state-of-the-art atmospheric aerosol  
896 instrumentation was deployed in Beijing, China (Liu et al. 2020). At the Beijing University of  
897 Chemical and Technology (BUCT), the Aerosol and Haze Laboratory (AHL) was established in  
898 2018 - 2019, providing novel insights into air pollution in a comprehensive manner. The station  
899 hosts comprehensive instrumentation to concentrations of atmospheric trace gases, aerosol particle  
900 size distributions and mass concentrations, particle chemical composition on the levels from  
901 molecules, clusters and nanometer to micrometer sized aerosol particles. For example, the first  
902 results showed increased cluster mode particle number concentrations during NPF events, whereas  
903 during haze days accumulation mode particle number concentrations were high (Zhou et al., 2020).  
904 The observations have enabled to quantify number emission factors and underlined the importance of  
905 traffic (Kontkanen et al. 2020). Daytime sulfuric acid concentrations in Beijing were typically  
906 around  $4.9 \times 10^6 \text{ cm}^{-3}$  (Lu et al. 2019). During these measurements, an evidence was found on  
907 significant nighttime sulphuric acid production, yielding gaseous sulphuric acid concentrations of  
908  $1.0$  to  $3.0 \times 10^6 \text{ cm}^{-3}$  (Guo et al., 2021). For further results, see also section 2.2.2 Urban air quality  
909 and megacities.

910

911 Besides Beijing, measurements have been performed in several other locations inside the PEEX area. We  
912 used novel instrumentation to measure new particle formation and its precursors at the background Fonovaya  
913 station in the Tomsk region (Russia, Siberia), at the Värriö subarctic research station (Finland), in Ny-  
914 Ålesund (Svalbard, Norway) and on the German icebreaker, the Polarstern, during the MOSAIC project. As  
915 an example, the first results from Fonovaya station are shown in Fig. 2. Thanks to these deployments, in the  
916 next years we will be able to understand the identity of NPF precursors in those remote places. This will help  
917 us to elucidate the human impact on aerosol formation and thereby on aerosol-cloud interactions at high  
918 latitudes. In Siberia, we will finally understand why new particle formation occurs infrequently, and  
919 hopefully also identify the human role in this phenomenon. In the Arctic, we will understand the marine  
920 influence on NPF and will find out the detailed mechanism that leads to the formation of small clusters that  
921 which initiate NPF.

922

923 Model developments were made at several scales. Aerosol-radiation and aerosol-cloud interactions are  
 924 among the main sources of uncertainties in climate models, and detailed information on anthropogenic  
 925 aerosol number emissions is needed to improve this situation. Anthropogenic aerosol number emissions in  
 926 current large-scale models are usually converted from corresponding mass emissions in pre-compiled  
 927 emission inventories using very simplistic methods. In the global aerosol-climate model ECHAM-HAM, the  
 928 anthropogenic particle number emissions, converted originally from the AeroCom mass emissions, were  
 929 replaced with recently-formulated number emissions from the Greenhouse Gas and Air Pollution Interactions  
 930 and Synergies (GAINS) model (Xausa et al., 2018). However, revisions are still needed in the new particle  
 931 formation and growth schemes currently applied in global modeling frameworks.

932

933 For regional and urban scales, a fully integrated /online coupled meteorology-chemistry-aerosol model  
 934 Enviro-HIRLAM was developed (Baklanov et al., 2017) and tested for several applications in Europe,  
 935 Russian Arctic and China (Shanghai) (Mahura et al., 2018, 2019). Key issues for seamless integrated  
 936 chemistry–meteorology modeling for Earth System prediction were analyzed and formulated (Baklanov et  
 937 al., 2018), highlighting the scientific issues and emerging challenges that require proper consideration to  
 938 improve the reliability and usability of these models for three main application areas: air quality,  
 939 meteorology, and climate modeling. Baklanov et al. (2018) also presents a synthesis of scientific progress in  
 940 the form of answers to nine key questions, and provides recommendations for future research directions and  
 941 priorities in the development, application, and evaluation of online coupled models.

942

### 943 2.2.2 Urban air quality and megacities (Q5)

944

945 The rapid urbanization and growing number of megacities and urban agglomerations requires new types of  
 946 research and services that make the best use of science and available technology. There are urgent needs for  
 947 examining what the rising number of megacities means for air pollution and local climate, and what effects  
 948 these changes have on global climate (Baklanov et al., 2016). Such integrated studies and services should  
 949 assist cities in facing hazards, such as storm surge, flooding, heat waves and air pollution episodes,  
 950 especially in changing climates (WMO, 2019). We discuss here the recent observation on the atmospheric  
 951 pollution in China and Russia.

952

#### 953 *Air quality in China – recent observations*

954

955 China is one of the regions with highest concentrations of fine PM<sub>2.5</sub> in the world (Wang et al., 2017a). This  
 956 has serious consequences on air pollution and the associated visibility reduction (haze) and adverse health  
 957 effects (Zhao et al., 2017). The number of haze days in China has been growing during the recent decades,  
 958 but detailed understanding of the factors governing the occurrence of haze is still not clear (Wang et al.,  
 959 2019). Both NO<sub>2</sub> and SO<sub>2</sub> concentrations showed increasing trends during the 2004-2012 period, and these  
 960 trends could be linked to increased power plant and traffic emissions (Wang et al., 2019). A key feature of

961 haze formation seems to be an increased inorganic fraction of the aerosol, suggesting that the reduction of  
962 nitrate, sulfate and their precursor gases would improve air quality and visibility in China (Wang et al.,  
963 2019). In northern China, PM<sub>2.5</sub> concentrations declined over the period 2013–2017, and approximately half  
964 of the inter-annual variability in this region was attributed to atmospheric circulation changes (Li et al.,  
965 2020b). The maximum daily 8-h average O<sub>3</sub> concentrations increased over most of northern China during the  
966 same time period, with again large influences due to atmospheric circulation on daily basis (Liu et al.,  
967 2019b).

968

969 Compared with most other urban environments investigated so far, measurements in urban China  
970 demonstrated a relatively frequent occurrence of atmospheric new particle formation (NPF), and the  
971 observed NPF events were typically characterized by high particle formation rates and strongly size-  
972 dependent growth of newly-formed particles (Kulmala et al., 2016b; Wang et al., 2017b; Chu et al., 2019).  
973 Since the first reported sub-3 nm particle measurements in China a few years ago (Xiao et al., 2015), new  
974 insight into the formation pathways of molecular clusters and their growth have been obtained, including the  
975 relative roles of gaseous sulfuric acid, amines, ammonia and organic vapors in these processes (Yao et al.,  
976 2018; Yan et al., 2021). While high pre-existing particle loadings appear to suppress NPF during severe haze  
977 periods in Chinese megacities, it is unclear how NPF is possible at all under less but still quite polluted  
978 conditions typical for these environments (Kulmala et al., 2017). Overall, the available observations suggest  
979 NPF to be a major source of aerosol particles in urban China, with potentially large effects on haze formation  
980 (Kulmala et al., 2021) and cloud properties (Chu et al., 2019).

981

982 Urban measurements of particle number size distributions give deep understanding into the sources and  
983 atmospheric processing of fine particles. The longest urban continuous record is from the SORPES station in  
984 the Yangtze River Delta (Qi et al., 2015), covering almost a decade of measurements, whereas the broadest  
985 size range (1.5 nm – 1 µm) was measured in the winter Beijing atmosphere (Zhou et al., 2020). The latter  
986 study found clear differences in particle sources in different size ranges: NPF was in general the largest  
987 source of clusters and nucleation mode (<25 nm) particles, while traffic contributed to all the size ranges and  
988 dominated both cluster and nucleation modes on haze days. Aitken mode (25–100 nm) particles originated  
989 mainly from local emissions, with additional contributions from regional and transported pollution as well as  
990 from the growth of nucleation mode particles. Regional and transported pollution were identified as the main  
991 source of accumulation mode (>100 nm) particles.

992

993 Air pollution and chemical transformation, including annual and seasonal variations of the concentrations of  
994 atmospheric constituents, were analyzed for North China for the period 2005–2015 (Bai et al., 2018a). A  
995 photochemical link that related the production of fine PM and O<sub>3</sub> to VOCs was detected, and this mechanism  
996 was found to be prominent in summer. An intensive measurement campaign (SORPES station, Yangtze  
997 River Delta) was carried out to investigate sulfate formation and associated nitrogen chemistry (Xie et al.,  
998 2015). That study highlighted the effect of NO<sub>x</sub> in enhancing the atmospheric oxidizing capacity, and

999 indicated a potentially very important impact of increasing NO concentrations on particulate pollution  
1000 formation and regional climate change in East Asia. In Changzhou, a highly-populated city in the Yangtze  
1001 River Delta, primary organic aerosol concentrations outweighed secondary ones, indicating an important role  
1002 of local anthropogenic emissions in aerosol pollution (Ye et al., 2017). The measurement also showed the  
1003 abundance of organic nitrogen compounds in water-soluble organic aerosol, suggesting that these  
1004 compounds are likely associated with traffic emissions.

1005

1006 Aerosol impacts on warm cloud properties were investigated over three major urban clusters in Eastern  
1007 China and East China Sea using multi-sensor satellite observations (Liu et al., 2017, 2018). In addition to the  
1008 amount of aerosol, evidence was provided that aerosol types and environmental conditions need to be  
1009 considered to understand the relationship between cloud properties and aerosols. Aerosol-cloud interactions  
1010 were found to be more complex and of greater uncertainty over land than over ocean.

1011

1012 The atmospheric boundary layer (ABL), and especially its dynamic behavior, is central to the evolution of  
1013 near-surface air pollution. Using atmospheric observations combined with theoretical arguments, Petäjä et al.  
1014 (2016) proposed a feedback mechanism connecting ABL properties with PM. According to such mechanism,  
1015 high concentrations of PM enhance the stability of an urban boundary layer (BL) decreasing its height, thus  
1016 causing further accumulation of pollution inside BL. Ding et al. (2016a) and Wang et al. (2018b)  
1017 demonstrated an important role of BC aerosols in this feedback using model simulations combined with  
1018 observations. A tight connection between the BL height and pollutant concentration, and indications of the  
1019 presence of the above feedback mechanism, was also found based on comprehensive observations made on a  
1020 325-m tower in Beijing (Wang et al., 2020). In order to understand these feedbacks, Kulmala (2018) and  
1021 Hari et al. (2016) emphasized the crucial role of continuous, comprehensive measurements on a network of  
1022 flagship stations in tackling the air pollution problem in urban China and megacities elsewhere in the world.  
1023 They also introduced a so-called “Stations for Measuring Atmospheric and Earth surface Relations”  
1024 (SMEAR) concept, which consists of integrated atmospheric and ecosystem observations allowing the  
1025 analysis of Earth surface – atmosphere feedbacks and interactions. The first SMEAR-type station in China,  
1026 the SORPES station located in the Yangtze River Delta, has been operating since 2011 (Ding et al., 2016b).

1027

### 1028 *Anthropogenic emissions and environmental pollution in Russia*

1029

1030 In the complex situation of the plurality of emissions, an important research task remains in the Moscow  
1031 megacity environment for the assessment of the air quality and potential sources through aerosol  
1032 composition analyses. Moscow aerosol pollution has been studied using a special AeroRadCity-2018  
1033 experiment (Chubarova et al., 2019) and satellite data with the application of new MAIAC/MODIS aerosol  
1034 algorithm with a 1-km resolution (Zhdanova et al., 2020). An advanced source apportionment for this  
1035 environment was performed using combined Fourier-transform infrared spectroscopy data and statistical  
1036 principal component analysis (Popovicheva et al., 2020b). The main principal component loadings revealed

1037 the source impacts of transport, biomass burning, biogenic, dust and secondary aerosol in spring.  
1038 Identification of biomass burning-affected periods discriminated the daily aerosol composition change with  
1039 respect to air mass transport and number of fires detected in the surrounding areas. Measurements of  
1040 particulate BC were conducted at an urban background site (Meteorological Observatory of MSU) during the  
1041 spring period of 2017-2018 (Popovicheva et al., 2020c). The mean BC concentrations displayed significant  
1042 diurnal variations, with a poorly prominent morning peak and minimum at daytime. BC mass concentrations  
1043 were higher at nighttime due the shallow boundary layer and intensive diesel traffic. The aerosol optical  
1044 thickness (AOT) over Moscow showed a pronounced seasonal cycle, with a summer maximum and winter  
1045 minimum (Chubarova et al., 2016a). It was found that during 2001–2014, the monthly-mean values of AOT  
1046 declined by 1–5% per year, and this decline was attributed to decreased emissions of aerosols and their  
1047 precursors.

1048

1049 In general, the atmospheric environment over remote areas of Siberia and Northern Asia is relatively clean  
1050 compared with other surrounding regions of Asia and Eastern Europe (Baklanov et al., 2013). However, air  
1051 pollution from Siberian industrial centers poses significant environmental threats. For Siberian cities (e.g.,  
1052 Norilsk, Barnaul, Novokuznetsk), the air quality is among the worst in the Russian and European cities.  
1053 Similar to Arctic cities, stable atmospheric stratification and temperature inversions dominate for more than  
1054 half a year. This leads to pollution accumulation near the surface, which influences ecosystems and people.  
1055 Moreover, not only severe climatic conditions, but also manmade impacts on the environment in industrial  
1056 areas and large cities have intensified. The impacts manifest themselves as the pollution of environment, land  
1057 use changes, hydrodynamic regimes and local climate. Ultimately, these impacts feed back to people,  
1058 affecting their health and well-being.

1059

1060 The Russian part of the Barents Euro-Arctic region includes severe emission ‘hot spots’ for air pollutants.  
1061 The Kola Peninsula, despite the presence of areas with undisturbed nature in the eastern part, is the most  
1062 industrially developed and urbanized region in the Russian Arctic. The main polluters are the smelters of the  
1063 Severonickel (Monchegorsk, central part of the peninsula) and the Pechenganickel (Nickel and Zapolyarnyi  
1064 near the Russian-Norwegian border) enterprises. For comparison, emissions of SO<sub>2</sub> from the Nickel smelter  
1065 alone are 5-6 times larger than the total Norwegian emissions (NILU, 2013). In 2015 the Norilsk Nickel in  
1066 Siberia - the biggest mining and the metallurgical complex - emitted about 1.9 million tons of SO<sub>2</sub> (GGO,  
1067 2016). With the nickel factory (located in the southern part of the city), copper factory (just to its north) and  
1068 metallurgical plant (12 km to the east), the city of Norilsk is influenced by heavy industry no matter which  
1069 way the wind blows. The Blacksmith Institute declared in 2007 that Norilsk is one of the top 10 worst-  
1070 polluted places in the world. The impacts of emissions are manifested as deterioration of forest ecosystems  
1071 and acidification of soils and surface waters (Derome and Lukina, 2011), even at considerable distances from  
1072 the smelters. Heavy metals and alkaline pollutants contaminate areas around the sources of pollution within a  
1073 few hundred kilometres, while acid sulphates can be transported over long distances (Mahura et al., 2018).

1074

1075 A recent analysis on the total deposition and loading on the population in North-Western Russia and  
1076 Scandinavian countries caused by the continuous sulfur emissions from the Cu-Ni smelters in Murmansk  
1077 indicates the dominance of wet deposition, especially in winter time (Mahura et al., 2018). North-Western  
1078 Russia is influenced more by the Severonikel emissions compared with countries in the Scandinavian  
1079 Peninsula. The cities of the Murmansk region (Kola Peninsula) are under highest impacts. On a yearly scale,  
1080 the individual loadings on population are at the largest level (up to 120 kg/person) in the Murmansk region,  
1081 much lower (15 kg/person) in northern Norway, and the smallest (< 5 kg/person) in eastern Finland, Karelia  
1082 Republic and Arkhangelsk region. Distinct seasonal variability was identified, with the lowest contribution  
1083 during summer and the highest contribution during winter-spring in Russia, during spring in Norway, and  
1084 during autumn in Finland and Sweden.

1085  
1086 The annual yearbook “The State of Atmospheric Pollution in Cities on the Territory of Russia” for 2018  
1087 (Roshydromet and GGO, 2019) states the highest atmospheric emissions of PM were observed in Siberian  
1088 and Ural cities. In Novokuznetsk and Omsk, the observed PM was the highest (> 30 000 tons per year) while  
1089 emissions from other cities such as Angarsk and Chelyabinsk were lower (< 20 000 tons per year). Note that  
1090 in the 2015-2019 yearbooks, emissions from only stationary sources were provided due to revisions  
1091 (approved and implemented in November 2019 by the Russian Ministry of Natural Resources and Ecology,  
1092 MNRE) of methods applied for estimation of emissions into the atmosphere from mobile sources. Depending  
1093 on a source type, different methods to calculate emissions are applied (MNRE, 2019). For the gaseous  
1094 compounds, such as SO<sub>2</sub>, the maximum emissions included very high from Siberian cities (e.g. Norilsk,  
1095 Novosibirsk, Novokuznetsk, Omsk, Ufa, Irkutsk, Angarsk) and from North-West Russia cities (Zapolyarny,  
1096 Nickel, Monchegorsk). High NO<sub>2</sub> emissions were observed in Novosibirsk, Omsk, Angarsk and  
1097 Chelyabinsk. The CO integral urban emissions depend on a city size. These varied from less than 10 Gg yr<sup>-1</sup>  
1098 <sup>1</sup> (for small regional centers like Vladimir, Kursk, Samara) to 406 and 804 Gg yr<sup>-1</sup> for large metropolitan  
1099 areas such as St. Petersburg and Moscow. As a whole, an analysis of spatio-temporal variation of trace gases  
1100 in the boundary layer over Russian cities indicated significant emission variations between the urban  
1101 environments and remote sites (Elansky et al., 2016).

1102 Cities, being not isolated systems, may distribute as much pollution to the surrounding areas as they receive  
1103 it from outside them or from remote regions. The analysis of the transboundary atmospheric transport  
1104 between Russian Siberia and bordering countries (e.g. China, Kazakhstan, and Mongolia) is part of a mutual  
1105 risk assessment for urban areas/ cities and their surroundings. For example, the city of Ulaanbaatar  
1106 (Mongolia) suffers from high levels of pollution due to excessive airborne particulate matter emanating from  
1107 coal combustion mixed with traffic emissions and resuspended soil dust, resulting in variable chemical  
1108 source profiles (Gunchin et al., 2019). Long-range transport from remote sources might be an additional  
1109 contributor. Moreover, there are indications that such transport of biomass burning emissions from Siberia  
1110 could lead to pollution episodes and impact on surface ozone as far as in western North America (Jaffe et al.,  
1111 2004).

1112

### 1113 2.2.3 Weather and atmospheric circulation (Q6)

1114

1115 The observed evolution of weather and climate represents the combined effects of external forcing (changes  
1116 in the concentrations of greenhouse gases and aerosols etc.) and internal variability, related to a large extent  
1117 to the atmospheric circulation. It is also affected by local factors, particularly urban heat islands in cities.

1118 Here we discuss these interconnected processes, focusing on cold and warm episodes, cyclone density and  
1119 atmosphere-ocean interactions, effects of circulation on temperature and moisture, cloudiness in the Arctic,  
1120 and boundary layer dynamics relevant to the Arctic-boreal region.

#### 1121 *Cold and warm episodes*

1122 The Arctic warming, as well as the Arctic amplification, have been associated with changes in atmospheric  
1123 large-scale circulation together affecting the European winter temperatures. In large parts of Europe, severe  
1124 cold (warm) winter events are significantly correlated with warm (cold) Arctic episodes (Vihma et al., 2020).

1125 Air mass trajectory analysis revealed that air masses associated with extreme cold (warm) events typically  
1126 originate from over continents (sea areas). Despite Arctic and European-wide warming, winter cooling has  
1127 occurred in northeastern Europe in cases of air masses arriving from the southeast (Vihma et al., 2020).

1128

#### 1129 *Cyclone density dynamics and atmosphere-ocean interaction*

1130 Transporting large amounts of heat and moisture from mid-latitudes to the central Arctic, synoptic-scale  
1131 cyclones are vital for the Arctic climate system. Recent findings, based on atmospheric reanalysis, above all  
1132 the global ERA-Interim reanalysis available from 1 January 1979 to 31 August 2019, are summarized below.  
1133 During 1979–2016 in winter (Dec, Jan, Feb), the cyclone density increased in the areas around Svalbard and  
1134 in northwestern Barents Sea, but decreased in southeastern Barents Sea (Wickström et al., 2020). This is  
1135 related to a shift to more meridional winter storm tracks in the Norwegian, Barents and Greenland Seas. The  
1136 shift is favored by a positive trend in the Scandinavian Pattern and, in the areas north of Svalbard, by a  
1137 significant increase in the Eddy Growth Rate (Wickström et al., 2020).

1138

1139 Numerical model simulations of the storm activity in the White, Baltic and Barents Seas were analyzed for  
1140 the period 1979-2015 (Myslenkov et al., 2018). A high interannual variability in the storm number was  
1141 observed for all studied seas. No significant trends in the storm number during the period 1979-2015 were  
1142 found in the studied sea areas. On average, the connection with global atmospheric circulation is stronger for  
1143 the Baltic Sea than for the other two seas. Also, the future changes of wind wave climate were analyzed.  
1144 According to the RCP8.5 scenario, in the second part of the 21st century the number of storm events will rise  
1145 in the Baltic and Barents Seas.

1146

1147 In the Bjerknes compensation, changes in atmospheric heat transport co-occur with opposing changes in  
1148 ocean heat transport. Observations and model simulations indicate a central role for ocean-atmosphere heat

1149 exchange in the Barents Sea area in maintaining this compensation in the Arctic (Bashmachnikov et al., 2018  
1150 a, 2018b).

1151

#### 1152 *Circulation effect on temperature*

1153 The effect of atmospheric circulation on temperature trends in years 1979-2018 was studied by Räisänen  
1154 (2019, 2021) using a trajectory-based method. He found that the circulation trends had reduced the annual  
1155 mean warming during this period in western and central Siberia locally by over 1°C, with a much larger  
1156 cooling effect in autumn and winter (Fig. 3). His findings also confirmed a circulation-induced amplification  
1157 of warming over the Barents and Kara seas particularly in winter. Yet, in most areas the circulation-related  
1158 temperature trends have varied strongly from month to month, leaving only a relatively small effect on the  
1159 annual mean temperature trends. The residual warming obtained after subtracting the circulation effect  
1160 therefore tends to have a smoother seasonal cycle than the observed temperature trends, in better agreement  
1161 with the multi-model mean trends in the CMIP5 simulations (Taylor et al., 2012).

1162

#### 1163 *Circulation effect on moisture*

1164 The effects of large-scale circulation on moisture, cloud and longwave radiation occur mostly via the impact  
1165 of horizontal moisture transport (Nygård et al., 2019). Evaporation is typically not efficient enough to shape  
1166 those distributions, and much of the moisture evaporated in the Arctic is transported southward (Nygård et  
1167 al., 2019). Strong moisture transport events avail a large part of the northwards moisture transport. The  
1168 meridional net transport is only a small part of the water vapor exchange between the Arctic and mid-  
1169 latitudes (Naakka et al., 2019). When a high-pressure pattern across the Arctic Ocean from Siberia to North  
1170 America is lacking, the amounts of moisture, clouds and downward longwave radiation are anomalously  
1171 high near the North Pole (Nygård et al., 2019). Using vertically-integrated water vapor as a metric, the Arctic  
1172 (north of 70°N) has experienced a robust moistening trend since 1979, and in absolute numbers this trend is  
1173 the smallest in March and the largest in August (Rinke et al., 2019). However, the relative trends are the  
1174 largest in winter. Although different atmospheric reanalysis are consistent in spatiotemporal trend patterns,  
1175 they scatter in the trend magnitudes.

1176

1177 Analysis of moisture and aridity estimated using the web-GIS "CLIMATE" and the ECMWF ERA-Interim  
1178 reanalysis data for Southern Siberia (50-65 °N, 60-120 °E) from 1979 to 2010 with a 0.75° × 0.75° grid  
1179 resolution showed that the mountain regions of Eastern Siberia have been come more arid each month during  
1180 the last 30 years (Ryazanova and Voropay, 2017). In Western Siberia, aridity increased in May and  
1181 decreased in June, while in the other months positive and negative trends were found. The greatest  
1182 differences in the trends of the aridity index, air temperature and precipitation were observed in July.

1183

#### 1184 *Cloudiness in Arctic*

1185



1186 The climatology and inter-annual variability of Arctic cloudiness remains a wildcard in regional climate  
 1187 change projections. Both climate models and satellite data products need *in situ* observations for calibration  
 1188 and validation. Chernokulsky et al. (2017) and Chernokulsky and Esau (2019) collected and processed  
 1189 manual cloud observations from meteorological stations in the PEEEX area. The cloud records in the Arctic  
 1190 are available since the end of the 19<sup>th</sup> century. Since 1936, cloud observations representatively cover the  
 1191 Eurasian Arctic. This permits reconstructions of cloud type and cloud cover climatologies as well as studies  
 1192 of inter-decadal variability of cloudiness. A problem of a special interest is related to the co-variability of the  
 1193 total cloud cover and sea ice concentration or extent. Both clouds and sea ice affect the surface heat balance  
 1194 through surface albedo, but their feedback mechanisms, dynamical impacts and climate sensitivities are  
 1195 different. Chernokulsky et al. (2017) found that the annual-mean total cloud cover (TCO) decreases during  
 1196 warmer climate periods with a lower sea ice concentration, but increases over sea ice in the Barents Sea as  
 1197 more moisture is transported into the Arctic at higher temperatures. Furthermore, the increasing TCO  
 1198 reduces the deficit of the surface heat, and the intra- and inter-annual variability of TCO over solid ice is  
 1199 higher than that over open water (Chernokulsky et al. 2017). Long-term cloud climatological analysis based  
 1200 on meteorological observations of the total and low cloud cover and cloud types from the Barents Sea to the  
 1201 Chukchi Sea showed that significant transitions between cloud types has been taken place, especially the  
 1202 low-level stratus and stratocumulus types have been transformed to convective cloud types (Chernokulsky  
 1203 and Esau, 2019). Chernokulsky and Esau (2019) addressed that their results are relevant for understanding  
 1204 Arctic cloud processes and feedbacks, and that new knowledge is needed to connect the changes in the  
 1205 Arctic radiation balance with the Arctic cloud cover—cloud type climatology.

1206

#### 1207 *Boundary layer dynamics and urban heat islands*

1208

1209 On the background of accelerated and amplified Arctic warming, anthropogenic heat release and metabolism  
 1210 of cities add up to persistent warm temperature anomalies in urbanized areas (Fig. 4). Indeed, if the climate  
 1211 change forcing approaches  $2 \text{ W m}^{-2}$ , the urban heat forcing could be  $10\text{-}100 \text{ W m}^{-2}$  (Konstantinov et al.,  
 1212 2018). The urban heating trapped in shallow planetary boundary layers is potent to rise the local  
 1213 temperatures by 1 to 10 °C or even more. This local climate phenomenon is known as the urban heat island  
 1214 (UHI) (Esau et al., 2020). A series of *in situ* and satellite UHI studies in the northern cities revealed strong  
 1215 and persistent warm temperature anomalies in almost all of 28 northern West Siberian cities (Miles and Esau,  
 1216 2017), in 5 cities covered by the UHIARC network (Konstantinov et al., 2019; Varentsov et al., 2018a) and  
 1217 in 57 Scandinavian cities (Miles and Esau, 2020). The mean wintertime temperature anomalies, the UHI  
 1218 intensity, varied from 0.8 K to 1.4 K and had extreme intensities of up to 7 K during cold anticyclone weather  
 1219 conditions. The complete dataset of surface UHI intensity derived from MODIS LST data products is freely  
 1220 available and published in Miles (2020). Such a UHI-induced strong mediation of cold temperature spells  
 1221 might cause significant socio-economic and environmental impacts in the cities (Konstantinov et al. 2018,  
 1222 Fig. 4). A survey of other UHI studies in 11 Arctic cities and towns confirmed that even relatively small

1223 cities at high latitudes may exhibit intensive UHIs. A recent analysis confirms the important role of the  
1224 surrounding temperature in explaining spatial-temporal variation of the UHI intensity (Miles and Esau,  
1225 2017). The major contribution to the UHI was revealed for water, sparse vegetation, grassland and scrubland.  
1226 The mechanisms and pathways of the UHI maintenance requires an involvement of numerical experiments  
1227 with turbulence-resolving models to advance the understanding of the local climate features (Urban Heat  
1228 Islands - UHIARC dataset see [http://urbanreanalysis.ru/uhi\\_arc.html](http://urbanreanalysis.ru/uhi_arc.html)). We would need a denser  
1229 meteorological network, especially high quality temperature data, to better understand the urban climatology  
1230 and the thawing processes in urban soils and to better assess climatic trends relevant to Arctic societies and  
1231 welfare (Konstantinov et al. 2018).

1232

1233 Urban climate anomalies may cause more extreme weather and climate phenomena in densely populated  
1234 megacities. The Moscow agglomeration – the largest megacity in the boreal continental climate within the  
1235 PEEEX domain – demonstrates profound effect of interactions between the UHI and urban winds, known as a  
1236 cross-over effect (Varentsov et al. 2018b). The UHI creates an urban heat “dome” with near-surface air  
1237 inflow into the urban central districts and air outflow at higher levels in the atmosphere. The air uplift in the  
1238 urban dome is connected to the increase in summer rainfall at the lee side and over the central urban districts.  
1239 Stable atmospheric stratification over rural area is strengthen by the downwind air motions coming from the  
1240 urban region.

1241

1242 Atmospheric boundary layer over the Arctic Ocean has been studied on the basis of tethered sonde sounding  
1243 observations over sea ice (Palo et al., 2017) and research aircraft observations over the open ocean and sea  
1244 ice (Suomi et al., 2016). Palo et al. (2017) found that in spring and summer, the occurrence and properties of  
1245 temperature inversions were controlled by the surface melt and warm air advection rather than surface net  
1246 radiation. During snow/ice melt, temperature inversions were frequently surface-based, and equally strong as  
1247 winter inversions over the Arctic Ocean. To better understand atmospheric boundary layer processes in the  
1248 Arctic, Suomi et al. (2016) developed a method to measure wind gusts from a research aircraft. It allows  
1249 wind gust observations at altitudes not reached by traditional weather mast observations. The observed gust  
1250 factors strongly depended on the surface roughness, which differed for sea ice and the open ocean.

1251

### 1252 2.3 ARCTIC-BOREAL AQUATIC SYSTEM

1253

1254 We discuss the recent results on Arctic sea ice dynamics and thermodynamics, snow depth and sea ice  
1255 thickness, sea ice research supporting navigation, and rare elements in snow and the ocean sediments,  
1256 especially from the perspective of improvements in the observation and modelling methods (Q7, section  
1257 3.3.1). We introduce new results on the Arctic marine ecosystem and focus on the primary production and  
1258 carbon cycle (Q8, section 3.3.2.). In section 3.3.3 for the Arctic – boreal lakes and rivers, we discuss the  
1259 browning of lakes and lake sediment with a special attention on the Selenga River system of Lake Baikal  
1260 (Q9).

1261  
1262 2.3.1 Changing water systems, snow, sea ice and ocean sediments (Q7)

1263

1264 *Sea ice and thermodynamics with atmospheric and ocean dynamics*

1265

1266 Referring to the earlier discussion in section 2.2.3 on atmospheric circulation, we address here how the sea  
1267 ice dynamics closely interacts with the atmospheric and ocean dynamics. A rapid decrease in the Arctic  
1268 Ocean ice cover, particularly in the Barents and Kara Seas, has been taking place since the late 1970s  
1269 simultaneously with the cooling of winters in central Eurasia (McCusker et al., 2016). This unexpected  
1270 winter cooling is related to increasing northeasterly winds over the southeastern flank of an anomalous high  
1271 that has developed over the northwestern coast of Russia (McCusker et al., 2016; Mori et al., 2019, Räisänen  
1272 2021). However, the causality between the atmospheric circulation changes and the Arctic sea ice decrease is  
1273 debated. Observations suggests a strong correlation between these two, but climate model simulations forced  
1274 by reduced ice cover produce much weaker circulation changes than observed, resulting in only weak  
1275 cooling in central Eurasia (Mori et al., 2014, 2019; McCusker et al., 2016). This suggests that either most  
1276 models are underestimating the sensitivity of the atmospheric circulation to sea ice decrease, supported by  
1277 Romanowsky et al. (2019), or that the circulation change has not been primarily caused by the decreasing sea  
1278 ice. In the latter case, the correlation between the reduced ice cover and atmospheric circulation would  
1279 mainly reflect the effect of circulation on sea ice. In support of this, Blackport et al. (2019) showed that a  
1280 reduced sea ice coincides with an anomalous heat flux from the atmosphere to the ocean, and that on the sub-  
1281 seasonal time scale, anomalies in atmospheric circulation tend to precede rather than follow those in sea ice.  
1282 Thus, while the reduced sea ice might partly explain the observed changes in atmospheric circulation (Mori  
1283 et al., 2019), the effect of circulation on sea ice appears to be stronger than the effect of sea ice on  
1284 circulation.

1285

1286 Considering atmosphere-ice interactions, Jakobson et al. (2019) studied the linkages between sea ice  
1287 concentration (SIC), atmospheric stratification, surface roughness and wind speed at the 10-m height (W10)  
1288 and 850-hPa level (W850). In all the seasons except summer, a reduction in SIC favored reduced  
1289 atmospheric stratification and aerodynamic surface roughness, which resulted in a stronger W10. The effect  
1290 was the strongest in autumn, and positive trends in W10 and its ratio to W850 typically occurred in regions  
1291 with the strongest negative trends in SIC. The relationships were stronger on inter-annual than on sub-  
1292 seasonal time scales. Large-scale atmospheric circulation, characterized, e.g., by the Dipole Anomaly (DA),  
1293 has also contributed to sea ice dynamics. A positive polarity in DA has contributed to the recent rapid loss of  
1294 summer sea ice in the Pacific part of the Arctic Ocean by bringing warmer air masses from the south and  
1295 transporting more ice towards the north enhancing the ice-albedo feedback (Lei et al., 2016). Another  
1296 example of ice dynamics affecting the ice-albedo feedback was the weakened Transpolar Drift Stream in  
1297 summer 2013. It reduced sea ice transport out of the Arctic Ocean, and restrained ice melt because of the low

1298 air temperatures, weakened albedo feedback, and a relative small oceanic heat flux in the central Arctic (Lei  
1299 et al., 2018).

1300 Solar radiation, being the main forcing factor for a sea ice melt in summer, is difficult to parameterize in  
1301 thermodynamic models. This is due to the large variability in the optical properties of sea ice in space and  
1302 time. A two-stream model provides a time-efficient parameterization of the apparent optical properties  
1303 (AOPs) for ponded sea ice, accounting for both absorption and scattering, and has a potential to be  
1304 implemented into sea-ice thermodynamic models to explain the role of melt ponds in the summer decay of  
1305 Arctic sea ice (Lu et al. 2016). This model was used to investigate the role of solar radiation in the Arctic sea  
1306 ice during the melting season considering layers of melt ponds, underlying sea ice, and ocean beneath the  
1307 ice. It was found that the energy absorption profiles depend strongly on the incident irradiance and ice  
1308 scattering, but only weakly on the pond depth. It seems that the incident solar energy is largely absorbed by  
1309 the melt pond rather than by the underlying sea ice (Lu et al., 2018a). The model was further applied to  
1310 investigate the influence of a surface ice lid on the optical properties of a melt pond. The thickness of the ice  
1311 lid determines the amount of solar energy absorbed. Visual inspections on the color of refreezing melt ponds  
1312 also help to judge the significance of the influence of the ice lid. This will allow for an accurate estimation  
1313 on the role of surface ice lid during field investigations on the optical properties of melt ponds (Lu et al.,  
1314 2018a). The modelled pond color agrees with field observations from the Arctic sea ice in summer. The  
1315 analysis of pond color is a new potential method to obtain ice thickness in summer, however, more validation  
1316 data and improvements to the radiative transfer model would be needed (Lu et al., 2018b).

1317

#### 1318 *Snow depth/mass and sea ice thickness*

1319 Snowpack on sea ice has a crucial role in insulating the sea ice from the colder atmosphere, accordingly  
1320 reducing sea ice growth in winter, effectively reflecting the incoming solar radiation, reducing sea ice melt in  
1321 spring and summer and contributing to its formation. The replacement of snow fall by rain strongly enhances  
1322 the ice-albedo feedback in the Arctic Ocean (Dou et al., 2019). Shalina and Sandven (2018) refined the  
1323 description of snow depth on sea ice in the central Arctic, providing new snow depth data for the Arctic  
1324 marginal seas. High autumn and winter precipitation and thinning Arctic sea ice make snow-ice formation  
1325 prevalent in the Atlantic sector of the Arctic (Merkouriadi et al., 2017).

1326

1327 Advance has been made in applying thermistor string based autonomous high-resolution Snow and Ice Mass  
1328 Balance (IMB) Array (SIMBA) buoys to measure snow depth and ice thickness (Figs. 5 and 6.). SIMBA has  
1329 a lower cost, allowing deployment in large numbers (Lei et al., 2015). The determination of snow depth and  
1330 ice thickness from SIMBA temperature profiles has so far been largely a manual process. A SIMBA-  
1331 algorithm was developed to process SIMBA data automatically (Liao et al., 2018), assuming a fixed snow-  
1332 ice interface. Snow-ice formation results in snow-ice interface moving upward. The SIMBA-algorithm was  
1333 further developed to tackle the moving interfaces (Cheng et al., 2020). The developed SIMBA-algorithm  
1334 works well in cold condition for lakes and Polar Oceans. For Polar Oceans, the snow and ice are close to

1335 isothermal during summer, which prevents the identification of interfaces on the basis of the temperature  
1336 gradient. Under such conditions, thermodynamic modelling yields valuable information on snow depth and  
1337 ice thickness (Tian et al., 2017).

1338 A challenge in sea ice thermodynamic modelling is the uncertainty in the magnitude of the oceanic heat flux  
1339 at the ice base, especially for land-fast sea ice. Yang et al. (2015) applied a one-dimensional thermodynamic  
1340 model to investigate impact factors on land-fast sea ice in the East Siberian Sea. The modelled snow cover  
1341 was less than 10 cm, having a small influence on the ice thickness, but surface albedo and oceanic heat  
1342 fluxes were critical.

1343

1344 Also in the terrestrial Arctic and boreal zone, there is a need for a better efficiency and coverage of an *in-situ*  
1345 snow observation network. Snow cover and snow mass are fundamental parameters for global energy and  
1346 water cycles, and the changes in the regional snowpack have societal impacts like on amount of drinking  
1347 water or capacity for the hydropower generation (Bormann et al., 2018). Snow depth data in the Arctic  
1348 region are available from the synoptic weather stations and snow mass data are systematically collected from  
1349 the snow courses, as demonstrated in Extended Data (fig. 2) by Pulliainen et al. (2020). The use of automatic  
1350 and cost-effective measurements together with harmonized snow measurement practices is the way forward.  
1351 A survey on a harmonized snow monitoring in Europe demonstrated that crucial parameters for operational  
1352 services, such as parameters characterizing precipitating and suspended snow, are measured by 74% of the  
1353 European snow network contributors (COST Action ES1404), but the parameters characterizing the snow  
1354 microstructural properties, electromagnetic properties and composition are currently measured by only 41%,  
1355 26% and 13%, respectively, of the network contributors (Pirazzini et al., 2018). The observations at the  
1356 continental scale, so far, demonstrate a widespread snow-cover retreat since the 1970's across the Northern  
1357 Hemisphere, particularly in the Arctic (Derksen et al., 2012; Bormann et al., 2018). On the contrary, the  
1358 results from the mountains are mixed and there is no consistent picture of what is happening at the regional  
1359 scale (Bormann et al., 2018). Pulliainen et al. (2020) provided new insight into the seasonal snow mass and  
1360 its trend by using a bias-corrected GlobSnow 3.0 estimates. Pulliainen et al. (2020) is now able to  
1361 demonstrate different continental trends based on the 39-year satellite record: a decrease in North America, a  
1362 negligible trend in Eurasia, and a high regional variability in both areas.

1363 *Sea ice research supporting navigation*

1364

1365 Recent research has addressed emerging opportunities for Arctic navigation and the importance of  
1366 operational sea ice analysis. Lei et al. (2015) showed trends along the Arctic Northeast Passage (NEP) and  
1367 demonstrated an increase in the spatially-averaged length of the open period (the ice concentration less than  
1368 50%) from 84 days in the 1980's to 114 days in the 2000s. The summer sea ice along the High-Latitude Sea  
1369 Route (HSR) north of the eastern Arctic islands has decreased during the last decade, with the ice-free period  
1370 reaching 42 days in 2012. The HSR avoids shallow waters along the coast, which easier the access to for  
1371 deeper-draft vessels (Lei et al., 2015). Considering operational sea ice analyses for the Bohai Sea, work has

1372 been done to combine thermodynamic modelling and Earth Observation (EO) data from synthetic aperture  
1373 radar (SAR) and microwave radiometers (Karvonen et al., 2017). The SAR-based discrimination between  
1374 sea ice and open-water works well, and areas of thinner and thicker ice can be distinguished. However, a  
1375 larger comprehensive training dataset is needed to set up an operational algorithm for the estimation of sea  
1376 ice concentration and for the weighting scheme for sea ice thickness (Karvonen et al., 2017).

1377

1378 Multi-decadal Arctic sea-ice state estimates are important for the strategic planning of Arctic navigation.  
1379 These estimates are usually based on climate models with a thermodynamic-dynamic sea-ice models. An up-  
1380 to-date assessment of large-scale sea-ice models was with the aid of sea-ice models as a climate model  
1381 component, a comprehensive review was carried out by Leppäranta et al. (2020). Specifically, Uotila et al.  
1382 (2015) found that a model with the subgrid-scale sea-ice thickness distribution reproduces more realistic sea  
1383 ice and upper ocean, due to better captured spring evolution, than a model with just single sea-ice thickness  
1384 category. In terms of validity of initial conditions for multi-decadal predictions, Uotila et al. (2019) analyzed  
1385 a set of ocean reanalysis products, including Arctic sea ice, and found that the multi-model set mean is a  
1386 useful product as a state estimate. This finding increases confidence toward the use of the combination of  
1387 ocean reanalysis for both initialization of multi-decadal predictions and analysis of multi-decadal variability.

1388

1389 *Ocean floor and Sediments: composition and fluxes*

1390

1391 A significant content of illite and muscovite among layer silicates in most of the ice-rafted sediments  
1392 samples taken from selected Arctic regions suggests that sources of the sedimentary material are mainly  
1393 mineralogically similar to modern bottom sediments of the East Siberian and Chukchi seas, as well as  
1394 presumably sediments of the eastern Laptev Sea. A significant kaolinite fraction in the samples from the  
1395 North Pole area can be caused by the influx of ice-rafted fine-grained sedimentary material from the  
1396 Beaufort or Chukchi seas, where kaolinite is supplied from the Bering Sea. The samples contained variable  
1397 proportions of erosion products of both mafic and felsic magmatic rocks and/or sufficiently mature  
1398 sedimentary rocks (Maslov et al., 2018a).

1399

1400 Quantification of CH<sub>4</sub> sources is fundamental information for the climate change mitigation (Fletcher and  
1401 Schaefer 2019). Methane stored in ocean floor reservoirs can reach the atmosphere in the form of bubbles or  
1402 dissolved in water. Methane hydrates could destabilize with rising temperatures, further increasing  
1403 greenhouse gas emissions in a warming climate. Subsea permafrost and hydrates in the East Siberian Arctic  
1404 Shelf (ESAS) are acting as a substantial carbon pool, and source of methane to the atmosphere. Annual  
1405 methane emissions of the region varies from 0.0 to 4.5 Tg CH<sub>4</sub> yr<sup>-1</sup> estimated by Berchet et al. (2016).  
1406 Yasunaka et al. (2018) estimated the monthly air-sea CO<sub>2</sub> fluxes in the Arctic Ocean and adjacent seas  
1407 located north of 60 degrees N for the period 1997 2014 and ended up to a net annual Arctic Ocean CO<sub>2</sub>  
1408 uptake of 180 ± 130 Tg C per year.

1409

1410 The Zeppelin Observatory data for 2014 suggest that the CH<sub>4</sub> fluxes from the Svalbard continental platform  
 1411 are smaller than 0.2 Tg yr<sup>-1</sup>. All estimates are in the lower range of values reported earlier (Pisso et al.,  
 1412 2016). Platt et al. (2018) reported a potential region with high ocean-atmosphere CH<sub>4</sub> flux located north of  
 1413 Svalbard, but addressed that at the time of the measurements the meteorological conditions were unique,  
 1414 including a short episode of the highly sensitive to emissions over an active seep site without a sensitivity to  
 1415 land-based emissions.

1416  
 1417 *River runoff affecting the hydrological processes at coastal marine environments*  
 1418

1419 The Arctic Ocean, including the Hudson Bay, receives 55.6 % of its river inflow from Russia, mostly via 19  
 1420 large rivers (Shiklomanov and Shiklomanov, 2003). This freshwater inflow of approximately 2920 km<sup>3</sup> per  
 1421 year (Shiklomanov, 2008) is associated with large sediment and heat transports, which together affect the  
 1422 hydrography, marine climate and ecosystems across the Siberian shelf seas (Magritsky et al., 2018). A major  
 1423 part of seasonal and interannual variations in the river runoff is anthropogenic, due to regulation in large  
 1424 reservoirs (Georgiadi et al., 2016). In addition, Magritsky et al. (2018) detected an increased runoff trend of  
 1425 5-10 %, compared to a reference period of 1936 to 1975, in most of the major Russian rivers discharging into  
 1426 the Arctic Ocean. This trend is mostly due to a climate-induced increase since the second half of 1980's  
 1427 (Magritsky et al., 2018). However, due to gaps in the monitoring programs, these estimates have a large  
 1428 uncertainty: focusing on river discharges from the six largest Eurasian rivers to the Arctic Ocean, estimates  
 1429 of the increase range from 7% (Peterson et al., 2002) to 1.5 % (Shiklomanov and Lammers, 2009).

1430  
 1431 Permafrost thawing has resulted in releases of old carbon storages, but so far there is no clear evidence on  
 1432 the impact of permafrost thawing on the net emissions of CO<sub>2</sub> and CH<sub>4</sub> to the atmosphere (IPCC, 2019). A  
 1433 potential explanation of no or weak net increase is that a fraction of the released methane has been taken by  
 1434 rivers instead of emitted to the atmosphere. Increased amounts of organic carbon in rivers impact the  
 1435 regional and global biochemical and methane cycles (Shakhova et al., 2007; Wild et al., 2019). With the  
 1436 accelerating permafrost thaw, also the atmospheric emissions are expected to increase, in particular for CO<sub>2</sub>  
 1437 but also for CH<sub>4</sub>. Expected future changes in river ice regime are consistent with the expected changes in the  
 1438 duration of the cold season and accumulated negative air temperatures. Significant changes are expected for  
 1439 the rivers in the Kola Peninsula and the lower reaches of the rivers Northern Dvina and Pechora, whereas the  
 1440 lowest changes are expected for the central parts of Eastern Siberia (Agafonova et al., 2017). Due to  
 1441 anthropogenic activities (above all industry, municipal services, and filling of reservoirs), water withdrawal  
 1442 from Russian Arctic rivers and related groundwater systems is approximately 20.6 km<sup>3</sup> per year, and it is  
 1443 expected to increase to 37 km<sup>3</sup> per year by 2025 to 2030 (Magritsky et al., 2018). Features of these changes  
 1444 at the marine margin of the Lena River delta are different compared to changes in the delta head area.

1445  
 1446 The hydrological representativeness of a glacier is a new characteristic, and of practical importance for  
 1447 basin-wide tasks of hydrology and glaciology. For its evaluation, it is proposed to replace the seasonal air

1448 temperatures with the glacier summer mass balance (BS) or to include BS in the multiple regression  
 1449 equations for calculating the runoff of rivers fed by melting of snow and ice. This method can be  
 1450 recommended for at least of some glaciers in the existing network of the World Glacier Monitoring Service  
 1451 (WGMS) (Konovalov et al., 2019).

1452

### 1453 2.3.2 Marine ecology (Q8)

1454

#### 1455 *Living marine organisms weaken or even subdue CO<sub>2</sub> accumulation*

1456 The important climatological role of the world's oceans is to reduce the CO<sub>2</sub> accumulation into the  
 1457 atmosphere through its absorption. This mechanism is ordinarily viable as the partial pressure of dissolved  
 1458 CO<sub>2</sub> in marine surface waters is less than the content of CO<sub>2</sub> in the overlying atmosphere. Due to the organic  
 1459 pump, a net draw down of atmospheric CO<sub>2</sub> into the ocean is put into effect. It proceeds in the process of  
 1460 sinking of particulate organic carbon of algal origin: organically bound CO<sub>2</sub> is released through  
 1461 remineralization and further accumulated in the deep ocean. In contrast, owing to the processes of carbonate  
 1462 counter pump, CaCO<sub>3</sub> is exported downward and, at depth, dissolves causing a net release of CO<sub>2</sub> to the  
 1463 atmosphere (Balch et al., 2016). However, there are living marine organisms that are able to weaken or even  
 1464 subdue CO<sub>2</sub> accumulation, at least within their habitat. Among this group of marine organisms, the leading  
 1465 role belongs to coccolithophores. Among marine bio systems, coccolithophores (class Primnesiophyceae) are  
 1466 most productive calcifying algae (Taylor et al., 2017). They both produce particulate inorganic carbon (in the  
 1467 form of calcite) and promote the increase of CO<sub>2</sub> partial pressure ( $p\text{CO}_2$ ) in the ambient marine surface  
 1468 waters. Thus, the biological activity of coccolithophores can exercise a direct influence on both the CO<sub>2</sub> flux  
 1469 exchange at the atmosphere-ocean interface and the marine carbonate chemistry system (CCS). The rain  
 1470 ratio, i.e. the ratio of particulate inorganic carbon to organic carbon, determines the intensity and direction of  
 1471 CO<sub>2</sub> flux at the atmosphere-ocean interface. In the case of coccolithophores, the rain ratio is above unity  
 1472 within their habitat area, which potentially can have climatic consequences but also drive alterations in  
 1473 marine CCSs (Balch 2018).

1474

1475 *Emiliania huxleyi* is the most widespread coccolithophorid algal species in Earth's oceans, which, in light of  
 1476 the above, naturally explains why this is one of the best-studied marine algae. Of all other coccolithophores,  
 1477 *E. huxleyi* is probably the most successful in forming extensive blooms in world-wide marine waters ranging  
 1478 from oligotrophic to eutrophic. Unlike diatoms and dinoflagellates, this alga is phenomenally immune to  
 1479 both light-limitation and very high light intensities. As high levels of incident light/irradiance enhance  
 1480 calcification (which is predominantly a light-dependent reaction), it is supposed that the calcification  
 1481 machinery enables *E. huxleyi* cells to resist photodamage through dissipating excess energy. This specialty is  
 1482 important in case of nutrient-depleted waters, especially in combination with the high affinity of *E. huxleyi*  
 1483 for nutrients including nitrogen but especially phosphorous. The property of both mixotrophic nutrition, and  
 1484 resistance, at least partial, to zooplankton grazing and virus attacks (due to cell's coverage by calcite  
 1485 scales/coccoliths) contribute to this alga ability to sustain a variety of unfavorable conditions and retain



1486 steadfastly its ecological niche (Godrijan et al, 2020). Thus, the elaborate biology of *E. huxleyi* cells imparts  
 1487 to them the intrinsic and rather rare property of pursuing growth-maximizing and loss-minimizing life  
 1488 strategies. This property reveals itself through multiple manifestations, two of which are vastness and  
 1489 sustainability of *E. huxleyi* bloom areas. A typical bloom surface is not less than thousands of square  
 1490 kilometers, but in many marine environments it is far larger (Kondrik et al., 2018b). For example, in some  
 1491 years, the value of  $S$  in the North and Norwegian Sea can be well above 100 000 km<sup>2</sup>, in the Bering Sea  
 1492 maximum bloom area ( $S$ ) values were registered at 250 000 km<sup>2</sup>, particularly large *E. huxleyi* bloom areas  
 1493 (up to 380 000 km<sup>2</sup>) were observed in the Barents Sea (Kondrik et al., 2017). Within the subpolar and polar  
 1494 zones of the Northern Hemisphere, in the waters around the Great Britain, in the North, Norwegian,  
 1495 Labrador, Greenland, Barents, and Bering seas *E. huxleyi* blooms occur annually although with largely  
 1496 varying intensity (Pozdnyakov et al., 2017). The duration of blooms in the Northern Atlantic and the Barents  
 1497 Sea is on average about three-four weeks. The moment of onset of the *E. huxleyi* bloom area maximum shifts  
 1498 from June-July to September-October for the seas located at the temperate, subpolar and polar latitudes of  
 1499 the Northern Hemisphere, respectively. This sequence mimics the flow pattern of the Gulf Stream. In the  
 1500 Bering Sea, the temporal pattern of  $S$  variations reveals two periods (1998-2001 and 2018-2020) of  
 1501 extraordinary intense *E. huxleyi* outbursts. It is hypothesized that this phenomenon was driven by massive  
 1502 advection of Fe-depleted North Pacific waters due to a significant weakening of the Alaskan Current. The  
 1503 latter is supposed to be a teleconnected aftermath of exceptionally strong El Niño events in 1996-1997 and  
 1504 2017, respectively (Pozdnyakov et al., 2020).

1505  
 1506 Satellite-borne estimations made during 1998-2018 showed that *E. huxleyi* outbursts resulted in a release of  
 1507 inorganic carbon (PIC) in the form of CaCO<sub>3</sub> in surface waters in amounts ranging from ~10 to several  
 1508 hundreds of kilotons. In the Barents Sea, the released PIC content varied between ~100 kt and 250-300 kt,  
 1509 whereas in the Bering Sea, during the two periods of exceptional activity, the PIC content was as high as 500  
 1510 kt (Kondrik et al., 2017). There is ample evidence that the release of PIC was accompanied by a significant  
 1511 increase in CO<sub>2</sub> partial pressure ( $\Delta p\text{CO}_2$ ) within the bloom area: between 1998 and 2016, the mean and  
 1512 maximum values of the ratio  $\Delta p\text{CO}_2/(\Delta p\text{CO}_2)_{\text{background}}$ , varied in the ranges of ~ (20-40)%, and ~(30- 60)%,  
 1513 respectively. The highest numbers were registered in the Bering and Barents seas (Kondrik et al., 2018a;  
 1514 2019). Also, there is space borne evidence for the atmospheric columnar  $\Delta\text{CO}_2$  enhancement ( $\Delta\text{CO}_2$ )<sub>atm</sub> over  
 1515 *E. huxleyi* blooms: numerous case studies in the aforementioned North Atlantic seas as well as in the Barents  
 1516 and Black seas proved that ( $\Delta\text{CO}_2$ )<sub>atm</sub> could reach 2-3 ppm (Kondrik et al., 2019; Morozov et al., 2019).

1517  
 1518 Notwithstanding the remarkable ability of *E. huxleyi* to grow under conditions unfavorable for algae of other  
 1519 functional groups (e.g. diatoms, flagellates, cyanobacteria), a highly irregular pattern of the registered two-  
 1520 decadal (1998-present) time series of  $S$ , PIC, and  $\Delta p\text{CO}_2$  are indicative of susceptibility of this alga outbursts  
 1521 to environmental conditions (Nissen et al., 2018; Kazakov et al., 2019; Silkin et al., 2019). Statistical  
 1522 prioritization of non-biogenic forcing factors (FFs) shows that the latter are sea- and time-period specific  
 1523 (Pozdnyakov et al., 2019). Thus, in the Barents Sea, sea water temperature (SWT) is the highest-ranked FF,

1524 followed by PAR (photosynthetic active radiation). In the Bering Sea, beyond the aforementioned periods  
 1525 (1998-2001 and 2018-present), sea surface salinity (SSS) is the FFs leader, with PAR as a runner up,  
 1526 whereas SWT is only third in the row. Although these assessments are done without explicitly considered  
 1527 nutrients concentrations (NCs), implicitly NCs were among the FFs. Indeed, arguably, variations in SWT,  
 1528 SSS, CHL, MLD, and surface current speed/advection (tested as FFs) indirectly account for the variations in  
 1529 NCs as well in such CCSs parameters as alkalinity and basicity (Durairaj et al., 2015; Pozdnyakov et al.,  
 1530 2019, and references therein).

1531

1532 In the long run, the steady accumulation of CO<sub>2</sub> into the atmosphere should closely be considered (Rivero-  
 1533 Calle et al., 2015). The action of a rising atmospheric CO<sub>2</sub> concentration is expected to proceed through a  
 1534 number of direct and indirect interactions (Fig. 7), both of which should ultimately cause alterations in the  
 1535 rain ratio. An increase in the atmospheric CO<sub>2</sub> concentration leads to the rising of the global temperature, and  
 1536 further to the strengthening of stratification, intensification of irradiance within the euphotic zone and cutting  
 1537 of nutrient fluxes from below. Although increases in CO<sub>2</sub> fluxes to the surface ocean cause a reduction of pH  
 1538 and CO<sub>3</sub><sup>2-</sup> levels in water, the large pool of HCO<sub>3</sub><sup>-</sup> remains to support the calcification machinery. Thus, it  
 1539 will lead to the establishment of environmental conditions unfavorable for non-calcifying phytoplankton  
 1540 (NCP), but beneficial (or at least enduring) for coccolithophores in general and *E. huxleyi* specifically. The  
 1541 reduction of NCP and uncontested growth of *E. huxleyi* drives a further reduction of dissolved CO<sub>2</sub>  
 1542 consumption by other groups of phytoplankton, increase in *p*CO<sub>2</sub> in the surface ocean and intensification of  
 1543 CO<sub>2</sub> fluxes into the atmosphere. Concurrently, through a system of feedback interactions, alterations in the  
 1544 rain ratio are bound to affect the carbon fluxes at the water-atmosphere interface. Therefore, the scenario of  
 1545 further increases atmospheric CO<sub>2</sub> concentration in the future, in all probability, implies a vaster proliferation  
 1546 of *E. huxleyi* in the world's oceans.

1547

1548 In combination with statistic-based-mathematical models of *E. huxley* blooms (Pozdnyakov et al., 2019), the  
 1549 available IPCC climate models permit mid-term projections of the forthcoming changes (Gnatiuk et al.,  
 1550 2020). However, our knowledge on the reciprocal influence of climate change and both the structure and  
 1551 functioning of marine ecosystems (even at the level of primary producers!) is still insufficient to confidently  
 1552 prognose the future dynamics of the *E. huxleyi* phenomenon. More studies are required even to fully  
 1553 understand the mechanism of intracellular light-dependent reaction of calcification, its dependency on both  
 1554 seawater carbonate chemistry and environmental FFs (Vihma et al., 2019). Creation of respective  
 1555 multidecadal databases (as in Kazakov et al., 2019) as well as further delivery of satellite and *in*  
 1556 *situ*/shipborne/laboratory data are necessary to improve our capacity to assess with certainty the  
 1557 climatological and ecological role of *E. huxleyi* blooms on regional and global scales (Fig. 7).

1558

1559 2.3.3 Lakes and rivers (Q9)

1560 *Organic carbon in lakes*

1561

1562 Spatial variability, an essential characteristic of lake ecosystems, has often been neglected in field research  
1563 and monitoring. The detected spatial "noise" strongly suggests that besides vertical variation also the  
1564 horizontal variation should be considered in the ecosystem monitoring and, most importantly when the role  
1565 of dissolved organic carbon (DOC) on the CO<sub>2</sub> flux is estimated (Manasypov et al., 2015; Leppäranta et al.,  
1566 2018). In natural waters with an increasing level of colored dissolved organic matter (CDOM) concentration,  
1567 the water color is shifted towards brown. The key "permanent" landscape variables, the coverage by lakes  
1568 and peatland in the catchment area can be strongly correlated with lake elevation above the sea level. A high  
1569 lake coverage indicates a low CDOM concentration, while a high peat coverage indicates the opposite  
1570 (Arvola et al., 2016). For example in Finland, recent results from inland water studies have not shown any  
1571 overall, consistent large-scale changes in CDOM concentrations over the last 101-year period (Arvola et al.,  
1572 2017). Rather, CDOM changes in individual lakes have been related to changes in land use in the drainage  
1573 basin. Manasypov et al. (2015) reported results from Siberian lakes, representing a discontinuous permafrost  
1574 zone, and addressed that although the concentration of most elements in the lakes are lowest in spring, the  
1575 maximal water coverage of land made it as an significant reservoir of DOC. The soluble metals in the water  
1576 column that can be easily mobilized to the hydrological network.

1577

1578 In very shallow freezing lakes, the volume liquid water is much reduced due to ice growth, and rejection of  
1579 nutrients and pollutants in the ice growth causes major enrichment of the water body. This has major  
1580 implications to the ecosystem of these lakes (Yang et al., 2016; Song et al., 2019). Freezing rejects some 80-  
1581 90 % of the impurities in freshwater lakes. On the other hand, ice cover accumulates atmospheric deposition  
1582 over several months but releases them into the water body within one month's melting phase. Rejection of  
1583 nutrients and pollutants in lake ice growth causes major enrichment of the water body in shallow lakes and  
1584 notable increases in nutrient concentrations in a shallow lake during seasonal ice growth (Fang et al., 2015).

1585

#### 1586 *Lake carbon balance*

1587

1588 Arctic and boreal lakes are an important natural source of CH<sub>4</sub> into the atmosphere (Bastviken et al, 2011).  
1589 Methane is produced mainly in the bottom sediments and/or hypolimnion, where most of the anaerobic  
1590 decomposition of organic matter take place, and then is either oxidized to CO<sub>2</sub> in the water column or  
1591 emitted to the atmosphere. At Kuivajärvi, a typical meso humid lake located in Southern Finland, it was  
1592 found that 91% of available CH<sub>4</sub> was oxidized in the active CH<sub>4</sub> oxidation zone during hypolimnetic hypoxia  
1593 (Saarela et al., 2020). In warm springs, the early onset of thermal stratification with cold and well-  
1594 oxygenated hypolimnion delays the period of hypolimnetic hypoxia and thus limiting the production of  
1595 methane. At Kuivajärvi measured CO<sub>2</sub> fluxes (F-CO<sub>2</sub>) showed that the lake acted as net source of carbon  
1596 during two open-water periods (Mammarella et al., 2015). During daytime, with typically high wind speeds,  
1597 shear-induced water turbulence controls the water-air gas transfer efficiency, thus enhancing the vertical  
1598 diffusive fluxes across the water-air interface. However, during calm nighttime conditions, buoyancy-driven  
1599 turbulent mixing, associated with penetrative cooling of surface water, controls the gas exchange, and simple

1600 wind speed-based transfer velocity models strongly underestimate F- CO<sub>2</sub> (Mammarella et al., 2015). Kiuru  
 1601 et al. (2018) developed a model simulating CO<sub>2</sub> dynamics of a boreal lake in warming climate. The  
 1602 simulations for 2070-2099 showed a 20–35% increase in the CO<sub>2</sub> flux from the lake compared to the  
 1603 reference period of 1980–2009.

1604

#### 1605 *Lake ice cover*

1606 Wei et al. (2016) studied the Lake Inari (67.14 N, 25.73 E), Finnish Lapland, in winters 1980/1981 -  
 1607 2012/2013, and observed an increasing trend in the air temperature during the freezing season, associated  
 1608 with an increasing trend in the water precipitation during winter. Low temperatures with less precipitation  
 1609 lead to the formation of columnar ice, while strong winds together with heavy snowfall favored granular ice  
 1610 formation. Karetnikov et al., (2017) analyzed long-term ice conditions in Lake Ladoga, Russia, for the period  
 1611 of 1913–2015 and showed that the mean freezing and breakup dates were November 26 and May 15,  
 1612 respectively, and that the annual frequency of complete freeze over of the lake was 0.83. The period from  
 1613 1990 to present was much milder than the preceding years. The annual increase in the ice concentration  
 1614 depended on the accumulated freezing-degree-days (AFDD) and the hypsographic curve, while the ice  
 1615 thickness increased with the square root of AFDD.

1616

1617 An analysis of a Siberian thermokarst lake located in the Lena River Delta, characterized as a floating ice  
 1618 lake, showed that the temporal dynamics and magnitude of heat fluxes and surface energy balance closures  
 1619 are substantially different depending on lake surface conditions (Franz et al., 2018). Sensible heat and latent  
 1620 heat fluxes, modelled using available heat bulk transfer models (Woolmay et al, 2015; Verburg and  
 1621 Antenucci, 2010; Andreas et al, 2002), tend to underestimate the measured fluxes and show less variability  
 1622 over freezing ice cover, melting ice in Spring, as well as over open water in Summer. However, the  
 1623 performance of these models depends also on the accuracy of meteorological and hydrological input  
 1624 parameters, which should be carefully measured especially during challenging winter conditions.

1625

1626 The seasonal lake ice cover is a sensitive indicator of climate variations in the Arctic (Kirillin et al., 2012;  
 1627 Leppäranta, 2015). To work more on this question, Lake Kilpisjärvi (surface 37.1 km<sup>2</sup>, max depth 57 m), a  
 1628 tundra lake in northern Finland, has been under an intensive ice-related field programs in recent years. The  
 1629 research covered the whole year but was focused on the melting period in May–June. The heat budget over  
 1630 the ice season was dominated by the radiation balance. Turbulent fluxes were significant before the freeze-up  
 1631 in fall, but in the ice season they were small. The evolution of ice thickness served as a very good  
 1632 approximation to the total surface heat flux (Leppäranta et al., 2017) (Fig. 8). In the melting stage, solar  
 1633 radiation, the strongest forcing of the water body beneath ice cover, breaks the stability and initiates  
 1634 convective turbulent mixing. This brings heat from the deeper water to ice, enhancing melting at the ice  
 1635 bottom (Kirillin et al., 2018). Thus, the common assumption of the heat flux from the water to ice to be due  
 1636 to molecular conduction does not hold in the melting stage but it is much higher. The ice–water interaction  
 1637 under lake ice has not been well covered in earlier studies of ice growth and melting.

1638

1639 The ice melting process was studied in detail in Lake Kilpijärvi. The melting progressed in the upper and  
1640 lower surfaces and in the interior, with proportions depending on the solar flux and optical properties of the  
1641 ice, and were therefore case-dependent. About one-third of the solar flux that penetrated the ice returned to  
1642 ice bottom, providing heat for melting. This was consistent with the under-ice results by Kirillin et al. (2018).  
1643 In 2013 a rapid ice breakage event completed the ice breakup in a short time interval, with final breakage at  
1644 the ice porosity 40-50%. A lake ice melting model should include the thickness and porosity of ice, with  
1645 porosity connected to an ice strength criterion (Leppäranta et al., 2019).

1646

#### 1647 *Lake Baikal and Selenga River delta*

1648 The Selenga River, the main tributary of Lake Baikal, has a catchment area of 450 000 km<sup>2</sup> in the boundary  
1649 region between Northern Mongolia and Southern Siberia. This area is well known by its climate, land use  
1650 and dynamic socioeconomic changes which might have negative impacts on the ecosystems of Lake Baikal  
1651 and thus was selected as PEEEX field laboratory within PEEEX subprogram Selenga-Baikal Network  
1652 ([www.atm.helsinki.fi/peex/index.php/baikal-selenga-network-basenet](http://www.atm.helsinki.fi/peex/index.php/baikal-selenga-network-basenet)). In the recent past, hydroclimatic  
1653 development together with land use changes led to a contaminant influx from mining areas and urban  
1654 settlements increased. Additional hydrological modifications due to the construction of dams and  
1655 abstractions/water diversions from the Selenga's Mongolian tributaries could lead to additional alterations  
1656 (Karthe et al., 2017b). In addition to Selenga River, a key issue for an improved understanding of regional  
1657 impacts of the environmental change is to disentangle the influence of climate change from that of other  
1658 pressures within the catchment (Lychagin et al., 2017). The PEEEX subprogram Selenga-Baikal Network  
1659 aims at integrated field-based and modeling knowledge to develop basin-wide conceptual framework of  
1660 riverine fluxes (Kasimov et al., 2017a; Karthe et al., 2019).

1661

1662 As a PEEEX field laboratory, regional large-scale assessments made it possible to predict the comprehensive  
1663 nature of hydrological and geochemical changes driven by climatic processes and human impacts. Heavy  
1664 metals in water and sediments (Kasimov et al., 2020a, 2020b) and fish communities (Kaus et al., 2017) were  
1665 measured since 2011 in over 50 locations around the catchment. The mining zones are potential hotspots for  
1666 increasing metal loads to downstream river systems. Several metals (Al, Cd, Fe, Mn, Pb and V) are exported  
1667 from mining sites to the downstream river system, as shown by net increasing mass flows. Based on a novel  
1668 partitioning coefficient approach (Table. 2), contrasting patterns with domination of both particulate and  
1669 dissolved phases in different parts of the basin were found. Such heterogeneity in the metal partitioning is  
1670 likely to be found in many large river systems.

1671

1672 Multi-scale modeling ranged from the basin wide (Malsy et al., 2017; Frolova et al., 2017) to specific sub-  
1673 regions, such as particular segments of the river system (Kaus et al., 2017; Thorslund et al., 2017; Garmayev  
1674 et al., 2019) or its delta (Chalov et al., 2017a, 2017b; Shinkareva et al., 2019), and identified reactions of  
1675 hydrogeochemical pathways on climate change. The mean flow reduction in the Selenga River was 3-5%

1676 during 2020's to 2030's and 4-25% during 2080's to 2090's, being a crucial driver of ongoing and future  
1677 hydrogeochemical changes. Increases in temperatures with permafrost thaw and the expansion of  
1678 agricultural, mining and urbanization processes may induce up to a 6% increase in the particulate modes and  
1679 3% in the dissolved modes of some metals in the river system (Chalov et al., 2018). Possible changes in the  
1680 number or magnitude of high-flow events, caused by climatic or other anthropogenic factors, could influence  
1681 the total sediment deposition, which was primarily found to occur during relatively short high-flow events.  
1682 Such potential changes have important implications to the possible spreading of polluted sediments (Pietron  
1683 et al., 2015) and their storage in the Selenga River Delta, which is an important wetland region forming the  
1684 geochemical barrier which mitigate pollution of Lake Baikal by riverine fluxes (Voropay and Kichigina,  
1685 2018, Chalov et al., 2015). The Selenga delta region sequester various metals bound to Selenga River  
1686 sediments (Chalov et al., 2015, Pietron et al., 2018). The water shortage decreases the processes of  
1687 suspended sediment retention in the delta. The seasonal hydrogeochemical patterns are explained by wetland  
1688 inundation during floods and channel erosion or Baikal wind surge during low flow periods (Chalov et al.,  
1689 2017a, 2017b).

1690

#### 1691 *Asian water lakes*

1692

1693 The largest internal drainage basins in the world are located in Central Asia, with a limited availability of  
1694 both surface and groundwater (Karthe et al., 2017a). Since the twentieth century, water resources of this  
1695 region have been over exploited and, for example, from small Mongolian headwater streams to the mighty  
1696 Aral Sea, surface waters have been partially desiccated. It seems that the implementation of the Integrated  
1697 Water Resources Management and water-food-energy nexus approaches would lead to a more  
1698 environmental-friendly future (Karthe et al., 2017). The lake-rich Qinghai-Tibet Plateau (QTP) has recently  
1699 been identified as the Third Pole of the Earth. Due to its high elevation and unique climate, QTP affects the  
1700 global and local climate and played an important role on the Central and Southern Asian water cycle (Zhang  
1701 et al., 2018). Lake-atmosphere interactions have been quantified over open-water periods, yet little is known  
1702 about the lake ice thermodynamics and heat and mass balance during the ice-covered season. A modelling  
1703 study for a thermokarst lake in the QTP was performed (Huang et al., 2019a). Strong diurnal cycles were  
1704 seen for all surface heat fluxes. The ice mass balance was dominated by the growth and melt at the base, but  
1705 the surface sublimation was also crucial for the ice loss, accounting for up to 40% of the maximum ice  
1706 thickness and 41% of the lake water loss during the ice-covered period. The strong penetration of solar  
1707 radiative flux is the dominant contributor to the high value of upward sensible heat flux at ice bottom,  
1708 resulting in a relatively thin ice cover compared with equivalent high-latitude climate.

1709

## 1710 2.4 SOCIETY

1711

1712 The anthropogenic impact has been addressed as one of the PEEEX themes for the society system. The  
 1713 discussion on the mitigation and adaptation, including urban infrastructure design and risk assessment, are  
 1714 addressed in this context (Q10, section 2.4.1). The social transformations are discussed in terms how local  
 1715 reindeer grazing interacts with the environment (Q11 section 2.4.2). The adaptive capacity of the Northern  
 1716 societies depends on their environment, demographic structure and economic capacity, and the  
 1717 environmental hazards and environmental health under changing climate are the key research areas in this  
 1718 context (Q12 section 2.4.3.).

1719

#### 1720 2.4.1. Anthropogenic impact (Q10)

1721

##### 1722 *Mitigation*

1723 Arctic climate change generates a need for long-term planning and development of new socio-economic  
 1724 infrastructures, such as dams, bridges, roads and transnational and regional energy networks. For this task,  
 1725 new climate-based forecasting tools, cost and operational risk estimates as well as other methods and tools  
 1726 for an infrastructure and urban design are needed. As an example, engineering calculations for maximal  
 1727 discharges were provided for the Nadym River in Russia (Shevnina et al., 2017). Badina (2018) introduced a  
 1728 method for the natural risk assessment by using indices based on socioeconomic potential data and spatial  
 1729 distribution of natural hazards. This method has been tested and used to identify the most vulnerable  
 1730 municipalities in South Siberia. Another example of new methods is a “Green Factor tool” to increase the  
 1731 share and effectiveness of green areas in urban environments and cities. An ambitious target set in this tool  
 1732 could encourage or force urban developers to aim higher with the planning of green areas and construction,  
 1733 however the existing regulations challenge the use of this approach (Juhola, 2018).

1734

1735 The energy production is of fundamental importance for the society functions, and new clean energy  
 1736 technologies are needed for hindering the climate change. The potential of hydropower production under  
 1737 probabilistic projections of annual runoff rate and future changes in the potential hydropower production  
 1738 need to be evaluated (Shevnina et al., 2019). All the Nordic countries are vulnerable to various degrees to  
 1739 potential cross-border impacts, due to their energy sectors being highly globalized and interconnected.  
 1740 However, cross-border impacts are not yet properly included in Nordic climate assessments or energy  
 1741 strategies. The EU’s new Green Deal is pivotal in this respect, as for the first time emissions along the whole  
 1742 supply chain (oil, gas, coal, renewables) become under scrutiny and as part of a normative governance.  
 1743 Therefore, policy makers and energy planners should be assisted in making comprehensive vulnerability  
 1744 assessments that address both domestic and international climate risks (Groundstroem and Juhola, 2019).

1745

#### 1746 2.4.2 Environmental impact (Q11)

1747

1748 *Reindeer (Rangifer tarandus L.) grazing and ground vegetation structure and biomass*

1749

1750 Reindeer (*Rangifer tarandus L.*) grazing in the North affects the ground vegetation structure and biomass and  
 1751 cover of lichens. It seems that reindeers affect GHG fluxes from the forest field layer. Grazing changes affect  
 1752 the vegetation composition and thereby emissions (Köster et al., 2018). Köster et al. (2017) provided detailed  
 1753 information on soil CO<sub>2</sub> effluxes, which were mostly affected by the year of measurement, time of  
 1754 measurement, soil temperature and also by the management, resulting in higher CO<sub>2</sub> emissions on the grazed  
 1755 areas. Soil moisture content did not affect the soil CO<sub>2</sub> efflux. For example, in the Finnish Lapland the  
 1756 average soil CO<sub>2</sub> efflux values were significantly higher in 2014 compared with 2013, mainly due to  
 1757 differences in the soil temperature at the beginning of the season (Köster et al., 2017). Furthermore, grazing  
 1758 significantly decreased the biomass and cover of lichens and also the amount of tree regeneration. In a  
 1759 subarctic mature pine forest, grazing did not affect the soil temperature or soil moisture. No statistically  
 1760 significant effect of grazing on the soil CO<sub>2</sub> efflux, soil C stock or soil microbial C biomass was found. The  
 1761 soil microbial N biomass was significantly lower in the grazed areas compared to the non-grazed areas. It  
 1762 seems that in the boreal subarctic coniferous forests, grazing by reindeer can be considered as "C neutral"  
 1763 (Köster et al., 2015). There is also indication that reindeer grazing affects the boreal forest soils e.g. their  
 1764 fungal community structure and litter degradation (Santalahti et al., 2018).

1765

#### 1766 2.4.3 Natural hazards (Q12)

1767

1768 Under this theme, the PEEEX research has so far focused on environmental health issues. These include  
 1769 diseases, impact of UV radiation, and air pollution in urban environments. The spread of diseases caused by  
 1770 living pathogens is basically determined by environmental conditions. Medico-geographical assessments are  
 1771 usually based on identification of the links between the spread of diseases and factors of the geographical  
 1772 environment.

1773

#### 1774 *Naturally-determined diseases*

1775 Climatic factors are deemed among the main determinants for the spread of naturally-determined diseases  
 1776 (Malkhazova et al., 2018). Emerging zoonotic diseases are expected to be particularly vulnerable to climate  
 1777 and biodiversity disturbances. Anthrax is an archetypal zoonosis that manifests its most significant burden on  
 1778 vulnerable pastoralist communities. Ezhova et al. (2021) investigated the dynamics of environmental factors  
 1779 that led to an anthrax outbreak in Yamal Peninsula, Siberia, during 2016. They found that the local  
 1780 permafrost was thawing rapidly for the last 6 years before the outbreak, supporting the hypothesized role of  
 1781 permafrost thaw in triggering this outbreak, and concluded further that the spread of anthrax was likely  
 1782 intensified by the extremely dry summer of 2016 in the region. Overall, the recent findings highlight the  
 1783 significance of warming temperatures for anthrax ecology in northern latitudes, and suggest potential  
 1784 mitigating effects of interventions targeting megafauna biodiversity conservation in grassland ecosystems  
 1785 and animal health promotion among small to midsize livestock herds (Walsh, et al., 2018). Equally important  
 1786 is the monitoring of climatic factors, such warming and precipitation extremes, in Arctic regions previously  
 1787 contaminated by Anthrax (Ezhova et al., 2021).



1788

1789 *UV variations*

1790 Different geophysical parameters affecting the UV molecular number density show that especially at high  
1791 altitudes, the increased surface albedo has a significant effect on the UV growth. The new parameterization  
1792 of the on-line UV tool (*momsu.ru/uv/*) for Northern Eurasia allows us to determine the altitude dependence  
1793 of UV and to estimate the possible effects of UV on human health considering different skin types and  
1794 various open body fraction for January and April conditions in the Alpine region (Chubarova et al., 2016b).  
1795 Using UV satellite retrievals, ERA-Interim data and the INM-RSHU chemistry-climate model, the changes  
1796 in the UV irradiance and UV resources were estimated over Northern Eurasia for the 1979-2015 period,  
1797 demonstrating significant UV increases over vast areas (Chubarova et al., 2020). Referring to long-term UV  
1798 measurements and model simulations in Moscow, a statistically significant positive trend of more than 5%  
1799 per decade since 1979 was evaluated (Chubarova et al., 2018). Related to the connection between UV  
1800 variation and stratospheric O<sub>3</sub>, see also the section 2.2.1 Atmospheric composition and chemistry.

1801

1802 *Examples of air pollution episodes*

1803

1804 Street-level urban air pollution is one of the key topics in urban environments. For example, in Norway,  
1805 Bergen, the most extreme cases of repetitive wintertime air pollution episodes, followed by increased large-  
1806 scale wind speeds above the valley, were transported by the local re-circulations to other less polluted areas  
1807 with only slow dilution. This result underlines the need for better described assumptions on transport paths  
1808 and weak dispersion in classical air pollution models, in order to improve the current air quality forecasts in  
1809 urban areas (Wolf- Grosse et al., 2017b). A link between the persistence of the flow above the Bergen valley  
1810 and the occurrence and severity of the local air pollution episodes was found. Analysis of the large-scale  
1811 circulation over the North Atlantic-European region, with respect to air pollution in Bergen, revealed that the  
1812 persistence in meteorological conditions connected with air pollution episodes is not necessarily caused by  
1813 large-scale anomalies of the atmospheric circulation over the Norwegian west coast, but rather connected  
1814 with anomalies as far away as Greenland (Wolf-Grosse et al., 2017a).

1815

1816 In Russia, especially intensive atmospheric pollution episodes have severe impacts on the environment and  
1817 human health. Popovicheva et al (2019b) analyzed the Tver region, north of Moscow, which was  
1818 considerably affected the secondary organic aerosol (SOA) formation originating from long-lasting peat bog  
1819 fires. Spectral absorbance characteristics were similar to peat burning and traffic source emissions during fire  
1820 and non-fire related days and confirmed the effect of transported peat smoke on air quality in a megacity  
1821 environment (Popovicheva et al., 2019b). Popovicheva et al. (2019b) also showed that long-term transport  
1822 from the North-West Russia and Scandinavia influence the local population.

1823

1824 Local Arctic air pollution alone can seriously affect public health and ecosystems locally, especially in  
1825 wintertime when the pollution can accumulate under inversion layers (Schmale et al., 2018a). We need more

1826 research on the contributing emission sources and the relevant atmospheric pollution mechanisms, and more  
 1827 detailed epidemiological or toxicological health impact studies in the Arctic. Socioeconomic changes  
 1828 (shipping, tourism, natural resources extraction, increasing number of population) are already taking place in  
 1829 the Arctic, and they will increase in the future. It is also expected that the emission types and magnitudes will  
 1830 increase the number of exposed individuals (Arnold et al., 2016). There is still a large variation in the amount  
 1831 of the location of emissions. Future predictions are even more difficult due to the yet unknown development  
 1832 of the Arctic economic activities and their emissions (Arnold et al., 2016, Schmale et al., 2018a, 2018b).

1833

### 1834 **3. SYNTHESIS AND FUTURE PROSPECTS**

1835

#### 1836 3.1 Future research needs from the system perspectives

1837

1838 For the Land ecosystem, the recent progress towards understanding of the Northern Eurasian Arctic - boreal  
 1839 land ecosystems (section 3.1) are dealing with improved methodologies relevant to land processes (Q1),  
 1840 observations on permafrost thawing (Q2), and observed changes in the Northern ecosystems, especially soil  
 1841 conditions (Q3).

1842

1843 Improved satellite-based methods and (validation) data together with better quantification and, especially,  
 1844 the scaling of the gross primary production (GPP) are enabling a better identification and quantification of  
 1845 Earth surface characteristics and ecosystem carbon balance compared with the earlier capacity (Gurchenkov  
 1846 et al., 2017, Rautiainen et al., 2016, Nitzbon et al., 2019, Boike et al., 2019, Terentieva et al., 2016), Zhang et  
 1847 al, 2018, Pulliainen et al., 2017, Matkala et al., 2020; Bondur and Chimitdorzhiev, 2008 a,b). Intensive  
 1848 research has been carried out on the quantification of the GPP, a key variable for biological activity, in  
 1849 different conditions and at different scales (Pulliainen 2017, Kulmala et al., 2019, Matkala et al., 2020).  
 1850 Further investigations are called for a more detailed understanding of the seasonal dynamics of the biological  
 1851 activity.

1852

1853 The Northern Eurasian ecosystems' tipping points are related to multiple simultaneous stress factors. The  
 1854 key stress factors here are the permafrost thawing and factors important for ecosystems, such as the  
 1855 prolongation of the growing season, increase in the mean temperature of the growing season and forest fires  
 1856 (Kukkonen et al. 2020, Biskaborn et al. 2019, Payne et al., 2016. Köster et al. 2016, Miles and Esau 2016,  
 1857 Miles et al., 2019). New evidence on the progress of permafrost thawing in Siberia has been introduced by  
 1858 Kukkonen et al. (2020) and Biskaborn et al. (2019). The permafrost thawing is also triggering yet not  
 1859 clearly-known processes related to changing fluxes, ecosystem processes and dynamics of greenhouse gas  
 1860 sinks and sources (Schuur et al., 2008, Thomson et al., 2017, Commane et al., 2017, Euskirchen et al., 2017,  
 1861 Dean et al., 2018, Thonat et al., 2017). The progress affecting permafrost thawing has not yet been analyzed  
 1862 in detail. For example, we need more information on the dynamics of how the thawing processes vary  
 1863 between soil types due to differences in water movement and, in the winter time, how the snow cover affects

1864 ground surface temperatures (Bartsch et al. 2010). In addition to permafrost processes, the recent advances in  
1865 observed changes in the Northern ecosystem reveal a significant role of soil processes in biogeochemical  
1866 cycles, especially the nitrogen cycle (Voigt et al., 2016, Pärn et al., 2018). Knowledge of the soil  
1867 microbiological composition and the effect of forest fires have been improved (Köster et al., 2015, 2016,  
1868 Zhang-Turpeinen et al., 2020), but further research is called for vegetation changes influencing the below-  
1869 ground microbiology, its composition and enzymatic activity (Payne et al., 2016. Köster et al. 2016). The  
1870 NDVI methods have made it possible to detect vegetation changes (Miles and Esau 2016). A range of  
1871 vegetation cover changes in Siberia have been reported, such as the Arctic greening and browning processes,  
1872 but e.g. the greening of Siberian cities remains an issue of intensive research also in the future (Miles and  
1873 Esau 2016, Miles et al., 2019).

1874 For the Atmospheric system, the recent progress in understanding the Northern Eurasian Arctic - boreal land  
1875 atmospheric system and the aspects of the megacity air quality (section 3.2) are dealing with atmospheric  
1876 composition changes (Q4), key feedbacks between climate and air quality (Q5), and synoptic scale weather  
1877 (Q6). Recent results demonstrate improved quantification of the carbon balance and CO<sub>2</sub> fluxes and  
1878 concentrations due to land use change, forest fires in Siberia, and new understanding of aerosol sources and  
1879 properties in the Arctic environment and across the Northern Eurasia (Pulliainen et al., 2017, Karelin et al.,  
1880 2017, Rakitin et al., 2018, Skorokhod et al., 2017, Alekseychik et al. 2017). However, most of the results  
1881 deal with atmospheric aerosol chemistry and physics in boreal and Arctic environments originating from  
1882 measurements in the few flagship stations in Finland and Russia (Kerminen et al., 2018, Wiedensohler et al.,  
1883 2019, Freud et al., 2017, Paasonen et al., 2018, Östrom et al., 2017, Kalogridis et al., 2018, Bondur et al.,  
1884 2016, Bondur and Ginzburg 2016, Bondur et al, 2019 c,d, Bondur and Gordo, 2018; Mikhailov et al., 2017,  
1885 Breider et al., 2017), indicating the need for a comprehensive station network in the PEEEX region. Black  
1886 carbon emitted by the Siberian forest fires and some other sources, and its long range transport to the Arctic,  
1887 are also widely discussed (Kalogridis et al., 2018, Bondur et al., 2016, Bondur and Ginzburg 2016,  
1888 Mikhailov et al., 2017, Breider et al., 2017, Shevchenko et al., 2015, Konovalov et al., 2018, Marelle et al.,  
1889 2018). In addition, measurements of ozone in the troposphere and stratosphere provide insight into  
1890 atmospheric chemistry in urban environments (Skorohod et al., 2017), UV radiation and human health  
1891 (Chubarova et al., 2019). Environmental health, including the impacts of air quality and UV radiation, is  
1892 foreseen as a high momentum research topic in the PEEEX domain, and further research is called for in this  
1893 area.

1894  
1895 Related to air pollution, we reported several new results on the dynamics between the haze pollution and  
1896 boundary layer meteorology in enhancing air pollution in megacity environments (Zhao et al., 2017, Ding et  
1897 al., 2016a, Wang et al., 2018b, Bai et al., 2018a, Ye et al., 2017). The long-term and comprehensive  
1898 measurements carried out especially at the SORPES station in Nanjing provide valuable data pools for such  
1899 studies (Ding et al., 2016a). However, the backbone of the recent progress has been the improved on-line  
1900 atmospheric measurements and the use of machine learning methods combined with different methodologies,  
1901 such as back trajectories together with the lidar and radiosonde data. In addition, improved models of

1902 emission inventories together with the ECHAM-HAM and GAINS models have led to a better quantification  
 1903 of aerosol number emissions. New knowledge has enabled the introduction of new theoretical arguments on  
 1904 the feedbacks between high aerosol concentrations and the urban boundary layer (Petäjä et al. 2016). New  
 1905 measurements have also been obtained from Siberian cities (Elansky et al., 2016, Chubarova et al., 2016a,  
 1906 Mahura et al., 2018). However, we are still in the early phase of having a holistic picture on large-scale  
 1907 feedbacks due to the lack of long-term, comprehensive measurements in these regions.

1908  
 1909 Changes in the atmospheric dynamics in the North have potential impacts on short-term local/regional and  
 1910 sub-seasonal to seasonal large-scale weather predictions, and on long-term projections on biogeochemical  
 1911 systems. It is therefore crucial to understand changes in boundary-layer processes as well as synoptic- and  
 1912 large-scale circulation in the Arctic and Northern Eurasia. Recent results show potential, but causally  
 1913 arguable, connections between the alarming sea ice decline, evaporation, cloudiness, atmospheric circulation  
 1914 and moisture transport as well as Arctic and European winter temperatures (Nygård et al., 2019, Rinke et al.,  
 1915 2019, McCusker et al., 2016, Mori et al., 2014, Blackport et al., 2019; Cohen et al., 2020). Further  
 1916 investigations are called for atmosphere-ice-ocean interactions, coupling between small-scale processes  
 1917 (such as clouds and turbulence) and synoptic-scale weather, as well as for polar prediction and extreme  
 1918 events. Furthermore, more quantitative knowledge is needed on pan-Arctic energy budgets (Spengler et al.,  
 1919 2016). The urban heat island (UHI) phenomena taking place in Arctic cities has received an increasing  
 1920 attention, and there is a special need for improved forecasting services for Arctic cities (Miles and Esau  
 1921 2017, Konstantinov et al., 2018, Varentsov et al., 2018b).

1922  
 1923 For the Water system, we discussed the Arctic sea ice dynamics and thermodynamics, snow depth and sea  
 1924 ice thickness, sea ice research supporting navigation, and rare elements in the snow and the ocean sediments,  
 1925 especially from the perspective of improvements in the observation and modelling methods (Q7, section  
 1926 3.3.1.). New evidence on atmosphere–Arctic sea ice interactions have been provided by Lei et al. (2018), and  
 1927 Jakobson et al. (2019). Lei et al. (2018) analyzed how the climate warming would affect the winter growth  
 1928 rate of thin and thick ice, and Jakobson et al. (2019) gave new insight into the relation between sea ice  
 1929 concentration and the wind speed. Furthermore, advance has been made in understanding the  
 1930 thermodynamics and metamorphosis of the snowpack on sea ice and their interactions with surface albedo  
 1931 changes (Dou et al., 2019). Operational sea ice analysis is increasingly important for the Arctic shipping and  
 1932 navigation (Lei et al., 2015, Karvonen et al., 2017). New results on rare elements, mineral composition and  
 1933 CO<sub>2</sub> and methane fluxes associated with ocean sediments have been attained (Maslov, et al., 2018, Yasunaka  
 1934 et al., 2018). This serves as an important information for mitigation plans, as well as for new estimates on the  
 1935 river runoff and discharge in Russian rivers into the Arctic seas (Grigoriev and Frolova 2018, Agafonova et  
 1936 al., 2017).

1937  
 1938 The marine Arctic ecosystems are under a progressive increase of anthropogenic impacts, the main issues  
 1939 calling for better understanding being the integrated effect of Arctic warming, ice and snow melt, ocean

1940 freshening, air quality and acidification of the Arctic marine ecosystems, primary production and carbon  
 1941 cycle (Q8, section 3.3.2). Quantitative information about the CO<sub>2</sub> accumulation into the ocean is having a  
 1942 high momentum. Marine organisms, such as coccolithoprip algae, are influencing the CO<sub>2</sub> flux exchange  
 1943 (Kondrik, et al., 2018b, Pozdnyakov et al., 2017). In addition to changing marine environments, the Arctic –  
 1944 boreal lakes and rivers may undergo changes in flooding, increasing the amount of fresh water and  
 1945 allochthonous materials (Q9, section 3.3.3). In addition to the Arctic Ocean, the ice and snow conditions of  
 1946 Northern lakes are under pressure. Lake Kilpisjärvi (Finland) (Arvola et al., 2017, Leppäranta et al., 2017)  
 1947 and Lake Ladoga (Russia) (Karetnikov et al., 2017) have been under an intensive research, and the recent  
 1948 results demonstrate changes in heat fluxes, ice cover periods and stratification. The browning of lakes and  
 1949 lake sediments were discussed, and new results were attained from the Selenga River of the Baikal Lake.  
 1950 Dramatic changes will be expected in the water runoff and in the amount of dissolved modes of metals, also  
 1951 having serious impact on the environmental health (Chalov et al., 2015, 2016, 2017 a, 2017b, Karthe et al.,  
 1952 2017 a, 2017b). As a comparison to the Northern high latitudes, we also discussed freezing lakes in Central  
 1953 Asia, where the climate is cold and arid. There the ice is typically snow-free, or possesses only a thin snow  
 1954 cover, allowing penetration of sunlight into the water body (Huang et al., 2019).

1955

1956 For the Societal system, the anthropogenic impact has been addressed as one of the main themes (Q10). The  
 1957 discussion on the mitigation and adaptation, including the urban infrastructure design (Juhola 2018) and risk  
 1958 assessment, were addressed in this context (section 3.4.1). In social transformations, a special attention was  
 1959 given to one of the most important local livelihoods in Lapland: reindeer grazing and how it interacts with  
 1960 the environment (Q11 section 3.4.2). The adaptive capacity of the Northern societies rest on their  
 1961 environment, demographic structure and economic activities (Q12). Referring to the earlier statement about  
 1962 the future research needs for the Atmospheric system with respect to environmental health, here again we  
 1963 would like to put an increasing attention to environmental health under changing climate, including the  
 1964 spread of diseases and air pollution and their combined effects (section 3.4.3.).

1965

1966 3.2 Feedback mechanisms under changing climate, cryosphere conditions and urbanization

1967

1968 During the recent years, Kulmala et al. (2004, 2020) have focused on the quantification of the Continental  
 1969 Biosphere-Aerosol-Cloud-Climate (COBACC) feedback loop relevant to the boreal region in Northern  
 1970 Eurasia. Previous results on the COBACC feedback loop addressed the role of BVOC emission dynamics  
 1971 (Arneth et al., 2016). Both higher temperatures and increased CO<sub>2</sub> concentrations are (separately) expected  
 1972 to increase emissions of biogenic volatile organic compounds (BVOCs) to the atmosphere. It also seems that  
 1973 the GPP is controlled by the BVOC effects on the clouds. Sporre et al. (2019) used an Earth System model to  
 1974 estimate aerosol scattering due to enhanced BVOC emissions and estimated the associated negative direct  
 1975 radiative effect (-0.06 W m<sup>-2</sup>). The total global radiative effect associated with this feedback was estimated to  
 1976 be -0.49 W m<sup>-2</sup> (Sporre et al., 2019), indicating that it has the potential to offset about 13 % of the forcing  
 1977 associated with a doubling of CO<sub>2</sub>. The direct effect of aerosol on GPP due to an increase in the fraction of

1978 diffuse radiation was estimated between 6 and 14% increase in GPP at maximum observed aerosol loading  
 1979 compared to low aerosol loading in Northern Eurasia forests (Ezhova et al., 2018b).  
 1980  
 1981 The results from the Tibetan plateau demonstrate notable feedbacks between vegetation, BVOC emissions  
 1982 and aerosol particles. The historical wetting of the TP region has increased the vegetation cover, allowing for  
 1983 feedback processes via biogenic aerosol formation and aerosol-cloud-precipitation interactions. A significant  
 1984 wetting trend since the early 1980's in Tibetan Plateau is most conspicuous in central and eastern Asia. Fang  
 1985 et al. (2019) hypothesized that the current warming may enhance emissions of biogenic volatile organic  
 1986 compounds (BVOC), which can increase secondary organic aerosols concentrations, contributing to the  
 1987 precipitation increase. The wetting trend can increase the vegetation cover and has a positive feedback on the  
 1988 BVOC emissions. The simulations suggest a significant contribution of increased BVOC emissions to the  
 1989 regional organic aerosol mass, and the simulated increase in BVOC emissions is significantly correlated with  
 1990 the wetting trend in Tibetan Plateau.  
 1991  
 1992 To estimate the net effects of various feedback mechanisms on land cover changes, photosynthetic activity,  
 1993 GHG exchange, BVOC emissions, formation of aerosols and clouds, and radiative forcing (Q14) calls for  
 1994 intensive collaboration and integration between the Arctic Ocean sciences and terrestrial sciences across the  
 1995 Pan-Arctic domain and across the Arctic and high-latitude domain. The Arctic greening and browning  
 1996 (section 3.1.3.) call for a multi-disciplinary scientific approach, improved modelling tools and new data to  
 1997 deeply understand the biosphere-atmosphere-anthroposphere interactions and feedbacks. Petäjä et al. (2020a,  
 1998 2020b) discussed the complexity of feedbacks, especially at the Arctic context, and the interplay between the  
 1999 temperature, GHG, permafrost, land cover and water bodies and between photosynthetic activity, aerosols,  
 2000 clouds and radiation budget. The current downturn of the arctic cryosphere (*section 3.1.2*), together with the  
 2001 changes in sea ice dynamics and glaciers and the permafrost thawing, affect bot marine and terrestrial carbon  
 2002 cycles in interconnected ways (*section 3.3.1*). Parmentier et al. (2017) discussed the changing arctic  
 2003 cryosphere and how the processes in the ocean and on land are too often studied as separate systems,  
 2004 although the sea ice decline connects the rapid warming of the Arctic, Arctic Ocean marine processes and  
 2005 air-sea exchange of CO<sub>2</sub>. Thus, the future priorities would be on the development of our modelling tools  
 2006 towards an all-scale modelling approach to cover the feedbacks, processes and interactions at the land-ocean  
 2007 interface and also in urban environments in the Arctic region. We also need to support the further  
 2008 development of the ground-based observation networks.  
 2009  
 2010 3.3 Climate scenarios for the Arctic-boreal region  
 2011  
 2012 Climate scenarios set the urgency for the mitigation and adaptation actions for the Northern Eurasian region.  
 2013 The Arctic-boreal region combines an area of both amplified climate change (Arctic amplification) and large  
 2014 diversity in the model predictions (Collins et al., 2013; Hoegh-Guldberg et al., 2018). Under the “low-to-  
 2015 medium” RCP4.5 forcing scenario (van Vuuren et al., 2011), the CMIP5 multi-model mean temperature

2016 changes during the 21<sup>st</sup> century indicate the strongest winter-time warming of >5 °C in the Arctic Ocean,  
 2017 whereas the majority of the terrestrial region will warm by 2–4 °C (Fig. 12). Even during summertime, the  
 2018 continental warming over the region will generally exceed 2 °C. It is important to note that the diversity of  
 2019 model projections is accentuated over the Arctic and Northern Eurasian domain: the mechanisms behind the  
 2020 Arctic amplification are implemented in varying details in the distinct models, and the associated interactions  
 2021 and feedback processes provide a diverse picture of the future in the Arctic-boreal regions.

2022  
 2023 In addition to considerable trends in atmospheric temperatures, the models further indicate prominent  
 2024 changes in precipitation (Collins et al., 2013, Hoegh-Guldberg et al., 2018). For the Arctic boreal region, this  
 2025 is largely depicted as an increasing rainfall during both winter and summer, extending to 15-25% over most  
 2026 of the terrestrial domain over the winter and somewhat less during summer (Fig. 9). Contemporary warm  
 2027 Arctic temperatures and large sea ice deficits (75% volume loss) demonstrate climate states outside our  
 2028 previous experience. The modeled changes in the Arctic cryosphere demonstrate that even limiting the global  
 2029 temperature increase to 2 °C will leave the Arctic a much different environment by mid-century, with less  
 2030 snow and sea ice, melted permafrost, altered ecosystems, and a projected annual mean Arctic temperature  
 2031 increase of +4 °C. Even under ambitious emission reduction scenarios, high-latitude land ice melt, including  
 2032 Greenland, are foreseen to continue due to internal lags, leading to accelerating global sea level rise  
 2033 throughout the century (Overland et al., 2019).

#### 2035 4. CONCLUDING REMARKS

2036  
 2037 Only the integration of different observing networks and programs into an inter-operable and integrated  
 2038 observation system can provide data needed for understanding the mechanisms of the Arctic-boreal system.  
 2039 There is a fundamental need for an integrated, comprehensive network of the-state-of-the art *in situ* stations  
 2040 measuring Earth surface – atmosphere interactions (Kulmala et al., 2016a, 2018; Uttal et al., 2016; Hari et  
 2041 al., 2016; Alekseychik et al., 2016; Vihma et al. 2019). The results obtained in the Pan Eurasian Experiment  
 2042 (PEEX) programme in Russian and China introduced in this paper are based on a combination of long-term  
 2043 observations and campaign data. In addition, the Arctic marine regions require comprehensive observations  
 2044 and subsequent synthesis, as these regions are under a lot of environmental stresses. Therefore, we need  
 2045 more *in situ* observations of the Arctic system covering the marine atmosphere, sea ice and ocean. However,  
 2046 there are pronounced technological and logistical challenges to setup such continuous, marine *in situ*  
 2047 observations (e.g. Vihma et al. 2019). Furthermore, improved monitoring is needed for river discharge and  
 2048 associated fluxes of greenhouse gases and other key compounds and more research on the understanding of  
 2049 coastal processes and atmospheric transport and specific regional socioeconomic issues and their interactions  
 2050 with changing environments (Vihma et al., 2019; Petäjä et al., 2020a).

2051  
 2052 The international organizations and bodies like the Arctic Council (SAON's Roadmap for Arctic Observing  
 2053 and Data Systems, ROADS), EU Horizon2020 (Blue Growth INTAROS and APPLICATE projects), GEO-

2054 CRI (high Mountains and cold regions), the Belmont Forum COPERNICUS and WMO are coordinating  
 2055 development of the Arctic data and services. New data products are expected from the large-scale MOSAiC  
 2056 campaign and projects like ERA-PLANET iCUPE (Petäjä et al. 2020b) or ArcticFLUX to monitor the  
 2057 interface between the marine Arctic and Eurasian continent. Also, national-based Arctic observations and  
 2058 research programs like AC<sup>3</sup> by German institutes play a significant role. Russia conducts extensive research  
 2059 in the Arctic region, notably on the manned drifting ice stations. These Arctic observation activities are  
 2060 coordinated and carried out by Roshydromet, universities and Russian Academy of Sciences' institutes.

2061

2062 Concerning global energy markets, the Arctic region holds 25 % or more of the world's undiscovered oil and  
 2063 gas reservoirs (Arctic Oil & Gas, 2008). The plans of China and Russia to build 'Ice Silk Road' along  
 2064 Northern Sea linking the China and Russia to Europe is highlighting the growing economic and strategic  
 2065 importances of the polar regions, and the increasing pressure on the Arctic environment and local  
 2066 communities. In addition, wide areas of the high latitudes and Arctic regions are under the pressure of the  
 2067 changing economic activities of the Arctic, and also under high pressures of the changing environment and  
 2068 climate. A comprehensive observation network providing in-situ data in close coordination with satellite  
 2069 observations and ground-based remote sensing is required to monitor the environmental impacts of the  
 2070 envisioned operations.

2071

2072 Over the last few years, Earth system science is driven by the need to understand the scientific processes of  
 2073 climate change and air quality, their interrelations with the Earth system and their societal impacts. The  
 2074 interplay between science, politics and business, and the analysis of the existing policies and strategies, help  
 2075 us to recognize and analyze new and emerging trends of Arctic governance (e.g. protection and resilience  
 2076 vis-a-vis economic activities), geopolitics (e.g. state sovereignty vis-a-vis internationalization), geo-  
 2077 economics (e.g. tourism vis-à-vis reindeer herding), and science (e.g. climate change). The intensive work  
 2078 towards the new Arctic observations and data systems, together with the intensive observations on the land –  
 2079 atmosphere interactions taking place at the high latitudes, will provide the baseline for cross disciplinary  
 2080 research era. PEEX is aimed for these directions.

2081

## 2082 **ACKNOWLEDGEMENTS**

2083

2084 We thank the following funding agencies and projects: Academy of Finland contracts: No 280700, 294600,  
 2085 296302 (Novel Assessment of Black Carbon in the Eurasian Arctic: From Historical Concentrations and  
 2086 Sources to Future Climate Impacts (NABCEA), 307331 (FCoE Atmospheric Sciences), 311932, 314798/99,  
 2087 315203, 317999, 337549 (Atmosphere and Climate Competence Center (ACCC), Jane and Aatos Erkkö  
 2088 Foundation, Russian Government megagrant project № 075-15-2021-574 "Megapolis - heat and pollution  
 2089 island: interdisciplinary hydroclimatic, geochemical and ecological analysis", Russian Foundation for Basic  
 2090 Research (RFBR) projects No. 17-29-05027 (Selenga-Baikal river system), 17-29-05102, 18-05-00306, 18-  
 2091 05-60037, 18-05-60219 (Arctic river), 18-35-20031, 18-44-860017, 18-45-700015, 18-05-60083 (Storm  
 2092 activity in the Barents Sea), 18-60084 (Dangerous impacts of large - scale industrial emissions on aerosol  
 2093 pollution and Arctic ecosystem), 19-05-50088, 19-05-00352, 19-55-80021 (MOST and DST studies), the  
 2094 IAO SB RAS supported by RFBR project No. 19-05-50024, Russian Science Foundation (RSF) projects;



2095 RSF project 21-17-00181 (Monitoring at Lena River catchment)" No.17-17-01117, 18-17-00076 (Long-term  
 2096 measurement of aerosol chemical composition in Central Siberia, 19-77-20109 (Black carbon emissions  
 2097 from Siberian fires), 19-77-30004 (Moscow environment), 19-77-300-12 (Measurement networks and field  
 2098 sites in Kola Peninsula), Yugra State University grant No.13-01-20/39, Ministry of Science and Higher  
 2099 Education of Russia - Agreement No.13.1902.21.0003, State assignment No. 0148-2019-0006, Project  
 2100 N75295423 launched by St. Petersburg State University, European Research Council (ERC) projects No.  
 2101 742206 (ATM-GTP), No. 850614 (CHAPAs), EU Horizon 2020 projects No. 727890 (Integrated Arctic  
 2102 Observing System, INTAROS), 689443 (Integrative and Comprehensive Understanding on Polar  
 2103 Environments, iCUPE), 654109 (Aerosol Clouds and Trace Gases Research Infrastructure, ACTRIS-2),  
 2104 EU7 FP MarcoPolo Grant No. 606953, Erasmus+ 561975-EPP-1-2015-1-FI-EPPKA2-CBHE-JP, Norwegian  
 2105 Research Council and the Belmont Forum project SERUS, No. 311986, National Natural Science  
 2106 Foundation of China Grant No. 41275137, ESA-MOST China Dragon Cooperation projects No. 10663 and  
 2107 32771 (Dragon 3 and 4). We are also thankful for the support of the Russian Government project  
 2108 "Megapolis - heat and pollution island: interdisciplinary hydroclimatic, geochemical and ecological  
 2109 analysis" and Russian Science Foundation (RSF) 21-17-00181 (Monitoring at Lena River catchment)"

2110 Our special thanks also to Mrs. Alla Borisova, INAR, University of Helsinki, for the technical editing of the  
 2111 manuscript.

2112

2113 **REFERENCES**

2114 Andreae, M. O., Andreae, T. W., and Ditas, F.: How frequent is new particle formation in the boundary layer  
 2115 over the remote temperate/boreal forest?, AGU Fall Meeting, San Francisco, USA,  
 2116 doi:10.1002/essoar.10501148.1, 2019.

2117 Aalto, J., Porcar-Castell, A., Atherton, J., Kolari, P., Pohja, T., Hari, P., Nikinmaa, E., Petäjä, T., and Bäck,  
 2118 J.: Onset of photosynthesis in spring speeds up monoterpene synthesis and leads to emission bursts, *Plant,*  
 2119 *Cell and Environment.*, 38, 2299-2312, 2015.

2120 Agafonova, S. A., Frolova, N. L., Surkova, G. V., and Koltermann, K., P.: Modern characteristics of the ice  
 2121 regime of Russian Arctic rivers and their possible changes in the 21st century, *Geogr. Environ. Sustain.*,  
 2122 10(4), 4-15, doi:10.24057/2071-9388-2017-10-4-4-15, 2017.

2123 Alekseychik, P., Lappalainen, H.K., Petäjä, T., Zaitseva, N., Heimann, M., Laurila, T., Lihavainen, H., Asmi,  
 2124 E., Arshinov, M., Shevchenko, V., Makshtas, A., Dubtsov, S., Mikhailov, E., Lapshina, E., Kirpotin, S.,  
 2125 Kurbatova, Y., Ding, A., Guo, H., Park, S., Lavric, J.V., Reum, F., Panov, A., Prokushkin, A., and Kulmala,  
 2126 M.: Ground-based station network in Arctic and Subarctic Eurasia: An overview, *Geogr. Environ. Sustain.*,  
 2127 9(2), 75-88, doi:10.24057/2071-9388-2016-9-2-19-35, 2016.

2128 Alekseychik, P., Mammarella, I., Karpov, D., Dengel, S., Terentieva, I., Sabrekov, A., Glagolev, M., and  
 2129 Lapshina, E.: Net ecosystem exchange and energy fluxes measured with the eddy covariance technique in a  
 2130 western Siberian bog, *Atmos. Chem. Phys.*, 17, 9333–9345, doi:10.5194/acp-17-9333-2017, 2017.

2131 AMAP, 2017: Arctic Pollution 2017. Arctic Monitoring and Assessment Programme (AMAP), Oslo,  
 2132 Norway.

- 2133 Andreae, M. O.: Emission of trace gases and aerosols from biomass burning – an updated assessment,  
2134 *Atmos. Chem. Phys.*, 19, 8523–8546, doi:10.5194/acp-19-8523-2019, 2019.
- 2135 Arneth, A., Harrison, S., Zaehle, S., Tsigaridis, K., Menon, S., Bartlein, P. J., Feichter, J., Korhola, A.,  
2136 Kulmala, M., O'Donnell, D., Schurgers, G., Sorvari, S., and Vesala, T.: Terrestrial biogeochemical feedbacks  
2137 in the climate system. *Nature Geosci*, 3, 525–532, <https://doi.org/10.1038/ngeo905>, 2010.
- 2138 Arneth, A., Makkonen, R., Olin, S., Paasonen, P., Holst, T., Kajos, M. K., Kulmala, M., Maximov, T.,  
2139 Miller, P. A., and Schurgers, G.: Future vegetation–climate interactions in Eastern Siberia: an assessment of  
2140 the competing effects of CO<sub>2</sub> and secondary organic aerosols, *Atmos. Chem. Phys.*, 16, 5243–5262,  
2141 doi:10.5194/acp-16-5243-2016, 2016.
- 2142 Arnold, S. R., Law, K. S., Brock, C. A., Thomas, J. L., Starkweather, S. M., von Salzen, K., Stohl, A.,  
2143 Sharma S., Lund, M. T., Flanner, M. G., Petaja, T., Tanimoto, H., Gamble, J., Dibb J. E., Melamed M.,  
2144 Johnson, N., Fidel, M., Tynkkynen, V.-P., Baklanov, A., Eckhardt, S., Monks, S. A., Browse, J., and Bozem,  
2145 H.: Arctic air pollution: Challenges and opportunities for the next decade, *Elementa: Science of the*  
2146 *Anthropocene*, 4:000104, <https://dx.doi.org/10.12952/journal.elementa.00010>. 2016.
- 2147 Arvola, L., Äijälä, C., and Leppäranta, M.: CDOM concentrations of large Finnish lakes relative to their  
2148 landscape properties, *Hydrobiologia*, 780(1), 37–46, doi:10.1007/s10750-016-2906-4, 2016.
- 2149 Arvola, L., Leppäranta, M., and Äijälä, C.: CDOM variations in Finnish lakes and rivers between 1913 and  
2150 2014, *Sci. Total Environ.*, 601, 1638–1648, doi:10.1016/j.scitotenv.2017.06.034, 2017.
- 2151 Asmi, E., Kondratyev, V., Brus, D., Laurila, T., Lihavainen, H., Backman, J., Vakkari, V., Aurela, M.,  
2152 Hatakka, J., Viisanen, Y., Uttal, T., Ivakhov, V., and Makshtas, A.: Aerosol size distribution seasonal  
2153 characteristics measured in Tiksi, Russian Arctic, *Atmos. Chem. Phys.*, 16, 1271–1287, doi:10.5194/acp-16-  
2154 1271-2016, 2016.
- 2155 Backman, J., Schmeisser, L., Virkkula, A., Ogren, J. A., Asmi, E., Starkweather, S., Sharma, S.,  
2156 Eleftheriadis, K., Uttal, T., Jefferson, A., Bergin, M., Makshtas, A., Tunved, P., and Fiebig, M.: On  
2157 Aethalometer measurement uncertainties and an instrument correction factor for the Arctic, *Atmos. Meas.*  
2158 *Tech.*, 10, 5039–5062, doi:10.5194/amt-10-5039-2017, 2017.
- 2159 Badina, S. V.: Socio-economic potential of municipalities in the context of natural risk (case study –  
2160 Southern Siberian regions), *IOP Conference Series: Earth and Environmental Science*, 190,  
2161 doi:10.1088/1755-1315/190/1/012001, 2018.
- 2162 Bai, J.H.: Estimation of the isoprene emission from the Inner Mongolia grassland, *Atmospheric Pollution*  
2163 *Research*, 6, 406–414, doi: 10.5094/APR.2015.045, 2015.
- 2164 Bai, J.H.: UV extinction in the atmosphere and its spatial variation in North China, *Atmos. Environ.*, 154,  
2165 318–330, doi:10.1016/j.atmosenv.2017.02.002, 2017a.

- 2166 Bai, J.H., Guenther, A., Turnipseed, A., Duhl, T., Greenberg J.: Seasonal and interannual variations in  
 2167 whole-ecosystem BVOC emissions from a subtropical plantation in China. *Atmospheric Environment*, 161,  
 2168 176-190. <http://dx.doi.org/10.1016/j.atmosenv.2017.05.002>, 2017b.
- 2169 Bai, J.H., de Leeuw, G., van der Ronald, A., De Smedt, I., Theys, N., Van Roozendaal, M., Sogacheva, L.,  
 2170 and Chai, W. H.: Variations and photochemical transformations of atmospheric constituents in North China,  
 2171 *Atmos. Environ.*, 189, 213-226, doi:10.1016/j.atmosenv.2018.07.004, 2018a.
- 2172 Bai, Y., Zhang, J., Zhang, S., Yao, F., and Magliulo, V.: A remote sensing-based two-leaf canopy  
 2173 conductance model: Global optimization and applications in modeling gross primary productivity and  
 2174 evapotranspiration of crops, *Remote Sensing of Environment*, 215, 411-437, doi:10.1016/j.rse.2018.06.005,  
 2175 2018b.
- 2176 Bai, J. H.: A calibration method of solar radiometers, *Atmos. Pollut. Res.*, 10(4), 1365-1373,  
 2177 doi:10.1016/j.apr.2019.03.011, 2019.
- 2178 Bai, J. H.: O<sub>3</sub> Concentration and its relation with BVOC emissions in a subtropical plantation. *Atmosphere*,  
 2179 12, 711. <https://doi.org/10.3390/atmos12060711>, 2021.
- 2180 Baklanov, A., Mahura, A., Nazarenko, L., Tausnev, N., Kuchin, A., and Rigina, O.: *Atmospheric Pollution  
 2181 and Climate Change in Northern Latitudes*, Russ. Acad. Sci., Apatity, Russia, 2012.
- 2182 Baklanov, A. A., Penenko, V. V., Mahura, A. G., Vinogradova, A. A., Elansky, N. F., Tsvetova, E. A.,  
 2183 Rigina, O. Y., Maksimenkov, L. O., Nuterman, R. B., Pogarskii, F. A., and Zakey, A.: Aspects of  
 2184 Atmospheric Pollution in Siberia, in *Regional Environmental Changes in Siberia and Their Global  
 2185 Consequences*, edited by: Groisman P. Y., and Gutman, G., 303–346, Springer, Dordrecht, Netherlands,  
 2186 2013.
- 2187 Baklanov, A., Molina, L.T., and Gauss, M.: Megacities, air quality and climate, *Atmospheric Environment*,  
 2188 126, 235-249, <https://doi.org/10.1016/j.atmosenv.2015.11.059>, 2016.
- 2189 Baklanov, A., Smith Korsholm, U., Nuterman, R., Mahura, A., Nielsen, K. P., Sass, B. H., Rasmussen, A.,  
 2190 Zakey, A., Kaas, E., Kurganskiy, A., Sørensen, B., and González-Aparicio, I.: Enviro-HIRLAM online  
 2191 integrated meteorology–chemistry modelling system: strategy, methodology, developments and applications  
 2192 (v7.2), *Geosci. Model Dev.*, 10, 2971–2999, <https://doi.org/10.5194/gmd-10-2971-2017>, 2017.
- 2193 Baklanov, A., Brunner, D., Carmichael, G., Flemming, J., Freitas, S., Gauss, M., Hov, O., R. Mathur, R.,  
 2194 Schlünzen, K., Seigneur, C., and Vogel, B.: Key issues for seamless integrated chemistry-meteorology  
 2195 modeling, *Bull. Amer. Meteor. Soc.*, doi:10.1175/BAMS-D-15-00166.1., 2018.
- 2196 Balch, W. M., Bates, N. R., Lam, P. J., Twining, B. S., Rosengard, S. Z., Bowler, B. C., and Rauschenberg,  
 2197 S.: Factors regulating the Great Calcite Belt in the Southern Ocean, and its biogeochemical significance,  
 2198 *Global Biogeochem. Cycles*, 30(8), 1124-1144, doi:10.1002/2016GB005414, 2016.

- 2199 Balch, W. M.: The ecology, biogeochemistry, and optical properties of coccolithophores, *Ann. Rev. Mar.*  
2200 *Sci.*, 109, 71-98, doi:10.1146/annurev-marine-121916-063319, 2018.
- 2201 Bartsch, A., Kumpula, T., Forbes, B.C. and Stammler F.: Detection of snow surface thawing and refreezing  
2202 in the Eurasian Arctic with QuikSCAT: implications for reindeer herding, *Ecol Appl.*, 20, 2346-58., doi:  
2203 10.1890/09-1927.1., 2010.
- 2204 Barreira, L. M. F., Duporté, G., Rönkkö, T., Parshintsev, J., Hartonen, K., Hyrsky, L., Heikkinen, E.,  
2205 Kulmala, M., and Riekkola, M.-L.: Field measurements of biogenic volatile organic compounds in the  
2206 atmosphere using solid-phase microextraction Arrow, *Atmos. Meas. Tech.*, 11, 881–893, 2018.
- 2207 Bashmachnikov, I.L., Yurova, A.Y., Bobylev, L.P., and Vesman, A. V.: Seasonal and Interannual Variations  
2208 of Heat Fluxes in the Barents Sea Region, *Izv., Atmos. Ocean. Phys.*, 54, 213–222,  
2209 doi:10.1134/S0001433818020032, 2018a.
- 2210 Bashmachnikov, I. L., Yurova, A.Y., Bobylev, L. P., Vesman, A.V.: Seasonal and interannual variations of  
2211 the heat fluxes in the Barents Sea region, *Izv. Atmos. Ocean. Phys.*, 54(2), 239-249,  
2212 doi:10.7868/S0003351518020149, 2018b.
- 2213 Beer, C., Reichstein, M., Tomelleri, E., Ciais, P., Jung, M., Carvalhais, N., Rödenbeck, C., Altfaf Arain,  
2214 A., Baldocchi, D., Bonan, G.B., Bondeau, A., Cescatti, A., Lasslop, G., Lindroth, A., Lomas, M.,  
2215 Luysaert, S., Margolis, H., Oleson, K.W., Rouspard, O., Veenendaal, E., Viovy, N., Williams, C., F Ian  
2216 Woodward, F.,I., and Papale, D.: Terrestrial gross carbon dioxide uptake: global distribution and covariation  
2217 with climate. *Science*, 329, 834–838, doi: 10.1126/science.1184984, 2010.
- 2218 Belikov, D., Arshinov, M., Belan, B., Davydov, D., Fofonov, A., Sasakawa, M., Machida, T.: Analysis of the  
2219 Diurnal, Weekly, and Seasonal Cycles and Annual Trends in Atmospheric CO<sub>2</sub> and CH<sub>4</sub> at Tower Network  
2220 in Siberia from 2005 to 2016, *Atmosphere*, 10 (11), 689, doi: 10.3390/atmos10110689, 2019.
- 2221 Berchet, A., Bousquet, P., Pison, I., Locatelli, R., Chevallier, F., Paris, J.-D., Dlugokencky, E. J., Laurila, T.,  
2222 Hatakka, J., Viisanen, Y., Worthy, D. E. J., Nisbet, E., Fisher, R., France, J., Lowry, D., Ivakhov, V., and  
2223 Hermansen, O.: Atmospheric constraints on the methane emissions from the East Siberian Shelf, *Atmos.*  
2224 *Chem. Phys.*, 16, 4147–4157, doi:10.5194/acp-16-4147-2016, 2016.
- 2225 Berezina, E., Moiseenko, K., Skorokhod, A., Elansky, N., Belikov, I., and Pankratova, N.: Isoprene and  
2226 monoterpenes over Russia and their impacts in tropospheric ozone formation, *Geogr., Environ., Sustain.*,  
2227 12(1), 63-74, doi:10.24057/2071-9388-2017-24, 2019.
- 2228 Bezuglaya, E. Y., Ed.: Air quality in largest cities of Russia for 10 years (1988-1997), Hydrometeoizdat, St.  
2229 Petersburg, Russia, 1999.
- 2230 Biskaborn, B. K., Smith, S. L., Noetzli, J., Matthes, H., Vieira, G., Streletskiy, D. A., Schoeneich, P.,  
2231 Romanovsky, V. E., Lewkowicz, A. G., Abramov, A., Allard, M., Boike, J., Cable, W. L., Christiansen, H.

- 2232 H., Delaloye, R., Diekmann, B., Drozdov, D., Etzelmüller, B., Grosse, G., ... and Lantuit, H.: Permafrost is  
 2233 warming at a global scale, *Nat. Commun.*, 10(1), 264, doi: 10.1038/s41467-018-08240-4, 2019.
- 2234 Blackport, R., Screen, J. A., van der Wiel, K., and Bintanja, R.: Minimal influence of reduced Arctic sea ice  
 2235 on coincident cold winters in mid-latitudes, *Nat. Clim. Change*, 9, 697–704, doi: 10.1038/s41558-019-0551-  
 2236 4, 2019.
- 2237 Bobylev, S.N., Chereshnya, O.Y., Kulmala, M., Lappalainen, H. K., Petäjä, T., Solov'eva, S.V., Tikunov,  
 2238 V.S., and Tynkkynen, V.-P.: Indicators for digitalization of sustainable development goals in PEEEX  
 2239 program, *J. Geogr. Sust.*, 11, 145-156, 2018.
- 2240 Boike, J., Nitzbon, J., Anders, K., Grigoriev, M., Bolshiyarov, D., Langer, M., Lange, S., Bornemann, N.,  
 2241 Morgenstern, A., Schreiber, P., Wille, C., Chadburn, S., Gouttevin, I., Burke, E., and Kutzbach, L.: A 16-  
 2242 year record (2002–2017) of permafrost, active-layer, and meteorological conditions at the Samoylov Island  
 2243 Arctic permafrost research site, Lena River delta, northern Siberia: an opportunity to validate remote-sensing  
 2244 data and land surface, snow, and permafrost models, *Earth Syst. Sci. Data*, 11, 261–299,  
 2245 <https://doi.org/10.5194/essd-11-261-2019>, 2019.  
 2246
- 2247 Bondur, G., and Vorobev, V. E.: Satellite Monitoring of Impact Arctic Regions, *Izv. Atmos. Ocean. Phys.*,  
 2248 51, 949–968, doi: 10.1134/S0001433815090054, 2015.
- 2249 Bondur, V. G., and Ginzburg, A. S.: Emission of carbon-bearing gases and aerosols from natural fires on the  
 2250 territory of Russia based on space monitoring, *Dokl. Earth Sci.*, 466(2), 148-152,  
 2251 doi:10.1134/s1028334x16020045, 2016.
- 2252 Bondur, V. G.: Satellite monitoring of trace gas and aerosol emissions during wildfires in Russia. *Izv.*  
 2253 *Atmos. Ocean. Phys.*, 52(9), 1078-1091, doi:10.1134/s0001433816090103, 2016.
- 2254 Bondur, V. G., Gordo, K. A., and Kladov, V. L.: Spacetime distributions of wildfire areas and emissions of  
 2255 carbon-containing gases and aerosols in northern eurasia according to satellite-Monitoring Data, *Izv. Atmos.*  
 2256 *Ocean. Phys.*, 53(9), 859-874, doi:10.1134/s0001433817090055, 2017.
- 2257 Bondur, V. G. and Gordo, K. A.: Satellite Monitoring of Burned out Areas and Emissions of Harmful  
 2258 Contaminants due to Forest and other Wildfires in Russia, *Izv., Atmos. Ocean. Phys.*, 54 (9),955–965, doi:  
 2259 10.1134/S0001433818090104, 2018.
- 2260 Bondur V. G., Chimitdorzhiev T. N., Dmitriev A. V., and Dagurov P. N.: Otsenka prostranstvennoy  
 2261 anizotropii neodnorodnostey lesnoy rastitelnosti pri razlichnykh azimutalnykh uglakh radarnogo  
 2262 polyarimetricheskogo zondirovaniya (Spatial anisotropy assessment of the forest vegetation heterogeneity at  
 2263 various azimuth angles of the radar polarimetric sensing), *Issledovanie Zemli iz kosmosa, Russia*, 3, 92-103,  
 2264 doi:10.31857/S0205-96142019392-103, 2019a.

- 2265 Bondur, V. G., Chimitdorzhiev, T. N., Dmitriev, A. V., Dagurov, P. N., Zakharov, A. I., and Zakharova, L.  
 2266 N.: Metody radarnej polyarimetrii dlya issledovaniya izmenenij mekhanizmov obratnogo rasseyaniya v  
 2267 zonah opolznej na primere obrusheniya sklona berega reki Bureya (Using radar polarimetry to monitor  
 2268 changes in backscattering mechanisms in landslide zones for the case study of the Bureya river bank  
 2269 collapse), *Issledovanie Zemli iz kosmosa.*, Russia, 4, 3-17, doi:10.31857/S0205-9614201943-17, 2019b.
- 2270 Bondur, V. G., Tsidilina, M. N., and Cherepanova, E.V.: Satellite Monitoring of Wildfire Impacts on The  
 2271 Conditions of Various Types of Vegetation Cover in The Federal Districts of the Russian Federation, *Izv.*  
 2272 *Atmos. Ocean. Phys.*, 55 (9), 1238–1253, doi:10.1134/s000143381909010X, 2019 (c).
- 2273 Bondur, V. G., Tsidilina, M. N., Kladov, V. L., and Gordo, K. A.: Irregular Variability of Spatiotemporal  
 2274 Distributions of Wildfires and Emissions of Harmful Trace Gases in Europe Based on Satellite Monitoring  
 2275 Data // *Doklady Earth Sciences*, Vol. 485, Part 2, pp. 461–464, doi: 10.1134/S1028334X19040202, 2019(d).
- 2276 Bondur, V. G., Zakharova, L. N., and Zakharov, A. I.: Monitoring of the landslide area state on Bureya river  
 2277 in 2018-2019 according to radar and optical satellite images, *Issledovanie Zemli iz kosmosa*, Russia, No. 6,  
 2278 26-35, doi:10.31857/S0205-96142019626-35, 2019(e).
- 2279 Bondur, V. G., Zakharova, L. N., Zakharov, A. I., Chimitdorzhiev, T. N., Dmitriev, A. V., and Dagurov,  
 2280 P.N.: Monitoring of landslide processes by means of L-band radar interferometric observations: Bureya river  
 2281 bank caving case // *Issledovanie Zemli iz kosmosa*, Russia, No. 5, 3-14, DOI:  
 2282 <https://doi.org/10.31857/S0205-9614201953-14>. 2019 (f).
- 2283 Bondur, V. G., Tsidilina, M. N., and Kladov, V. L.: Irregular Variability of Spatiotemporal Distributions of  
 2284 Wildfires and Emissions of Harmful Trace Gases in Europe Based on Satellite Monitoring Data, *Dokl. Earth*  
 2285 *Sc.*, 485, 461–464, <https://doi.org/10.1134/S1028334X19040202>, 2019.
- 2286 Bondur, V. G., Mokhov, I. I., Voronova, O. S., and Sitnov, S. A.: Satellite Monitoring of Siberian Wildfires  
 2287 and Their Effects: Features of 2019 Anomalies and Trends of 20-Year Changes, *Doklady Earth Sciences*,  
 2288 492, 1, 370–375. doi: 10.1134/S1028334X20050049, 2020.
- 2289 Bormann, K. J., Brown, R. D., Derksen, C., and Painter, T. H.: Estimating snow-cover trends from space,  
 2290 *Nat. Clim. Chang.*, 8, 924-928, 2018.
- 2291 Boy, M., Thomson, E. S., Acosta Navarro, J.-C., Arnalds, O., Batchvarova, E., Bäck, J., Berninger, F., Bilde,  
 2292 M., Brasseur, Z., Dagsson-Waldhauserova, P., Castarède, D., Dalirian, M., de Leeuw, G., Dragosics, M.,  
 2293 Duplissy, E.-M., Duplissy, J., Ekman, A. M. L., Fang, K., Gallet, J.-C., Glasius, M., Gryning, S.-E., Grythe,  
 2294 H., Hansson, H.-C., Hansson, M., Isaksson, E., Iversen, T., Jonsdottir, I., Kasurinen, V., Kirkevåg, A.,  
 2295 Korhola, A., Krejci, R., Kristjansson, J. E., Lappalainen, H. K., Lauri, A., Leppäranta, M., Lihavainen, H.,  
 2296 Makkonen, R., Massling, A., Meinander, O., Nilsson, E. D., Olafsson, H., Pettersson, J. B. C., Prisle, N. L.,  
 2297 Riipinen, I., Roldin, P., Ruppel, M., Salter, M., Sand, M., Seland, Ø., Seppä, H., Skov, H., Soares, J., Stohl,  
 2298 A., Ström, J., Svensson, J., Swietlicki, E., Tabakova, K., Thorsteinsson, T., Virkkula, A., Weyhenmeyer, G.  
 2299 A., Wu, Y., Zieger, P., and Kulmala, M.: Interactions between the atmosphere, cryosphere, and ecosystems

- 2300 at northern high latitudes, *Atmos. Chem. Phys.*, 19, 2015–2061, <https://doi.org/10.5194/acp-19-2015-2019>,  
2301 2019.
- 2302 Breider, T.J., Mickley, L.J., Jacob, D.J., Ge, C., Wang, J., Sulprizio, M.P., Croft, B., Ridley, D.A.,  
2303 McConnell, J.R., Sharma, S., Husain, L., Dutkiewicz, V. A., Eleftheriadis, K., Skov, H., and Hopke, P. K.:  
2304 Multidecadal trends in aerosol radiative forcing over the Arctic: Contribution of changes in anthropogenic  
2305 aerosol to Arctic warming since 1980, *J. Geophys. Res.: Atmos.*, 122, 3573-3594,  
2306 <https://doi.org/10.1002/2016JD025321>, 2017.
- 2307 Burkhard, B., Kroll, F., Müller, F., and Windhorst, W. F., Landscapes' Capacities to Provide Ecosystem  
2308 Services – a Concept for Land-Cover Based Assessments, *Landscape Online* 15(1), 1-12, DOI:  
2309 10.3097/LO.200915, 2009.
- 2310 Chalov, S. R., Jarsjo, J., Kasimov, N. S., Romanchenko, A. O., Pietron, J., Thorslund, J., and Promakhova,  
2311 E. V.: Spatio-temporal variation of sediment transport in the Selenga River Basin, Mongolia and Russia,  
2312 *Environ. Earth Sci.*, 73(2), 663-680, doi:10.1007/s12665-014-3106-z, 2015.
- 2313 Chalov, S. R., Bazilova, V. O., and Tarasov, M. K.: Modelling suspended sediment distribution in the  
2314 Selenga River Delta using LandSat data, in *Integrating Monitoring and Modelling for Understanding,  
2315 Predicting and Managing Sediment Dynamics*, edited by: Collins, A., Stone, M., Horowitz, A., and Foster, I.,  
2316 Copernicus Gesellschaft, Gottingen, Germany, 375, 19-22, 2017a.
- 2317 Chalov, S., Thorslund, J., Kasimov, N., Aybullaev, D., Ilyicheva, E., Karthe, D., Kositsky, A., Lychagin,  
2318 M., Nittrouer, J., Pavlov, M., Pietron, J., Shinkareva, G., Tarasov, M., Garmaev, E., Akhtman, Y., and Jarsjö,  
2319 J.: The Selenga River delta: a geochemical barrier protecting Lake Baikal waters, *Regional Environ. Change*,  
2320 17, 2039-2053, doi: 10.1007/s10113-016-0996-1, 2017b.
- 2321 Chalov, S. R., Millionshchikova, T. D., and Moreido, V. M.: Multi-Model Approach to Quantify Future  
2322 Sediment and Pollutant Loads and Ecosystem Change in Selenga River System, *Water Resour.*, 45, S22-S34,  
2323 doi:10.1134/s0097807818060210, 2018.
- 2324 Che, Y., Xue, Y., Mei, L., Guang, J., She, L., Guo, J., Hu, Y., Xu, H., He, X., Di, A., and Fan, C.: Technical  
2325 note: Intercomparison of three AATSR Level 2 (L2) AOD products over China, *Atmos. Chem. Phys.*, 16,  
2326 9655–9674, <https://doi.org/10.5194/acp-16-9655-2016>, 2016.
- 2327 Cheng, Y., Cheng, B., Zheng, F., Vihma, T., Kontu, A., Yang, Q. and Liao, Z.: Air/snow, snow/ice and  
2328 ice/water interfaces detection from high-resolution vertical temperature profiles measured by ice mass-  
2329 balance buoys on an Arctic lake. *Annals of Glaciology*, accepted (2020).
- 2330 Chernokulsky, A. V., Esau, I., Bulygina, O. N., Davy, R., Mokhov, II, Outten, S., and Semenov, V. A.:  
2331 Climatology and interannual variability of cloudiness in the Atlantic Arctic from surface observations since  
2332 the late nineteenth century, *J. Clim.*, 30(6), 2103-2120, doi:10.1175/jcli-d-16-0329.1, 2017.

- 2333 Chernokulsky, A., and Esau, I.: Cloud cover and cloud types in the Eurasian Arctic in 1936–2012. *Int. J.*  
 2334 *Climatol.*, **39**(15), 5771–5790, <https://doi.org/10.1002/joc.6187>, 2019
- 2335 Chu, B., Kerminen, V.-M., Bianchi, F., Yan, C., Petäjä, T. and Kulmala, M.: Atmospheric new particle  
 2336 formation in China, *Atmos. Chem. Phys.*, **19**, 115–138, 2019.
- 2337 Chubarova, N. Y., Poliukhov, A. A., and Gorlova, I. D.: Long-term variability of aerosol optical thickness in  
 2338 Eastern Europe over 2001–2014 according to the measurements at the Moscow MSU MO AERONET site  
 2339 with additional cloud and NO<sub>2</sub> correction, *Atmos. Meas. Tech.*, **9**, 313–334, [https://doi.org/10.5194/amt-9-](https://doi.org/10.5194/amt-9-313-2016)  
 2340 [313-2016](https://doi.org/10.5194/amt-9-313-2016), 2016a.
- 2341 Chubarova, N., Zhdanova, Y., and Nezval, Y.: A new parameterization of the UV irradiance altitude  
 2342 dependence for clear-sky conditions and its application in the on-line UV tool over Northern Eurasia, *Atmos.*  
 2343 *Chem. Phys.*, **16**, 11867–11881, <https://doi.org/10.5194/acp-16-11867-2016>, 2016b.
- 2344 Chubarova, N. E., Pastukhova, A. S., and Galin, V. Y.: Long-Term Variability of UV Irradiance in the  
 2345 Moscow Region according to Measurement and Modeling Data, *Izv. Atmos. Ocean. Phys.*, **54**, 139–146,  
 2346 <https://doi.org/10.1134/S0001433818020056>, 2018.
- 2347 Chubarova, N. E., Androsova, E. E., Kirsanov, A. A., Vogel, B., Vogel, H., Popovicheva, O. B., and Rivin,  
 2348 G. S.: Aerosol and Its Radiative Effects during the Aeroradcity 2018 Moscow Experiment, *Geography,*  
 2349 *Environment, Sustainability*, **12**, 114–131, <https://doi.org/10.24057/2071-9388-2019-72> 2019a.
- 2350 Chubarova, N. E., Timofeev, Y. M., Virolainen, Y. A., and Polyakov, A. V.: Estimates of UV indices during  
 2351 the periods of reduced ozone content over Siberia in Winter-Spring 2016, *Atmos. Oceanic Opt.*, **32**, 177–179,  
 2352 [doi:10.1134/s1024856019020040](https://doi.org/10.1134/s1024856019020040), 2019b.
- 2353 Chubarova, N. E., Pastukhova, A.S., Zhdanova, E.Y., Volpert, E.V., Smyshlyaev and S.P., and Galin, V.Y.:  
 2354 Effects of Ozone and Clouds on Temporal Variability of Surface UV Radiation and UV Resources over  
 2355 Northern Eurasia Derived from Measurements and Modeling., *Atmosphere*, **11**, 59, 2020.
- 2356 Cohen, J., X. Zhang, T., Jung, R. Kwok, J., Overland, T., Ballinger, U.S., Bhatt, H. W., Chen, D., Coumou,  
 2357 S., Feldstein, H., Gu, D., Handorf, G., Henderson, M., Ionita, M., Kretschmer, F., Laliberte, S., Lee, H. W.,  
 2358 Linderholm, W., Maslowski, Y., Peings, K., Pfeiffer, I., Rigor, T., Semmler, J., Stroeve, P.C., Taylor, S.,  
 2359 Vavrus, T., Vihma, S., Wang, M., Wendisch, Y., Wu, and Yoon, J.: Divergent consensus on Arctic  
 2360 amplification influence on midlatitude severe winter weather. *Nature Climate Change*, **10**, 20–29,  
 2361 [doi:10.1038/s41558-019-0662-y](https://doi.org/10.1038/s41558-019-0662-y), 2020.
- 2362 Collins, M., Knutti, R., Arblaster, J., Dufresne, J.-L., Fichet, T., Friedlingstein, P., Gao, X., Gutowski,  
 2363 W.J., Johns, T., Krinner, G., Shongwe, M., Tebaldi, C., Weaver, A.J., and Wehner, M.: Long-term climate  
 2364 change: Projections, commitments and irreversibility, in *Climate Change 2013: The Physical Science Basis.*  
 2365 Contribution of Working Group I to the Fifth Assessment Report of the Intergovernmental Panel on Climate  
 2366 Change, edited by: Stocker, T.F., Qin, D., Plattner, G.-K., Tignor, M., Allen, S.K., Doschung, J., Nauels,



- 2367 A., Xia, Y., Bex, V., and Midgley, P.M., Cambridge University Press, Cambridge, United-Kingdom, 1029-  
2368 1136, doi:10.1017/CBO9781107415324.024, 2013.
- 2369 Commane, R., Lindaas, J., Benmergui, J., Luus K. A., Chang, R. Y.-W., Daube, B. C., Euskirchen, E. S.,  
2370 Henderson, J. M., Karion, A., Miller, J. B., Miller, S. M., Parazoo, N. C., Randerson, J. T., Sweeney, C.,  
2371 Tans, P., Thoning, K., Veraverbeke, S., Miller, C. E., and Wofsy, S. C.: Carbon dioxide sources from Alaska  
2372 driven by increasing early winter respiration from Arctic tundra, *PNAS*, 114(21), 5361-5366, 2017.
- 2373 Coumou, C., Petoukhov, V., Rahmstorf, S., Petri, S., and Schellnhuber, H.-J.: Quasi-resonant circulation  
2374 regimes and hemispheric synchronization of extreme weather in boreal summer, *Proc. Natl. Acad. Sci.*, 111,  
2375 12 331–12336, <https://doi.org/10.1073/pnas.1412797111>, 2014.
- 2376 Dada, L., Paasonen, P., Nieminen, T., Buenrostro Mazon, S., Kontkanen, J., Peräkylä, O., Lehtipalo, K.,  
2377 Hussein, T., Petäjä, T., Kerminen, V.-M., Bäck, J. and Kulmala, M.: Long-term analysis of clear-sky new  
2378 particle formation events and nonevents in Hyytiälä, *Atmos. Chem. Phys.*, 17, 6227-6241, 2017.
- 2379 Dada, L., Chellapermal, R., Buenrostro Mazon, S., Paasonen, P., Lampilahti, J., Manninen, H. E., Junninen,  
2380 H., Petäjä, T., Kerminen, V.-M., and Kulmala, M.: Refined classification and characterization of atmospheric  
2381 new-particle formation events using air ions, *Atmos. Chem. Phys.*, 18, 17883–17893,  
2382 <https://doi.org/10.5194/acp-18-17883-2018>, 2018.
- 2383 Dagsson-Waldhauserova, P., Meinander, O.: Atmosphere-cryosphere interaction in the Arctic, at high  
2384 latitudes and mountains with focus on transport, deposition and effects of dust, black carbon, and other  
2385 aerosols., *Front. Earth Sci.*, 7, 337, <https://www.frontiersin.org/articles/10.3389/feart.2019.00337/full>, 2019.
- 2386 Dave, B., and Kobayashi, Y.: China's silk road economic belt initiative in Central Asia: economic and  
2387 security implications, *Asia Europe Journal*, 16, 1-15. doi:10.1007/s10308-018-0513-x, 2018.
- 2388 Davy, R., and Esau, I.: Differences in the efficacy of climate forcings explained by variations in atmospheric  
2389 boundary layer depth, *Nat. Commun.*, 7, 8, doi:10.1038/ncomms11690, 2016.
- 2390 Davy, R., Esau, I., Chernokulsky, A., Outten, S., and Zilitinkevich, S.: Diurnal asymmetry to the observed  
2391 global warming, *Int. J. Climatol.*, 37, 79-93, doi:10.1002/joc.4688, 2017.
- 2392 Dean, J. F., Middelburg, J. J., Röckmann, T., Aerts, R., Blauw, L. G., Egger, M., Jetten, M. S. M., de Jong,  
2393 A. E. E., Meisel, O. H., Rasigraf, O., Slomp, C. P., in't Zandt, M. H., and Dolman, A. J.: Methane feedbacks  
2394 to the global climate system in a warmer world, *Rev. Geophys.*, 56(1), 207-250,  
2395 <https://doi.org/10.1002/2017RG00055>, 2018.
- 2396 Derksen, C., and Brown, R.: Spring snow cover extent reductions in the 2008-2012 period exceeding climate  
2397 model predictions, *Geophys. Res. Lett.*, 39, L19504, 2012.
- 2398 Derome, J., and Lukina, N.: Interaction between environmental pollution and land-cover/land-use change in  
2399 Arctic areas, in: *Eurasian Arctic Land Cover and Land Use in a Changing Climate*, edited by: Gutman, G.,  
2400 and Reissell, A., 6, 269–290, Springer, Amsterdam, Netherlands, 2011.

- 2401 Ding, A. J., Huang, X., Nie, W., Sun, J. N., Kerminen, V.-M., Petäjä, T., Su, H., Chen, Y. F., Yang, X.-Q.,  
 2402 Wang, M. H., Chi, X. G., Wang, J. P., Virkkula, A., Guo, W. D., Yuan, J., Wang, S. Y., Zhang, R. J., Wu, Y.  
 2403 F., Song, Y. Zhu, T., Zilitinkevich, S., Kulmala, M., and Fu, C. B.: Enhanced haze pollution by black carbon  
 2404 in megacities in China, *Geophys. Res. Lett.*, 43, 2873-2879, doi:10.1002/2016GL067745, 2016a.
- 2405 Ding, A. J., Nie, W., Huang, X., Chi, X., Sun, J., Kerminen, V.-M., Xu, Z., Guo, W., Petäjä, T., Yang, X.,  
 2406 Kulmala, M., and Fu, G.: Long-term observation of pollution-weather/climate interactions at the SORPES  
 2407 station: a review and outlook, *Front. Environ. Sci. Eng.*, 10, doi:10.1007/s11783-016-0877-3, 2016b.
- 2408 Dou, T., Xiao, C., Liu, J., Han, W., Du, Z., Mahoney, A. R., Jones, J., and Eicken, H.: A key factor initiating  
 2409 surface ablation of Arctic sea ice: earlier and increasing liquid precipitation, *The Cryosphere*, 13, 1233–  
 2410 1246, <https://doi.org/10.5194/tc-13-1233-2019>, 2019.
- 2411 Dragosics, M., Meinander, O., Jonsdottir, T., Durig, T., De Leeuw, G., Palsson, F., Dagsson-Waldhauserová,  
 2412 P., and Thorsteinsson, T.: Insulation effects of Icelandic dust and volcanic ash on snow and ice, *Arab. J.*  
 2413 *Geosci.*, 9, 126, DOI:10.1007/s12517-015-2224-6, 2016.
- 2414 Duporte, G., Parshintsev, J., Barreira, L. M. F., Hartonen, K., Kulmala, M., and Riekkola, M. L.: Nitrogen-  
 2415 containing low volatile compounds from pinonaldehyde-dimethylamine reaction in the atmosphere: a  
 2416 laboratory and field study, *Environ. Sci. Technol.*, 50(9), 4693-4700, doi:10.1021/acs.est.6b00270, 2016.
- 2417 Durairaj, P., Sarangi, R., Ramalingam, S., Thirunavukarassu, T., and Chauhan, P.: Seasonal nitrate  
 2418 algorithms for nitrate retrieval using OCEANSAT-2 and MODIS-AQUA satellite data, *Environ. Monit.*  
 2419 *Assess.*, 187, 176-189, doi: 10.1007/s10661-015-4340-x, 2015.
- 2420 Dyukarev, E.A., Godovnikov, E.A., Karpov, D.V., Kurakov, S.A., Lapshina, E.D., Filippov, I.V., Filippova,  
 2421 N.V., and Zarov, E.A.: Net ecosystem exchange, gross primary production and ecosystem respiration in  
 2422 ridge-hollow complex at Mukhrino Bog, *Geography, Environment, Sustainability*, 12(2), 227-244,  
 2423 doi.10.24057/2071-9388-2018-77, 2019.
- 2424 Elansky, N. F., Lavrova, O. V., Skorokhod, A. I., and Belikov, I. B.: Trace gases in the atmosphere over  
 2425 Russian cities, *Atmos. Environ.*, 143, 108-119, doi:10.1016/j.atmosenv.2016.08.046, 2016.
- 2426 Esau, I., Miles, V. V., Davy, R., Miles, M. W., and Kurchatova, A.: Trends in normalized difference  
 2427 vegetation index (NDVI) associated with urban development in northern West Siberia, *Atmos. Chem. Phys.*,  
 2428 16, 9563–9577, <https://doi.org/10.5194/acp-16-9563-2016>, 2016.
- 2429 Esau, I., Varentsov, M., Laruelle, M., Miles, M. W., Konstantinov, P., Soromotin, A., Baklanov, A. A., and  
 2430 Miles, V. V.: Warmer Climate of Arctic Cities, Chapter 3 in the monography “The Arctic: Current Issues and  
 2431 Challenges”, Edited by: Pokrovsky, O., NOVA Publishers, ISBN: 978-1-53617-306-2,  
 2432 <https://novapublishers.com/shop/the-arctic-current-issues-and-challenges/>, 2020.
- 2433 Euskirchen, E. S., Bret-Harte, M. S., Shaver, G. R., Edgar, C. W., and Romanovsky, V. E.: Long-term  
 2434 release of carbon dioxide from arctic tundra ecosystems in northern Alaska, *Ecosystems*, 1–15, 2017.

- 2435 Evangeliou, N., Shevchenko, V. P., Yttri, K. E., Eckhardt, S., Sollum, E., Pokrovsky, O. S., Kobelev, V. O.,  
2436 Korobov, V. B., Lobanov, A. A., Starodymova, D. P., Vorobiev, S. N., Thompson, R. L., and Stohl, A.:  
2437 Origin of elemental carbon in snow from western Siberia and northwestern European Russia during winter–  
2438 spring 2014, 2015 and 2016, *Atmos. Chem. Phys.*, 18, 963–977, <https://doi.org/10.5194/acp-18-963-2018>,  
2439 2018.
- 2440 Ezhova, E., Orlov, D., Suhonen, E., Kaverin, D., Mahura, A., Gennadinik, V., Kukkonen, I., Drozdov, D.,  
2441 Lappalainen, H. K., Melnikov, V., Petäjä, T., Kerminen, V.-M., Zilitinkevich, S., Malkhazova, S. M.,  
2442 Christensen, T. R., and Kulmala, M.: Climatic Factors Influencing the Anthrax Outbreak of 2016 in Siberia,  
2443 Russia. *EcoHealth*, <https://doi.org/10.1007/s10393-021-01549-5>, 2021.
- 2444 Ezhova, E., Kerminen, V.-M., Lehtinen, K. E. J., and Kulmala, M.: A simple model for the time evolution of  
2445 the condensation sink in the atmosphere for intermediate Knudsen numbers, *Atmos. Chem. Phys.*, 18, 2431–  
2446 2442, <https://doi.org/10.5194/acp-18-2431-2018>, 2018a.
- 2447 Ezhova, E., Ylivinkka, I., Kuusk, J., Komsaare, K., Vana, M., Krasnova, A., Noe, S., Arshinov, M., Belan,  
2448 B., Park, S.-B., Lavrič, J. V., Heimann, M., Petäjä, T., Vesala, T., Mammarella, I., Kolari, P., Bäck, J.,  
2449 Rannik, Ü., Kerminen, V.-M., and Kulmala, M.: Direct effect of aerosols on solar radiation and gross  
2450 primary production in boreal and hemiboreal forests, *Atmos. Chem. Phys.*, 18, 17863–17881,  
2451 <https://doi.org/10.5194/acp-18-17863-2018>, 2018b.
- 2452 Fang, K., Makkonen, R., Guo, Z., and Seppä, H.: An increase in the biogenic aerosol concentration as a  
2453 contributing factor to the recent wetting trend in Tibetan Plateau. *Sci Rep* 5, 14628,  
2454 <https://doi.org/10.1038/srep14628>, 2015.
- 2455 Fang, Y., Changyou, L., Leppäranta, M., Xiaonghong, S., Shengnan, Z., and Chengfu, Z.: Notable increases  
2456 in nutrient concentrations in a shallow lake during seasonal ice growth, *Water Science and Technology*,  
2457 74(12), 2773-2783, 2016.
- 2458 Fang, K. , Makkonen, R. , Guo, Z , Zhao , Y., and Seppä, H.: An increase in the biogenic aerosol  
2459 concentration as a contributing factor to the recent wetting trend in Tibetan Plateau, *Scientific Reports* , 5 ,  
2460 14628, DOI: 10.1038/srep14628, 2015.
- 2461 Fletcher, S. E. M., and Schaefer, H.: Rising methane: a new climate challenge, *Science*, 364, 932-933, 2019.
- 2462 Franz, D., Mammarella, I., Boike, J., Kirillin, G., Vesala, T., Bornemann, N., Larmanou, E., Langer, M., and  
2463 Sachs, T.: Lake-Atmosphere Heat Flux Dynamics of a Thermokarst Lake in Arctic Siberia, *J. Geophys. Res.:*  
2464 *Atmos.*, 123(10), 5222-5239, doi:10.1029/2017jd027751, 2018.
- 2465 Freud, E., Krejci, R., Tunved, P., Leaitch, R., Nguyen, Q. T., Massling, A., Skov, H., and Barrie, L.: Pan-  
2466 Arctic aerosol number size distributions: seasonality and transport patterns, *Atmos. Chem. Phys.*, 17, 8101–  
2467 8128, <https://doi.org/10.5194/acp-17-8101-2017>, 2017.

- 2468 Frolova, N.L., Belyakova, P.A., Grigoriev, V.Y. *et al.* : Runoff fluctuations in the Selenga River Basin, Reg  
 2469 Environ Change, 17, 1965–1976, [doi.org/10.1007/s10113-017-1199-0](https://doi.org/10.1007/s10113-017-1199-0), 2017.
- 2470
- 2471 Fu, B. J., and Forsius, M.: Ecosystem services modeling in contrasting landscapes, *Landscape Ecol.*, 30(3),  
 2472 375-379, doi:10.1007/s10980-015-0176-6, 2015.
- 2473 Garmaev, E. Z., Kulikov, A. I., Tsydypov, B. Z., Sodnomov, B. V., and Ayurzhanayev, A. A.: Environmental  
 2474 Conditions Of Zakamensk Town (Dzhida River Basin Hotspot), *Geography, Environment,  
 2475 Sustainability*,12(3), 224-239, <https://doi.org/10.24057/2071-9388-2019-32>, 2019.
- 2476 Georgiadi, A. G., Koronkevich, N. I., Milyukova, I. P., and Barabanova, E. A.: Integrated projection for  
 2477 runoff changes in large Russian river basins in the XXI Century, *Geography, Environment, Sustainability*,  
 2478 9(2), 38-46, 2016.
- 2479 GGO: Air quality in cities of Russia during the year 2015, St. Petersburg, Voeikov Main Geophysical  
 2480 Observatory, RosHydroMet, 2016.
- 2481 Giamarelou, M., Eleftheriadis, K., Nyeki, S., Tunved, P., Torseth, K., and Biskos, G.: Indirect evidence of  
 2482 the composition of nucleation mode atmospheric particles in the high Arctic, *J. Geophys. Res.: Atmos.*,  
 2483 121(2), 965-975, doi:10.1002/2015jd023646, 2016.
- 2484 Gil, J., Pérez, T., Boering, K., Martikainen, P. J., and Biasi, C.: Mechanisms responsible for high N<sub>2</sub>O  
 2485 emissions from subarctic permafrost peatlands studied via stable isotope techniques, *Global Biogeochem.  
 2486 Cycles*, 31(1), 172, doi:10.1002/2015GB005370, 2017.
- 2487 Glagolev, M.V., Ilyasov, D. V. I., Terentieva, E., Sabrekov, A. F., Yu Mochenov, S., and Maksutov, S. S.:  
 2488 Methane and carbon dioxide fluxes in the waterlogged forests of south and middle taiga of Western Siberia,  
 2489 *IOP Conf. Ser.: Earth Environ. Sci.*, 138 012005, 2018.
- 2490 Gnatiuk, N., Radchenko, I., Davy, R., Morozov E., and Bobylev, L.: Simulation of factors affecting  
 2491 *Emiliana huxleyi* blooms in Arctic and sub-Arctic seas by CMIP5 climate models: model validation and  
 2492 selection, *Biogeosciences*, 17, 1199–1212. doi: 10.5194/bg-17-1199-2020, 2020.
- 2493 Godrijan, J., Drapeau, D., and Balch, W. M.: Mixotrophic uptake of organic compounds by coccolithophores,  
 2494 *Limnol. Ocean.*, Early bird publication, <https://doi.org/10.1002/lno.11396>, 2020.
- 2495 Gordov, E.P., Okladnikov, I.G., Titov, A.G., Voropay N.N., Ryazanova A.A., and Lykosov V.N.:  
 2496 Development of Information-computational Infrastructure for Modern Climatology, *Russ. Meteorol. Hydrol.*,  
 2497 43, 722–728, <https://doi.org/10.3103/S106837391811002X>, 2018.
- 2498 Granath, G., Rydin, H., Baltzer, J. L., Bengtsson, F., Boncek, N., Bragazza, L., Bu, Z.-J., Caporn, S. J. M.,  
 2499 Dorrepaal, E., Galanina, O., Gałka, M., Ganeva, A., Gillikin, D. P., Goia, I., Goncharova, N., Hájek, M.,  
 2500 Haraguchi, A., Harris, L. I., Humphreys, E., Jiroušek, M., Kajukało, K., Karofeld, E., Koronova, N. G.,

- 2501 Kosykh, N. P., Lamentowicz, M., Lapshina, E., Limpens, J., Linkosalmi, M., Ma, J.-Z., Mauritz, M., Munir,  
2502 T. M., Natali, S. M., Natcheva, R., Noskova, M., Payne, R. J., Pilkington, K., Robinson, S., Robroek, B. J.  
2503 M., Rochefort, L., Singer, D., Stenøien, H. K., Tuittila, E.-S., Vellak, K., Verheyden, A., Waddington, J. M.,  
2504 and Rice, S. K.: Environmental and taxonomic controls of carbon and oxygen stable isotope composition in  
2505 Sphagnum across broad climatic and geographic ranges, *Biogeosciences*, 15, 5189–5202,  
2506 <https://doi.org/10.5194/bg-15-5189-2018>, 2018.
- 2507 Grigoriev, V.Y., and Frolova, N.L.: Terrestrial water storage change of European Russia and its impact on  
2508 water balance, *Geography, Environment, Sustainability*, 11(1), 38-50. [https://doi.org/10.24057/2071-9388-](https://doi.org/10.24057/2071-9388-2018-11-1-38-50)  
2509 [2018-11-1-38-50](https://doi.org/10.24057/2071-9388-2018-11-1-38-50), 2018.
- 2510 Groundstroem, F., and Juhola, S.: A framework for identifying cross-border impacts of climate change on  
2511 the energy sector, *Environment Systems and Decisions*, 39(1), 3-15, doi:10.1007/s10669-018-9697-2, 2019.
- 2512 Gunchin, G., Manousakas, M., Osan, J., Karydas, A. G., Eleftheriadis, K., Lodoysamba, S., Shagjjamba, D.,  
2513 Migliori, A., Padilla-Alvarez, R., Strelis, C., and Darby, I.: Three-year long source apportionment study of  
2514 airborne particles in Ulaanbaatar using x-ray fluorescence and positive matrix factorization, *Aerosol and Air*  
2515 *Quality Research*, 19(5), 1056-1067, doi:10.4209/aaqr.2018.09.0351, 2019.
- 2516 Guo, Y., Yan, C., Li, C., Feng, Z., Zhou, Y., Lin, Z., Dada, L., Stolzenburg, D., Yin, R., Kontkanen, J.,  
2517 Daellenbach, K. R., Kangasluoma, J., Yao, L., Chu, B., Wang, Y., Cai, R., Bianchi, F., Liu, Y., and Kulmala,  
2518 M.: Formation of Nighttime Sulfuric Acid from the Ozonolysis of Alkenes in Beijing, *Atmos. Chem. Phys.*  
2519 *Discuss.*, <https://doi.org/10.5194/acp-2019-1111>, in review, 2020.
- 2520 Gurchenkov, A. A., Murynin, A. B., Trekin, A. N., and Ignatyev, V. Y.: Object-oriented classification of  
2521 substrate surface objects in Arctic impact regions aerospace monitoring, *Herald of the Bauman Moscow*  
2522 *State Technical University*, 135-146. doi:10.18698/1812-3368-2017-3-135-146, 2017.
- 2523 Göckede, M., Kittler, F., Kwon, M. J., Burjack, I., Heimann, M., Kolle, O., Zimov, N., and Zimov, S.:  
2524 Shifted energy fluxes, increased Bowen ratios, and reduced thaw depths linked with drainage-induced  
2525 changes in permafrost ecosystem structure, *The Cryosphere*, 11, 2975–2996, [https://doi.org/10.5194/tc-11-](https://doi.org/10.5194/tc-11-2975-2017)  
2526 [2975-2017](https://doi.org/10.5194/tc-11-2975-2017), 2017.
- 2527 Göckede, M., Kwon, M. J., Kittler, F., Heimann, M., Zimov, N., and Zimov, S.: Negative feedback processes  
2528 following drainage slow down permafrost degradation, *Glob. Change Biol.*, 25, 3254– 3266,  
2529 <https://doi.org/10.1111/gcb.14744>, 2019.
- 2530 Hao, L., Garmash, O., Ehn, M., Miettinen, P., Massoli, P., Mikkonen, S., Jokinen, T., Roldin, P., Aalto, P.,  
2531 Yli-Juuti, T., Joutsensaari, J., Petäjä, T., Kulmala, M., Lehtinen, K. E. J., Worsnop, D. R., and Virtanen, A.:  
2532 Combined effects of boundary layer dynamics and atmospheric chemistry on aerosol composition during  
2533 new particle formation periods, *Atmospheric Chemistry and Physics*, 18(23), 17705-17716. doi:10.5194/acp-  
2534 [18-17705-2018](https://doi.org/10.5194/acp-18-17705-2018), 2018.

- 2535 Hari, P. & Kulmala, M.: Station for Measuring Ecosystem–Atmosphere Relations (SMEAR II). *Boreal Env.*  
2536 *Res.* 10: 315–322, 2005.
- 2537
- 2538 Hari, P., Andreae M., Kabat P., and Kulmala M.: A comprehensive network of measuring stations to  
2539 monitor climate change. *Boreal Env. Res.* 14: 442-446, 2009.
- 2540
- 2541 Hari, P., Petäjä, T., Bäck, J., Kerminen, V.-M., Lappalainen, H. K., Vihma, T., Laurila, T., Viisanen, Y.,  
2542 Vesala, T., and Kulmala, M.: Conceptual design of a measurement network of the global change, *Atmos.*  
2543 *Chem. Phys.*, 16, 1017-1028, doi:10.5194/acp-16-1017-2016, 2016.
- 2544 Hari, P., Kerminen, V.-M., Kulmala, L., Kulmala, M., Noe, S., Petäjä, T., Vanhatalo, A., and Bäck, J.:  
2545 Annual cycle of Scots pine photosynthesis, *Atmos. Chem. Phys.*, 17, 15045–15053, doi:10.5194/acp-17-  
2546 15045-2017, 2017.
- 2547 Heikkilä, A., Makelä, J. S., Lakkala, K., Meinander, O., Kaurola, J., Koskela, T., Karhu, J. M., Karppinen,  
2548 T., Kyrö, E., and De Leeuw, G.: In search of traceability: two decades of calibrated Brewer UV  
2549 measurements in Sodankyla and Jokioinen, *Geoscientific Instrumentation, Methods and Data Systems*, 5(2),  
2550 531-540, doi:10.5194/gi-5-531-2016, 2016.
- 2551 Heintzenberg, J., Tunved, P., Galí, M., and Leck, C.: New particle formation in the Svalbard region 2006–  
2552 2015, *Atmos. Chem. Phys.*, 17, 6153–6175, doi:10.5194/acp-17-6153-2017, 2017.
- 2553 Helin, A., Sietiö, O.-M., Heinonsalo, J., Bäck, J., Riekkola, M.-L., and Parshintsev, J.: Characterization of  
2554 free amino acids, bacteria and fungi in size-segregated atmospheric aerosols in boreal forest: seasonal  
2555 patterns, abundances and size distributions, *Atmos. Chem. Phys.*, 17, 13089–13101, doi.org/10.5194/acp-17-  
2556 13089-2017, 2017.
- 2557 Hellén, H., Praplan, A. P., Tykkä, T., Ylivinkka, I., Vakkari, V., Bäck, J., Petäjä, T., Kulmala, M., and  
2558 Hakola, H.: Long-term measurements of volatile organic compounds highlight the importance of  
2559 sesquiterpenes for the atmospheric chemistry of a boreal forest, *Atmos. Chem. Phys.*, 18, 13839–13863,  
2560 <https://doi.org/10.5194/acp-18-13839-2018>, 2018.
- 2561 Hinzman, L.D., Bettez, N.D., Bolton, W.R. et al. :Evidence and Implications of Recent Climate Change in  
2562 Northern Alaska and Other Arctic Regions, *Climatic Change*, 72, 251–298, [doi.org/10.1007/s10584-005-](https://doi.org/10.1007/s10584-005-5352-2)  
2563 [5352-2](https://doi.org/10.1007/s10584-005-5352-2), 2005.
- 2564 Hoegh-Guldberg, O., Jacob, D., Taylor, M., Bindi, M., Brown, S., Camilloni, I., Diedhiou, A.,  
2565 Djalante, R., Ebi, K. L., Engelbrecht, F., Guiot, J., Hijioka, Y., Mehrotra, S., Payne, A., Seneviratne, S. I.,  
2566 Thomas, A., Warren, R., and Zhou, G.: Impacts of 1.5°C Global Warming on Natural and Human Systems,  
2567 in: *Global Warming of 1.5°C: An IPCC Special Report on the impacts of global warming of 1.5°C above*  
2568 *pre-industrial levels and related global greenhouse gas emission pathways, in the context of*  
2569 *strengthening the global response to the threat of climate change, sustainable development, and efforts to*

- 2570 eradicate poverty, edited by: Masson-Delmotte, V., Zhai, P., Pörtner, H.-O., Roberts, D., Skea, J., Shukla, P.  
 2571 R., Pirani, A., Moufouma-Okia, W., Péan, C., Pidcock, R., Connors, S., Matthews, J. B. R., Chen, Y., Zhou,  
 2572 X., Gomis, M. I., Lonnoy, E., Maycock, T., Tignor, M., and Waterfield, T., WMO, Geneva, Switzerland,  
 2573 2018.
- 2574 Hong, J., Kim, J., Nieminen, T., Duplissy, J., Ehn, M., Äijälä, M., Hao, L. Q., Nie, W., Sarnela, N., Prisle, N.  
 2575 L., Kulmala, M., Virtanen, A., Petäjä, T., and Kerminen, V.-M.: Relating the hygroscopic properties of  
 2576 submicron aerosol to both gas- and particle-phase chemical composition in a boreal forest environment,  
 2577 *Atmos. Chem. Phys.*, 15, 11999–12009, <https://doi.org/10.5194/acp-15-11999-2015>, 2015.
- 2578 Huang, W., Cheng, B., Zhang, J., Zhang, Z., Vihma, T., Li, Z., and Niu, F.: Modeling experiments on  
 2579 seasonal lake ice mass and energy balance in the Qinghai–Tibet Plateau: a case study, *Hydrol. Earth Syst.*  
 2580 *Sci.*, 23, 2173–2186, 2019a.
- 2581 Huang, W., Zhang, J., Leppäranta, M., Li, Z., Cheng, B. and Lin, Z. 2019b. Thermal structure and water-ice  
 2582 heat transfer in a shallow ice–covered thermokarst lake in central Qinghai-Tibet Plateau, *Journal of*  
 2583 *Hydrology*, 578, [124122], 2019b.
- 2584 Hölttä, T., Lintunen, A., Chan, T., Mäkelä, A., and Nikinmaa, E.: A steady state stomatal model of balanced  
 2585 leaf gas exchange, hydraulics and maximal source-sink flux, *Tree Physiology*, 37, 851–868, doi:  
 2586 10.1093/treephys/tpx011, 2017.
- 2587 IPCC: Special Report on the Ocean and Cryosphere in a Changing Climate, edited by Pörtner, H.-O.,  
 2588 Roberts, D.C., Masson-Delmotte, V., Zhai, P., Tignor, M., Poloczanska, E., Mintenbeck, K., Alegría, A.,  
 2589 Nicolai, M., Okem, A., Petzold, J., Rama, B., and Weyer, N. M., 2019.
- 2590 IPCC, 2021: Climate Change 2021: The Physical Science Basis. Contribution of Working Group I to the  
 2591 Sixth Assessment Report of the Intergovernmental Panel on Climate Change[Masson-Delmotte, V., P. Zhai,  
 2592 A. Pirani, S. L. Connors, C. Péan, S. Berger, N. Caud, Y. Chen, L. Goldfarb, M. I. Gomis, M. Huang, K.  
 2593 Leitzell, E. Lonnoy, J.B.R. Matthews, T. K. Maycock, T. Waterfield, O. Yelekçi, R. Yu and B. Zhou (eds.)].  
 2594 Cambridge University Press. In Press. Summary for Policymakers IPCC, 2021: Summary for Policymakers.  
 2595 In: Climate Change 2021: The Physical Science Basis. Contribution of Working Group I to the Sixth  
 2596 Assessment Report of the Intergovernmental Panel on Climate Change[Masson-Delmotte, V., P. Zhai, A.  
 2597 Pirani, S. L. Connors, C. Péan, S. Berger, N. Caud, Y. Chen, L. Goldfarb, M. I. Gomis, M. Huang, K.  
 2598 Leitzell, E. Lonnoy, J.B.R. Matthews, T. K. Maycock, T. Waterfield, O. Yelekçi, R. Yu and B. Zhou (eds.)].  
 2599 Cambridge University Press. In Press.
- 2600 Ivakhov, V. M., Paramonova, N. N., Privalov, V. I., Zinchenko, A. V., Loskutova, M. A., Makshtas, A. P.,  
 2601 Kustov, V. Y., Laurila, T., Aurela, M., and Asmi, E.: Atmospheric Concentration of Carbon Dioxide at Tiksi  
 2602 and Cape Baranov Stations in 2010–2017, *Russ. Meteorol. Hydrol.*, 44, 291–299,  
 2603 doi:10.3103/s1068373919040095, 2019.

- 2604 Jaffe, D., Bertschi, I., Jaegle, L., Novelli, P., Reid, J. S., Tanimoto, H., Vingarzan, R. and Westphal, D. L.:  
2605 Long-range transport of Siberian biomass burning emissions and impact on surface ozone in western North  
2606 America, *Geophys. Res. Lett.*, 31(16), L16106, doi:10.1029/2004GL020093, 2004.
- 2607 Jakobson, L., T. Vihma, and E. Jakobson,: Relationships between Sea Ice Concentration and Wind Speed  
2608 over the Arctic Ocean during 1979–2015., *J. Climate*, 32, 7783–7796, [https://doi.org/10.1175/JCLI-D-19-](https://doi.org/10.1175/JCLI-D-19-0271.1)  
2609 0271.1, 2019.
- 2610 Juhola, S.: Planning for a green city: The Green Factor tool, *Urban Forestry and Urban Greening*, 34, 254-  
2611 258, doi:10.1016/j.ufug.2018.07.019, 2018.
- 2612 Juutinen, S., Virtanen, T., Kondratyev, V., Laurila, T., Linkosalmi, M., Mikola, J., Nyman, J., Räsänen, A.,  
2613 Tuovinen, J.-P., and Aurela, M.: Spatial variation and seasonal dynamics of leaf-area index in the arctic  
2614 tundra-implications for linking ground observations and satellite images, *Environ. Res. Lett.*, 12(9), 10,  
2615 doi:10.1088/1748-9326/aa7f85, 2017.
- 2616 Kalogridis, A.C., Popovicheva, O.B., Engling, G., Diapouli, E., Kawamura, K., Tachibana, E., Ono, K.,  
2617 Kozlov, V.S., and Eleftheriadis, K.: Smoke aerosol chemistry and aging of Siberian biomass burning  
2618 emissions in a large aerosol chamber, *Atmos. Environ.*, 185,15-28, 2018.
- 2619 Kangasluoma, J., Ahonen, L. R., Laurila, T., Cai, R., Enroth, J., Mazon, S., Korhonen, F., Aalto, P.,  
2620 Kulmala, M., Attoui, M. and Petäjä, T.: Laboratory verification of a new high flow differential mobility  
2621 particle sizer, and field measurements in Hyytiälä, *J Aerosol Sci*, 124, 1-9, 2018.
- 2622 Karelin, D. V., Goryachkin, S. V., Zamolodchikov, D. G., Dolgikh, A. V., Zazovskaya, E. P., Shishkov, V.  
2623 A., and Kraev, G. N.: Human footprints on greenhouse gas fluxes in cryogenic ecosystems, *Dokl. Earth Sc.*,  
2624 477, 1467–1469, doi:10.1134/S1028334X17120133, 2017.
- 2625 Karetnikov, S., Leppäranta, M., and Montonen, A.: A time series of over 100 years of ice seasons on Lake  
2626 Ladoga, *Journal of Great Lakes Research*, 43(6), 979-988, doi:10.1016/j.jglr.2017.08.010, 2017.
- 2627 Karthe, D., Abdullaev, I., Boldgiv, B., Borchardt, D., Chalov, S., Jarsjö, J., Li, L., and Nittrouer, J.A.: Water  
2628 in Central Asia: an integrated assessment for science-based management, *Environmental Earth Sciences*,  
2629 76(20), 15, doi:10.1007/s12665-017-6994-x, 2017a.
- 2630 Karthe, D., Chalov, S., Moreido, V., Pashkina, M., Romanchenko, A., Batbayar, G., Kalugin, A., Westphal,  
2631 K., Malsy, M., and Flörke, M.: Assessment of runoff, water and sediment quality in the Selenga River basin  
2632 aided by a web-based geoservice, *Water Resources*, 44(3), 399-416, 2017b.
- 2633 Karthe D., Chalov S., Gradel A., and Kusbach A.: Special issue: Environment change on the Mongolian  
2634 plateau: atmosphere, forests, soils and water, *Geography, Environment, Sustainability*, 12(3), 60-65,  
2635 doi:10.24057/2071-9388-2019-1411, 2019.



- 2636 Karvonen, J., Shi, L., Cheng, B., Similä, M., Mäkynen, M., and Vihma, T.: Bohai Sea ice parameter  
2637 estimation based on thermodynamic ice model and Earth observation data, *Remote Sensing*, 9, 234,  
2638 doi:10.3390/rs9030234, 2017.
- 2639 Kasimov, N., Karthe, D., and Chalov, S.: Environmental change in the Selenga River—Lake Baikal Basin,  
2640 *Reg. Environ. Chang.*, 17, 1945–1949, 2017a.
- 2641 Kasimov, N. S., Kosheleva, N. E., Nikiforova, E. M., and Vlasov, D. V.: Benzo a pyrene in urban  
2642 environments of eastern Moscow: pollution levels and critical loads, *Atmos. Chem. Phys.*, 17(3), 2217–2227,  
2643 doi:10.5194/acp-17-2217-2017, 2017b.
- 2644 Kasimov, N., Shinkareva, G., Lychagin, M., Kosheleva, N., Chalov, S., Pashkina, M., Thorslund, J., and  
2645 Jarsjö, J.: River water quality of the selenga-baikal basin: Part i—spatio-temporal patterns of dissolved and  
2646 suspended metals, *Water*, 12(8), 2137, 2020a.
- 2647
- 2648 Kasimov, N., Shinkareva, G., Lychagin, M., Chalov, S., Pashkina, M., Thorslund, J., and Jarsjö, J.: River  
2649 water quality of the selenga-baikal basin: part ii — metal partitioning under different hydroclimatic  
2650 conditions, *Water*, 12(9), 2392, 2020b.
- 2651
- 2652 Kaus, A., Schäffer, M., Karthe, D., Büttner, O., von Tümpling, W., and Borchardt, D.: Regional patterns of  
2653 heavy metal exposure and contamination in the fish fauna of the Kharaa River basin, Mongolia, *Reg.  
2654 Environ. Change*, 17, 2023–2037, doi: 10.1007/s10113-016-0969-4, 2017.
- 2655 Kazakov, E., Kondrik, D., and Pozdnyakov, D.: A synthetic satellite dataset of the spatio-temporal  
2656 distributions of *Emiliania huxleyi* blooms and their impacts on Arctic and sub-Arctic marine environments  
2657 (1998–2016), *Earth Systems Science Data*, 11, 119–128, doi: 10.5194/essd-11-119-2019, 2019.
- 2658 Kecorius, S., Vogl, T., Paasonen, P., Lampilahti, J., Rothenberg, D., Wex, H., Zeppenfeld, S., van Pinxteren,  
2659 M., Hartmann, M., Henning, S., Gong, X., Welti, A., Kulmala, M., Stratmann, F., Herrmann, H., and  
2660 Wiedensohler, A.: New particle formation and its effect on cloud condensation nuclei abundance in the  
2661 summer Arctic: a case study in the Fram Strait and Barents Sea, *Atmos. Chem. Phys.*, 19, 14339–14364, doi:  
2662 10.5194/acp-19-14339-2019, 2019.
- 2663 Kerminen, V.-M., Chen, X., Vakkari, V., Petäjä, T., Kulmala, M., and Bianchi, F.: Atmospheric new particle  
2664 formation and growth: review of field observations, *Environ. Res. Lett.*, 13, 103003, doi: 10.1088/1748-  
2665 9326/aadf3c, 2018.
- 2666 Kim, J., Kim, H. M., Cho, C.-H., Boo, K.-O., Jacobson, A. R., Sasakawa, M., Machida, T., Arshinov, M.,  
2667 and Fedoseev, N.: Impact of Siberian observations on the optimization of surface CO<sub>2</sub> flux, *Atmos. Chem.  
2668 Phys.*, 17, 2881–2899, <https://doi.org/10.5194/acp-17-2881-2017>, 2017.

- 2669 Kirillin, G., Leppäranta, M., Terzhevik, A., Bernhardt, J., Engelhardt, C., Granin, N., Golosov, S., Efremova,  
2670 T., Palshin, N., Sherstyankin, P., Zdorovenova, G., and Zdorovenov, R.: Physics of seasonally ice-covered  
2671 lakes: major drivers and temporal/spatial scales, *Aquatic Ecol.*, 74, 659–682, 2012.
- 2672 Kirillin, G., Aslamov, I., Leppäranta, M., and Lindgren, E.: Turbulent mixing and heat fluxes under lake ice:  
2673 the role of seiche oscillations, *Hydrology of Earth System Sciences*, 22(12), 6493–6504, doi:10.5194/hess-  
2674 22-6493-2018, 2018.
- 2675 Kirschke, S., Bousquet, P., Ciais, P., Saunois, M., Canadell, J. G., Dlugokencky, E. J., Bergamaschi, P.  
2676 Bergmann, D., Blake, D. R., Bruhwiler, L., Cameron-Smith, P., Castaldi, S., Chevallier, F., Feng, L., Fraser,  
2677 A., Heimann, M., Hodson, E. L., Houweling, S., Josse, B., Fraser, P. J., Krummel, P. B., Lamarque, J.-F.,  
2678 Langenfelds, R. L., Le Quere, C., Naik, V., O’Doherty, S., Palmer, P. I., Pison, I., Plummer, D., Poulter, B.,  
2679 Prinn, R. G., Rigby, M., Ringeval, B., Santini, M., Schmidt, M., Shindell, D. T., Simpson, I. J., Spahni, R.,  
2680 Steele, L. P., Strode, S. A., Sudo, K., Szopa, S., van der Werf, G.R., Voulgarakis, A., van Weele, M., Weiss,  
2681 R. F., Williams, J. E., and Zeng, G.: Three decades of global methane sources and sinks, *Nature Geoscience*,  
2682 6(10), 813–823, doi: 10.1038/ngeo1955, 2013.
- 2683 Kiselev, M. V., Voropay, N. N., and Cherkashina, A. A.: influence of anthropogenic activities on the  
2684 temperature regime of soils of the South-Western Baikal region, *IOP Conf. Ser.: Earth Environ. Sci.*, 381,  
2685 012043, doi: 10.1088/1755-1315/381/1/012043, 2019.
- 2686 Kittler, F., Heimann, M., Kolle, O., Zimov, N., Zimov, S., and Göckede, M.: Long-term drainage reduces  
2687 CO<sub>2</sub> uptake and CH<sub>4</sub> emissions in a Siberian permafrost ecosystem, *Global Biogeochemical Cycles*, 31,  
2688 1704–1717. doi: 10.1002/2017GB005774, 2017.
- 2689 Kiuru, P., Ojala, A., Mammarella, I., Heiskanen, J., Kämäräinen, M., Vesala, T. and Huttula, T.: Effects of  
2690 Climate Change on CO<sub>2</sub> Concentration and Efflux in a Humic Boreal Lake: A Modeling Study, *Journal of*  
2691 *Geophysical Research, Biogeosciences*, 123, 7, 2212–2233, 2018.
- 2692 Kondrik, D., Pozdnyakov, D., and Pettersson, L.: Particulate inorganic carbon production within *E. huxleyi*  
2693 blooms in subpolar and polar seas: a satellite time series study (1998–2013), *International Journal of Remote*  
2694 *Sensing*, 38:22, 6179–6205, doi: 10.1080/01431161.2017.1350304, 2017.
- 2695 Kondrik, D. V., Pozdnyakov, D. V., and Johannessen, O. M.: Satellite evidence that *E. huxleyi*  
2696 phytoplankton blooms weaken marine carbon sinks, *Geophys. Res. Lett.*, 5, 846–854. doi:  
2697 10.1002/2017GL076240, 2018a.
- 2698 Kondrik, D. V., Pozdnyakov, D. V., and Pettersson, L. H.: Tendencies in Coccolithophorid Blooms in Some  
2699 Marine Environments of the Northern Hemisphere according to the Data of Satellite Observations in 1998–  
2700 2013. *Izv. Atmos. Ocean. Phys.*, 53, 955–964, doi: 10.1134/S000143381709016X, 2018b.
- 2701 Kondrik, D. V., Kazakov, E. E., Pozdnyakov, D. V., and Johannessen, O. M.: Satellite evidence for  
2702 enhancement of the column mixing ratio of atmospheric CO<sub>2</sub> over *E. huxleyi* blooms, *Transactions of the*

- 2703 Karelian Research Centre of the Russian Academy of Sciences, *Limnologia i Oceanologia* series, 9, 1-11,  
2704 doi: 10/17076/lim1107, 2019.
- 2705 Konovalov, I. B., Lvova, D. A., Beekmann, M., Jethva, H., Mikhailov, E. F., Paris, J.-D., Belan, B. D.,  
2706 Kozlov, V. S., Ciaïș, P., and Andreae, M. O.: Estimation of black carbon emissions from Siberian fires using  
2707 satellite observations of absorption and extinction optical depths, *Atmos. Chem. Phys.*, 18, 14889–14924,  
2708 doi: 10.5194/acp-18-14889-2018, 2018.
- 2709 Konovalov V., Rets E., and Pimankina N.: Interrelation between glacier summer mass balance and runoff in  
2710 mountain river basins, *Geography, Environment, Sustainability*, 12(1), 23-33, doi: 10.24057/2071-9388-  
2711 2018-26, 2019.
- 2712 Konstantinov, P. I., Grishchenko, M. Y., and Varentsov, M. I.: Mapping urban heat islands of arctic cities  
2713 using combined data on field measurements and satellite images based on the example of the city of Apatity  
2714 (Murmansk Oblast), *Izv. Atmos. Ocean. Phys.*, 51(9), 992-998, doi:10.1134/s000143381509011x, 2015.
- 2715 Konstantinov, P., Varentsov, M., and Esau, I.: A high density urban temperature network deployed in several  
2716 cities of Eurasian Arctic, *Environ. Res. Lett.*, 13(7), 12, doi:10.1088/1748-9326/aacb84, 2018.
- 2717 Kontkanen, J., Paasonen, P., Aalto, J., Back, J., Rantala, P., Petäjä, T., and Kulmala, M.: Simple proxies for  
2718 estimating the concentrations of monoterpenes and their oxidation products at a boreal forest site, *Atmos.*  
2719 *Chem. Phys.*, 16(20), 13291-13307, doi:10.5194/acp-16-13291-2016, 2016.
- 2720 Kontkanen, J., Deng, C., Fu, Y., Dada, L., Zhou, Y., Cai, J., Daellenbach, K.R., Hakala, S., Kokkonen, T.V.,  
2721 Lin, Z., Liu, Y., Wang, Y., Yan, C., Petäjä, T., Jiang, J., Kulmala, M. and Paasonen, P. : Size-resolved  
2722 particle number emissions in Beijing determined from measured particle size distributions, *Atmos. Chem.*  
2723 *Phys.* 20, 11329-11348, 2020.
- 2724 Kooijmans, L. M. J., Sun, W., Aalto, J., Erkkilä, K.M., Maseyk, K., Seibt, U., Vesala, T., Mammarella, I.,  
2725 and Chen, H.: Influences of light and humidity on carbonyl sulfide-based estimates of photosynthesis,  
2726 *Proceedings of the National Academy of Sciences*, 116 (7), 2470-2475, doi:10.1073/pnas.1807600116, 2019.
- 2727 Korneykova, M. V., and Evdokimova, G. A.: Microbiota of the ground air layers in natural and industrial  
2728 zones of the Kola Arctic, *J Environ. Sci. Health A*, 53(3), 271-277, doi:10.1080/10934529.2017.1397444,  
2729 2018a.
- 2730 Korneikova, M. V., Redkina, V. V., and Shalygina, R. R.: Algological and mycological characterization of  
2731 soils under pine and birch forests in the Pasvik Reserve, *Eurasian Soil Science*, 51(2), 211-220,  
2732 doi:10.1134/s1064229318020047, 2018b.
- 2733 Koronatova, N. G., & Milyaeva, E. V.: Plant community succession in post-mined quarries in the northern-  
2734 taiga zone of West Siberia. *Contemporary Problems of Ecology*, 4(5), 513–518, 2011.

- 2735 Kukkonen, I., Ezhova, E., Suhonen, E. A. J., Lappalainen, H. K., Gennadinik, V., Ponomareva, O., Gravis,  
 2736 A., Miles, V., Kulmala, M., Melnikov, V., and Drozdov, D.: Observations and modelling of ground  
 2737 temperature evolution in the discontinuous permafrost zone in Nadym, North-West Siberia, *Permafrost and*  
 2738 *Periglacial Processes*, 1– 17, doi:10.1002/ppp.2040, 2020.
- 2739 Kulmala, M., Vehkamäki, H., Petäjä, T., Dal Maso, M., Lauri, A., Kerminen, V.-M., Birmili, W., and  
 2740 McMurry, P.H.: Formation and growth rates of ultrafine atmospheric particles: a review of observations,  
 2741 *Journal of Aerosol Science*, 35, 143-176, doi:10.1134/S1995425511050, 2004.
- 2742 Kulmala, M.: Atmospheric chemistry: China’s choking cocktail, *Nature*, 526, 497-499,  
 2743 doi:10.1038/526497a, 2015a.
- 2744 Kulmala, M., Lappalainen, H. K., Petäjä, T., Kurten, T., Kerminen, V.-M., Viisanen, Y., Hari, P., Sorvari, S.,  
 2745 Bäck, J., Bondur, V., Kasimov, N., Kotlyakov, V., Matvienko, G., Baklanov, A., Guo, H. D., Ding, A.,  
 2746 Hansson, H.-C., and Zilitinkevich, S.: Introduction: The Pan-Eurasian Experiment (PEEX) –  
 2747 multidisciplinary, multiscale and multicomponent research and capacity-building initiative, *Atmos. Chem.*  
 2748 *Phys.*, 15, 13085-13096, doi:10.5194/acp-15-13085-2015, 2015b.
- 2749 Kulmala, M., Lappalainen, H. K., Petäjä, T., Kerminen, V.-M., Viisanen, Y., Matvienko, G., Melnikov, V.,  
 2750 Baklanov, A., Bondur, V., Kasimov, N., and Zilitinkevich, S.: Pan-Eurasian Experiment (PEEX) Program:  
 2751 Grant Challenges in the Arctic-boreal context, *J. Geography Environment Sustainability*, 2, 5–18, 2016a.
- 2752 Kulmala, M., Petäjä, T., Kerminen, V. M., Kujansuu, J., Ruuskanen, T., Ding, A., Nie, W., Hu, M., Wang,  
 2753 Z., Wu, Z., and Wang, L.: On secondary new particle formation in China, *Front. Environ. Sci. Eng.*, 10, 8,  
 2754 doi:10.1007/s11783-016-0850-1, 2016b.
- 2755 Kulmala, M., Kerminen, V.-M., Petäjä, T., Ding, A. J., and Wang L.: Atmospheric gas-to-particle  
 2756 conversion: why NPF events are observed in megacities?, *Faraday Discuss.*, 200, 271-288,  
 2757 doi:10.1039/c6fd00257a, 2017.
- 2758 Kulmala, M.: Build a global Earth observatory, *Nature*, 553, 21-23, doi: 10.1038/d41586-017-08967-y, 2018.
- 2759 Kulmala, L., Pumpanen, J., Kolari, P., Dengel, S., Berninger, F., Köster, K., Matkala, L., Vanhatalo, A.,  
 2760 Vesala, T., and Bäck, J.: Inter- and intra-annual dynamics of photosynthesis differ between forest floor  
 2761 vegetation and tree canopy in a subarctic Scots pine stand, *Agricultural and Forest Meteorology*, 271, 1-11,  
 2762 doi: 10.1016/j.agrformet.2019.02.029, 2019.
- 2763 Kulmala, M., Dada, L., Daellenbach, K. R., Yan, C., Stolzenburg, D., Kontkanen, J., Ezhova, E., Hakala, S.,  
 2764 Tuovinen, S., Kokkonen, T. V., Kurppa, M., Cai, R., Zhou, Y., Yin, R., Baalbaki, R., Chan, T., Chu, B.,  
 2765 Deng, C., Fu, Y., Ge, M., He, H., Heikkinen, L., Junninen, H., Liu, Y., Lu, Y., Nie, W., Rusanen, A.,  
 2766 Vakkari, V., Wang, V., Yang, G., Yao, L., Zheng, J., Kujansuu, J., Kangasluoma, J., Petäjä, T., Paasonen, P.,  
 2767 Järvi, L., Worsnop, D., Ding, A., Liu, Y., Wang, L., Jiang, J., Bianchi, F., and Kerminen, V.-M.: Is reducing

- 2768 new particle formation a plausible solution to mitigate particulate air pollution in Beijing and other Chinese  
2769 megacities?, *Faraday Discussions*, doi: 10.1039/D0FD00078G.2021.
- 2770 Kwon, M. J., Beulig, F., Ilie, I., Wildner, M., Küsel, K., Merbold, L., Mahecha, M. D., Zimov, N., Zimov, S.  
2771 A., Heimann, M., Schuur, E. A. G., Kostka, J. E., Kolle, O., Hilke, I. and Göckede, M.: Plants,  
2772 microorganisms, and soil temperatures contribute to a decrease in methane fluxes on a drained Arctic  
2773 floodplain, *Glob. Change Biol.*, 23, 2396-2412, doi:10.1111/gcb.13558, 2017.
- 2774 Kwon, M. J., Natali, S. M., Hicks Pries, C. E., Schuur, E. A., Steinhof, A., Crummer, K. G., Zimov, N.,  
2775 Zimov, S. A., Heimann, M., Kolle, O., and Göckede, M.: Drainage enhances modern soil carbon contribution  
2776 but reduces old soil carbon contribution to ecosystem respiration in tundra ecosystems, *Glob. Change Biol.*,  
2777 25, 1315– 1325, doi: 10.1111/gcb.14578, 2019.
- 2778 Kühn, T., Kupiainen, K., Miinalainen, T., Kokkola, H., Paunu, V.-V., Laakso, A., Tonttila, J., Van  
2779 Dingenen, R., Kulovesi, K., Karvosenoja, N., and Lehtinen, K. E. J.: Effects of black carbon mitigation on  
2780 Arctic climate, *Atmos. Chem. Phys.*, 20, 5527–5546, doi: 10.5194/acp-20-5527-2020, 2020.
- 2781 Köster, E., Köster, K., Berninger, F., and Pumpanen, J.: Carbon dioxide, methane and nitrous oxide fluxes  
2782 from podzols of a fire chronosequence in the boreal forests in Värriö, Finnish Lapland, *Geoderma Regional*,  
2783 5, 181-187, doi:10.1016/j.geodrs.2015.07.001, 2015.
- 2784 Köster, E., Köster, K., Berninger, F., Prokushkin, A., Aaltonen, H., Zhou, X., and Pumpanen, J.: Changes in  
2785 fluxes of carbon dioxide and methane caused by fire in Siberian boreal forest with continuous permafrost,  
2786 *Journal of Environmental Management*, 228, 405-415, doi:10.1016/j.jenvman.2018.09.051, 2018.
- 2787 Köster, K., Berninger, F., Köster, E., and Pumpanen, J.: Influences of reindeer grazing on above- and  
2788 belowground biomass and soil carbon dynamics, *Arctic Antarctic and Alpine Res.*, 47(3), 495-503,  
2789 doi:10.1657/aaar0014-062, 2015.
- 2790 Köster, K., Berninger, F., Heinonsalo, J., Lindén, A., Köster, E., Ilvesniemi, H., and Pumpanen J.: The long-  
2791 term impact of low-intensity surface fires on litter decomposition and enzyme activities in boreal coniferous  
2792 forests, *Int. J Wildland Fire*, 25(2), 213-223, doi:10.1071/wf14217\_co, 2016.
- 2793 Köster, K., Köster, E., Berninger, F., Heinonsalo, J., and Pumpanen, J.: Contrasting effects of reindeer  
2794 grazing on CO<sub>2</sub>, CH<sub>4</sub>, and N<sub>2</sub>O fluxes originating from the northern boreal forest floor. *Land Degradation  
2795 and Development*, 29(2), 374-381, doi:10.1002/ldr.2868, 2018.
- 2796 Köster, K., Köster, E., Kulmala, L., Berninger, F., and Pumpanen, J.: Are the climatic factors combined with  
2797 reindeer grazing affecting the soil CO<sub>2</sub> emissions in subarctic boreal pine forest? *Catena*, 149, 616-622,  
2798 doi:10.1016/j.catena.2016.06.011, 2017.
- 2799 Lan, H., Holopainen, J., Hartonen, K., Jussila, M., Ritala, M. and Riekkola, M.-L.: Fully automated online  
2800 dynamic in-tube extraction for continuous sampling of volatile organic compounds in air, *Anal. Chem.*, 91,  
2801 8507, 2019.

- 2802 Lappalainen, H.K., Kulmala, M. and Zilitinkevich, S. (Eds.): Pan Eurasian Experiment (PEEX) Science Plan,  
 2803 web: [www.atm.helsinki.fi/peex](http://www.atm.helsinki.fi/peex), ISBN 978-951-51-0587-5 (printed), ISBN 978-951-51-0588-2 (online),  
 2804 2015.
- 2805 Lappalainen H.K., Petäjä T., Kujansuu J., Kerminen V., Shvidenko A., Bäck J., Vesala T., Vihma T., De  
 2806 Leeuw G., Lauri A., Ruuskanen T., Lapshin V.B., Zaitseva N., Glezer O., Arshinov M., Spracklen D.V.,  
 2807 Arnold S.R., Juhola S., Lihavainen H., Viisanen Y., Chubarova N., Chalov S., Filatov N., Skorokhod A.,  
 2808 Elansky N., Dyukarev E., Esau I., Hari P., Kotlyakov V., Kasimov N., Bondur V., Matvienko G., Baklanov  
 2809 A., Mareev E., Troitskaya Y., Ding A., Guo H., Zilitinkevich S., and Kulmala M.: Pan-Eurasian Experiment  
 2810 (PEEX) –a research initiative meeting the grand challenges of the changing environment of the northern Pan-  
 2811 Eurasian arctic-boreal areas, *J. Geography Environment Sustainability*, 2(7), 13-48, doi:10.24057/2071-  
 2812 9388-2014-7-2-13-48, 2014.
- 2813 Lappalainen, H. K., Kerminen, V.-M., Petäjä, T., Kurten, T., Baklanov, A., Shvidenko, A., Bäck, J., Vihma,  
 2814 T., Alekseychik, P., Andreae, M. O., Arnold, S. R., Arshinov, M., Asmi, E., Belan, B., Bobylev, L., Chalov,  
 2815 S., Cheng, Y., Chubarova, N., de Leeuw, G., Ding, A., Dobrolyubov, S., Dubtsov, S., Dyukarev, E., Elansky,  
 2816 N., Eleftheriadis, K., Esau, I., Filatov, N., Flint, M., Fu, C., Glezer, O., Gliko, A., Heimann, M., Holtslag, A.  
 2817 A. M., Hörrak, U., Janhunen, J., Juhola, S., Järvi, L., Järvinen, H., Kanukhina, A., Konstantinov, P.,  
 2818 Kotlyakov, V., Kieloaho, A.-J., Komarov, A. S., Kujansuu, J., Kukkonen, I., Duplissy, E.-M., Laaksonen, A.,  
 2819 Laurila, T., Lihavainen, H., Lisitzin, A., Mahura, A., Makshtas, A., Mareev, E., Mazon, S., Matishov, D.,  
 2820 Melnikov, V., Mikhailov, E., Moisseev, D., Nigmatulin, R., Noe, S. M., Ojala, A., Pihlatie, M., Popovicheva,  
 2821 O., Pumpanen, J., Regerand, T., Repina, I., Shcherbinin, A., Shevchenko, V., Sipilä, M., Skorokhod, A.,  
 2822 Spracklen, D. V., Su, H., Subetto, D. A., Sun, J., Terzhevik, A. Y., Timofeyev, Y., Troitskaya, Y.,  
 2823 Tynkkynen, V.-P., Kharuk, V. I., Zaytseva, N., Zhang, J., Viisanen, Y., Vesala, T., Hari, P., Hansson, H. C.,  
 2824 Matvienko, G. G., Kasimov, N. S., Guo, H., Bondur, V., Zilitinkevich, S., and Kulmala, M.: Pan-Eurasian  
 2825 Experiment (PEEX): towards a holistic understanding of the feedbacks and interactions in the land–  
 2826 atmosphere–ocean–society continuum in the northern Eurasian region, *Atmos. Chem. Phys.*, 16, 14421–  
 2827 14461, <https://doi.org/10.5194/acp-16-14421-2016>, 2016.
- 2828 Lappalainen, H.K., Kulmala, M., Kujansuu, J., Petäjä, T., Mahura, A., de Leeuw, G., Zilitinkevich, S.,  
 2829 Juustila, M., Kerminen, V.M., Bornstein, B. and Jiahua, Z.: The Silk Road agenda of the Pan-Eurasian  
 2830 Experiment (PEEX) program, *Big Earth Data*, 2(1), 8-35, doi:10.1080/20964471.2018.1437704, 2018.
- 2831 Lei, R. B., Xie, H. J., Wang, J., Leppäranta, M., Jonsdottir, I., and Zhang, Z. H.: Changes in sea ice  
 2832 conditions along the Arctic Northeast Passage from 1979 to 2012, *Cold Regions Science and Technology*,  
 2833 119, 132-144. doi:10.1016/j.coldregions.2015.08.004, 2015.
- 2834 Lei, R., Tian-Kunze, X., Leppäranta, M., Wang, J., Kaleschke, L., and Zhang, Z.: Changes in summer sea  
 2835 ice, albedo, and portioning of surface solar radiation in the Pacific sector of Arctic Ocean during 1982-2009,  
 2836 *J. Geophys. Res.: Oceans*, 121(8), 5470-5486, doi:10.1002/2016jc011831, 2016.

- 2837 Lei, R. B., Cheng, B., Heil, P., Vihma, T., Wang, J., Ji, Q., and Zhang, Z. H.: Seasonal and interannual  
2838 variations of sea ice mass balance from the Central Arctic to the Greenland Sea, *J. Geophys. Res.: Oceans*,  
2839 123(4), 2422-2439, doi:10.1002/2017jc013548, 2018.
- 2840 Leino, K., Nieminen, T., Manninen, H. E., Petäjä, T., Kerminen, V.-M., and Kulmala, M.: Intermediate ions  
2841 as a strong indicator of new particle formation bursts in a boreal forest, *Boreal Environ. Res.*, 21(3-4), 274-  
2842 286, 2016.
- 2843 Leppäranta, M.: Structure and properties of lake ice. *Freezing of Lakes and the Evolution of their Ice Cover*,  
2844 Springer, Berlin/Heidelberg, Germany, 51–90. doi: 10.1007/978-3-642-29081-7\_3, 2015.
- 2845 Leppäranta, M., Lindgren, E., and Shirasawa, K.: The heat budget of Lake Kilpisjärvi in the Arctic tundra,  
2846 *Hydrol. Res.*, 48(4), 969-980, doi:10.2166/nh.2016.171, 2017.
- 2847 Leppäranta, M., Lewis, J. E., Heini, A., and Arvola, L.: Spatial statistics of hydrography and water chemistry  
2848 in a eutrophic boreal lake based on sounding and water samples, *Environ. Monit. Assess.*, 190(7), 378,  
2849 doi:10.1007/s10661-018-6742-z, 2018.
- 2850 Leppäranta, M., Lindgren, E., Wen, L. and Kirillin, G.: Ice cover decay and heat balance in Lake Kilpisjärvi  
2851 in Arctic tundra, *Journal of Limnology*, 78(2). doi: 10.4081/jlimnol.2019.1879, 2019.
- 2852 Leppäranta, M., Meleshko, V., Uotila, P., and Pavlova, T.: Sea ice modelling, 315-387, *Sea Ice in the Arctic*  
2853 (Springer, Cham), 2020.
- 2854 Li, H., Väiliranta, M., Mäki, M., Kohl, L., Sannel, B., Pumpanen, J., Koskinen, M., Bäck, J. and Bianchi, F.:  
2855 Overlooked organic vapor emissions from thawing Arctic permafrost, *Environmental Research Letters* 15,  
2856 Issue 10, id.104097, 12 pp., 2020a.
- 2857 Li, M., Wang, L., Liu, J., Gao, W., Song, T., Sun, Y., Li, L., Li, X., Wang, Y., Liu, L. and Daellenbach,  
2858 K.R., Paasonen, P.J., Kerminen, V.-M., Kulmala, M., and Wang Y.: Exploring the regional pollution  
2859 characteristics and meteorological formation mechanism of PM<sub>2.5</sub> in North China during 2013–2017,  
2860 *Environment international*, 134, 105283, 2020b.
- 2861 Liao, Z., Cheng, B., Zhao, J., Vihma, T., Jackson, K., Yang, Q., Yang, Y., Zhang, L., Li, Z., Qiu, Y., and  
2862 Cheng, X.: Snow depth and ice thickness derived from SIMBA ice mass balance buoy data using an  
2863 automated algorithm, *Int. J. Digital Earth*, 12(8), 962-979, doi:10.1080/17538947.2018.1545877, 2018.
- 2864 Lin, X., Rogers, B. M., Sweeney, C., Chevallier, F., Arshinov, M., Dlugokencky, E., Machida, T., Motoki  
2865 Sasakawa, Tans, P., Keppel-Aleks, G.: Siberian and temperate ecosystems shape Northern Hemisphere  
2866 atmospheric CO<sub>2</sub> seasonal amplification, *PNAS*, 117 (35), 21079-21087, doi:10.1073/pnas.1914135117 ,  
2867 2020.
- 2868 Lintunen, A., Paljakka, T., Salmon, Y., Dewar, R., Riikonen, A, and Hölttä, T.: The influence of soil  
2869 temperature and water content on belowground hydraulic conductance and leaf gas exchange in mature trees  
2870 of three boreal species, *Plant, Cell and Environment*, 43, 532-547, doi: 10.1111/pce.13709, 2020.

- 2871 Liu, Y.C., Yan, C., Feng, Z., Zheng, F., Fan, X., Zhang, Y., Li, C., Zhou, Y., Lin, Z., Guo, Y., Zhang, Y.,  
 2872 Ma, L., Zhou, W., Liu, Z., Dada, L., Dällenbach, K., Kontkanen, J., Cai, R., Chan, T., Chu, B., Du, W., Yao,  
 2873 L., Wang, Y., Cai, J., Kangasluoma, J., Kokkonen, T., Kujansuu, J., Rusanen, A., Deng, C., Fu, Y., Yin, R.,  
 2874 Li, X., Lu, Y., Liu, Y., Lian, C., Yang, D., Wang, W., Ge, M., Wang, Y., Worsnop, D.R., Junninen, H., He,  
 2875 H., Kerminen, V.-M., Zheng, J., Wang, L., Jiang, J., Petäjä, T., Bianchi, F. and Kulmala, M. : Continuous  
 2876 and comprehensive atmospheric observation in Beijing: a station to understand the complex urban  
 2877 atmospheric environment, *Big Earth Data*, 4, 295-321, 2020.
- 2878 Liu, J., Wang, L., Li, M., Liao, Z., Sun, Y., Song, T., Gao, W., Wang, Y., Li, Y., Ji, D., Hu, B., Kerminen,  
 2879 V.-M., Wang, Y., and Kulmala, M.: Quantifying the impact of synoptic circulation patterns on ozone  
 2880 variability in northern China from April to October 2013–2017, *Atmos. Chem. Phys.*, 19, 14477–14492,  
 2881 doi:10.5194/acp-19-14477-2019, 2019 a.
- 2882 Liu, W., Atherton, J., Möttus, M., Gastellu-Etchegorry, J.P., Malenovský, Z., Raunonen, P., Åkerblom, M.,  
 2883 Mäkipää, R. and Porcar-Castell, A.: Simulating solar-induced chlorophyll fluorescence in a boreal forest  
 2884 stand reconstructed from terrestrial laser scanning measurements, *Remote Sensing of Environment*, 232,  
 2885 111274, 2019b.
- 2886 Liu, Y., de Leeuw, G., Kerminen, V.-M., Zhang, J., Zhou, P., Nie, W., Qi, X., Hong, J., Wang, Y., Ding, A.,  
 2887 Guo, H., Krüger, O., Kulmala, M., and Petäjä, T.: Analysis of aerosol effects on warm clouds over the  
 2888 Yangtze River Delta from multi-sensor satellite observations, *Atmos. Chem. Phys.*, 17, 5623–5641,  
 2889 doi:10.5194/acp-17-5623-2017, 2017.
- 2890 Liu, Y., Zhang, J., Zhou, P., Lin, T., Hong, J., Shi, L., Yao, F., Wu, J., Guo, H., and de Leeuw, G.: Satellite-  
 2891 based estimate of the variability of warm cloud properties associated with aerosol and meteorological  
 2892 conditions, *Atmos. Chem. Phys.*, 18, 18187–18202, doi:10.5194/acp-18-18187-2018, 2018.
- 2893 López-Blanco, E., Exbrayat, J.-F., Lund, M., Christensen, T. R., Tamstorf, M. P., Slevin, D., Hugelius, G.,  
 2894 Bloom, A. A., and Williams, M.: Evaluation of terrestrial pan-Arctic carbon cycling using a data-  
 2895 assimilation system, *Earth Syst. Dynam.*, 10, 233–255, doi:10.5194/esd-10-233-2019, 2019.
- 2896 Lu, P., Leppäranta, M., Cheng, B., and Li, Z.: Influence of melt-pond depth and ice thickness on Arctic sea-  
 2897 ice albedo and light transmittance, *Cold Regions Science and Technology*, 124, 1-10,  
 2898 doi:10.1016/j.coldregions.2015.12.010, 2016.
- 2899 Lu, P., Cheng, B., Leppäranta, M., and Li, Z. J.: Partitioning of solar radiation in Arctic sea ice during melt  
 2900 season, *Oceanologia*, 60(4), 464-477, doi:10.1016/j.oceano.2018.03.002, 2018a.
- 2901 Lu, P., Leppäranta, M., Cheng, B., Li, Z., Istomina, L., and Heygster, G.: The color of melt ponds on Arctic  
 2902 sea ice, *The Cryosphere*, 12, 1331–1345, doi:10.5194/tc-12-1331-2018, 2018b.
- 2903 Lu, Y., Yan, C., Fu, Y., Chen, Y., Liu, Y., Yang, G., Wang, Y., Bianchi, F., Chu, B., Zhou, Y., Yin, R.,  
 2904 Baalbaki, R., Garmash, O., Deng, C., Wang, W., Liu, Y.C., Petäjä, T., Kerminen, V.-M., Jiang, J., Kulmala,



- 2905 M. and Wang, L. : A proxy for atmospheric daytime gaseous sulfuric acid concentration in urban Beijing,  
2906 *Atmos. Chem. Phys.* 19, 1971-1983, 2019.
- 2907 Luoma, K., Virkkula, A., Aalto, P.P, Petäjä, T., and Kulmala, M.: Over a 10-year record of aerosol optical  
2908 properties at SMEAR II, *Atmos. Chem. Phys.*, 19, 11363–11382, doi:10.5194/acp-19-11363-2019, 2019.
- 2909 Lychagin, M., Chalov, S., Kasimov, N., Shinkareva, G., Jarsjo, J., and Thorslund, J.: Surface water pathways  
2910 and fluxes of metals under changing environmental conditions and human interventions in the Selenga River  
2911 system, *Environ. Earth Sci.*, 76(1), 14, doi:10.1007/s12665-016-6304-z, 2017.
- 2912 Ma,J., Yan, X., Dong, W. et al.: Gross primary production of global forest ecosystems has been  
2913 overestimated, *Sci Rep* 5, 10820, doi:10.1038/srep10820, 2015.
- 2914 Magritsky, D. V., Frolova, N. L. , Evstigneev, V. M. , Povalishnikova, E. S. , Kireeva, M. B., and  
2915 Pakhomova, O. M.: Long-term changes of river water inflow into the seas of the Russian Arctic sector,  
2916 *Polarforschung*, 87(2),177-194, doi: 10.2312/polarforschung.87.2.177, 2018.
- 2917 Mahura A., Baklanov A., Sørensen, J. H., Svetlov, A., and Koshkin, V.: Assessment of Long-Range  
2918 Transport and Deposition from Cu-Ni Smelters of Russian North. In "Air, Water and Soil Quality Modelling  
2919 for Risk and Impact Assessment", *Security Through Science, Series C - Environmental Security*. Eds. A.  
2920 Ebel, T. Davitashvili, Springer Elsevier Publishers, pp. 115-124, 2007.
- 2921 Mahura, A., Gonzalez-Aparacio, I., Nuterman, R., and Baklanov, A.: Seasonal Impact Analysis on  
2922 Population due to Continuous Sulphur Emissions from Severonikel Smelters of the Kola Peninsula.  
2923 *Geography, Environment, Sustainability*, 11(1), 130-144, doi:10.24057/2071-9388-2018-11-1-130-144,  
2924 2018.
- 2925 Malkhazova, S. M., Mironova, V. A., Orlov, D. S., and Adishcheva, O. S.: Influence of climatic factor on  
2926 naturally determined diseases in a regional context, *Geography, Environment, Sustainability*, 11(1), 157-170,  
2927 doi:10.24057/2071-9388-2018-11-1-157-170, 2018.
- 2928 Malsy, M., Flörke, M., and Borchardt, D.:What drives the water quality changes in the Selenga basin:  
2929 climate change or socio-economic development?, *Reg Environ Chang.*, 17, 1977–1989 doi:10.1007/s10113-  
2930 016-1005-4, 2017.
- 2931 Mammarella, I., Nordbo, A., Rannik, Ü., Haapanala, S., Levula, J., Laakso, H., Ojala, A., Peltola, O.,  
2932 Heiskanen, J., Pumpanen, J. and Vesala, T.: Carbon dioxide and energy fluxes over a small boreal lake in  
2933 Southern Finland, *J. Geophys. Res.: Biogeosciences*, 120(7), 1296-1314, doi:10.1002/2014jg002873, 2015.
- 2934 Manasyrov, R. M., Vorobyev, S. N., Loiko, S. V., Krivtsov, I. V., Shirokova, L. S., Shevchenko, V. P.,  
2935 Kirpotin, S. N., Kulizhsky, S. P., Kolesnichenko, L. G., Zemtsov, V. A. and Sinkinov, V. V.: Seasonal  
2936 dynamics of thermokarst lake chemical composition in discontinuous permafrost zone of Western Siberia,  
2937 *Biogeosciences*, 12, 3009-3028, 2015.

- 2938 Marelle, L., Raut, J. C., Law, K. S., and Duclaux, O.: Current and future arctic aerosols and ozone from  
 2939 remote emissions and emerging local sources-modeled source contributions and radiative effects, *J.*  
 2940 *Geophys. Res.: Atmos.*, 123(22), 12942-12963, doi:10.1029/2018jd028863, 2018.
- 2941 Maslov, A. V., Shevchenko, V. P., Bobrov, V. A., Belogub, E. V., Ershova, V. B., Vereshchagin, O. S., and  
 2942 Khvorov, P. V.: Mineralogical-geochemical features of ice-rafted sediments in some arctic regions,  
 2943 *Lithology and Mineral Resources*, 53(2), 110-129, doi:10.1134/s0024490218020037, 2018a.
- 2944 Maslov, A. V., Shevchenko, V. P., Kuznetsov, A. B., and Stein, R.: Geochemical and Sr-Nd-Pb-isotope  
 2945 characteristics of ice-rafted sediments of the Arctic Ocean, *Geochem. Int.*, 56(8), 751-765,  
 2946 doi:10.1134/s0016702918080050, 2018b.
- 2947 Matkala, L., Kulmala, L., Kolari, P., Aurela, M., and Bäck, J.: Resilience of carbon dioxide and water  
 2948 exchange to extreme weather events in subarctic Scots pine and Norway spruce stands, *Agricultural and*  
 2949 *Forest Meteorology*, 296, 108239, 2020.
- 2950 McCusker, K., Fyfe, J., and Sigmond, M.: Twenty-five winters of unexpected Eurasian cooling unlikely due  
 2951 to Arctic sea-ice loss, *Nature Geoscience* 9, 838–842, doi:10.1038/ngeo2820, 2016.
- 2952 Meinander, O., Heikkinen, E., Aurela, M., and Hyvärinen, A.: Sampling, Filtering, and Analysis Protocols to  
 2953 Detect Black Carbon, Organic Carbon, and Total Carbon in Seasonal Surface Snow in an Urban Background  
 2954 and Arctic Finland (>60° N), *Atmosphere*, 11, 923. doi:10.3390/atmos11090923, 2020a.
- 2955 Meinander, O., Kontu, A., Kouznetsov, R., Sofiev, M.: Snow Samples Combined with Long-Range  
 2956 Transport Modeling to Reveal the Origin and Temporal Variability of Black Carbon in Seasonal Snow in  
 2957 Sodankylä (67° N), *Front. Earth Sci.*, 8, 13,  
 2958 <https://www.frontiersin.org/articles/10.3389/feart.2020.00153/full>, 2020b.
- 2959 Merkouriadi, I., Cheng, B., Graham, R. M., Rösel, A., and Granskog, M. A.: Critical role of snow on sea ice  
 2960 growth in the Atlantic sector of the Arctic Ocean. *Geophysical Research Letters*, 44.  
 2961 doi:10.1002/2017GL075494, 2017
- 2962 Merkouriadi, I., Cheng, B., Graham, R. M., Rösel, A., and Granskog, M. A.: Critical role of snow on sea ice  
 2963 growth in the Atlantic sector of the Arctic Ocean, *Geophys. Res. Lett.*, 44, doi: 10.1002/2017GL075494,  
 2964 2018.
- 2965 Mikhailov, E. F., Mironova, S. Y., Makarova, M. V., Vlasenko, S. S., Ryshkevich, T. I., Panov, A. V., and  
 2966 Andreae, M. O.: Studying seasonal variations in carbonaceous aerosol particles in the atmosphere over  
 2967 central Siberia, *Izv. Atmos. Oceanic Phys.*, 51(4), 423-430, doi:10.1134/s000143381504009x, 2015a.
- 2968 Mikhailov, E. F., Mironov, G. N., Pöhlker, C., Chi, X., Krüger, M. L., Shiraiwa, M., Förster, J.-D., Pöschl,  
 2969 U., Vlasenko, S. S., Ryshkevich, T. I., Weigand, M., Kilcoyne, A. L. D., and Andreae, M. O.: Chemical  
 2970 composition, microstructure, and hygroscopic properties of aerosol particles at the Zotino Tall Tower

- 2971 Observatory (ZOTTO), Siberia, during a summer campaign, *Atmos. Chem. Phys.*, 15, 8847–8869,  
2972 doi:10.5194/acp-15-8847-2015, 2015b.
- 2973 Mikhailov, E. F., Mironova, S., Mironov, G., Vlasenko, S., Panov, A., Chi, X., Walter, D., Carbone, S.,  
2974 Artaxo, P., Heimann, M., Lavric, J., Pöschl, U., and Andreae, M. O.: Long-term measurements (2010–2014)  
2975 of carbonaceous aerosol and carbon monoxide at the Zotino Tall Tower Observatory (ZOTTO) in central  
2976 Siberia, *Atmos. Chem. Phys.*, 17, 14365–14392, doi:10.5194/acp-17-14365-2017, 2017.
- 2977 Mikola, J., Virtanen, T., Linkosalmi, M., Vähä, E., Nyman, J., Postanogova, O., Räsänen, A., Kotze, D. J.,  
2978 Laurila, T., Juutinen, S., Kondratyev, V., and Aurela, M.: Spatial variation and linkages of soil and  
2979 vegetation in the Siberian Arctic tundra – coupling field observations with remote sensing data,  
2980 *Biogeosciences*, 15, 2781–2801, doi:10.5194/bg-15-2781-2018, 2018.
- 2981 Miles, V. V., and Esau, I.: Spatial heterogeneity of greening and browning between and within bioclimatic  
2982 zones in northern West Siberia, *Environ. Res. Lett.*, 11(11), 12, doi:10.1088/1748-9326/11/11/115002, 2016.
- 2983 Miles, V., and Esau, I.: Seasonal and Spatial Characteristics of Urban Heat Islands (UHIs) in Northern West  
2984 Siberian Cities., *Remote Sens.*, 9, 989, 2017.
- 2985 Miles, M. W., Miles, V., and Esau, I.: Varying climate response across the tundra, forest–tundra and boreal  
2986 forest biomes in northern West Siberia, *Environ. Res. Lett.*, 14, 075008, doi:10.1088/1748-9326/ab2364,  
2987 2019.
- 2988 Miles, V., and Esau, I.: Surface urban heat islands in 57 cities across different climates in northern  
2989 Fennoscandia, *Urban Climate*, 31, 10.1016/j.uclim.2019.100575, 2020.
- 2990 Miles, V.: Arctic surface Urban Heat Island (UHI), MODIS Land Surface Temperature (LST) data, 2000-  
2991 2016. Arctic Data Center. doi:10.18739/A2TB0XW4T, 2020.
- 2992 MNRE (2019): Methods for calculating emissions of pollutants into the atmosphere from stationary sources.  
2993 Ministry of Natural Resources and Ecology. In Russian  
2994 ([www.mnr.gov.ru/docs/metodiki\\_rascheta\\_vybrosov\\_vrednykh\\_zagryaznyayushchikh\\_veshchestv\\_v\\_atmosf\\_ernyy\\_vozdukh\\_statsionarn/perechen](http://www.mnr.gov.ru/docs/metodiki_rascheta_vybrosov_vrednykh_zagryaznyayushchikh_veshchestv_v_atmosf_ernyy_vozdukh_statsionarn/perechen)), 2019.  
2995  
2996
- 2997 Mori, M., Watanabe, M., Shiogama, H., Inoue, J., and Kimoton, M.: Robust Arctic sea-ice influence on the  
2998 frequent Eurasian cold winters in past decades, *Nat. Geosci.*, 7, 869–873, doi:10.1038/ngeo2277, 2014.
- 2999 Mori, M., Kosaka, Y., Watanabe, M., Nakamura, H., and Kimoto, M.: A reconciled estimate of the influence  
3000 of Arctic sea-ice loss on recent Eurasian cooling, *Nat. Clim. Change*, 9, 123–129, doi: 10.1038/s41558-018-  
3001 0379-3, 2019.
- 3002 Morozov, E. A., Kondrik, D. V., Chepikova, S. S., and Pozdnyakov, D. V.: Atmospheric columnar CO<sub>2</sub>  
3003 enhancement over *E. huxleyi* blooms: case studies in the North Atlantic and Arctic waters. *Transactions of*

- 3004 the Karelian Research Centre of the Russian Academy of Sciences, *Limnologia i Oceanologia* series, 3, 1-6.  
3005 doi:10.17076/lim989, 2019.
- 3006 Myslenkov S., Medvedeva A., Arkhipkin V., Markina M., Surkova G., Krylov A., Dobrolyubov S.,  
3007 Zilitinkevich S., and Koltermann P.: Long-term statistics of storms in the Baltic, Barents and White Seas and  
3008 their future climate projections, *Geography, environment, sustainability*, 11, 93-112, doi:10.24057/2071-  
3009 9388-2018-11-1-93-112, 2018.
- 3010 Mäki, M., Krasnov, D., Hellén, H., Noe, S. M., and Bäck, J.: Stand type affects fluxes of volatile organic  
3011 compounds from the forest floor in hemiboreal and boreal climates, *Plant Soil*, 441, 363–381,  
3012 doi:10.1007/s11104-019-04129-3, 2019.
- 3013 Naakka, T., Nygård, T., Vihma, T., Graversen, R., and Sedlar, J.: Atmospheric moisture transport between  
3014 mid-latitudes and the Arctic: regional, seasonal and vertical distributions, *Int. J. Climatol.*, 32, 1–18,  
3015 doi:10.1002/joc.5988, 2019.
- 3016 Natali, S.M., Watts, J.D., Rogers, B.M., Potter, S., Ludwig, S. M., Selbmann, A. K., Sullivan, P.F. Abbott, B.  
3017 W., Arndt, K. A., Birch, L., Björkman, M.P., Bloom, A., Celis, G., Christensen, T. R., Christiansen, C. T.,  
3018 Commane, R., Cooper, E. J., Crill, P., Czimeczik, C., Davydov, S., Du, J., Egan, J.E., Elberling, B.,  
3019 Euskirchen, B.S., Friborg, T., Genet, H., Göckede, M., Goodrich, J.P., Grogan, P., Helbig, M., Jafarov, E.E.,  
3020 Jastrow, J. D., Kalhori, A.A.M., Kim, Y. Kimball, J. S., Kutzbach, L., Lara, M. J, Larsen, K., S., Lee, B.-Y.,  
3021 Liu, Z., Lorant, M. M., Lund, M., Lupascu, M., Madani, N., Malhotra, A., Matamala, R., McFarland, J.,  
3022 McGuire, A. D., Michelsen, A., Minions, C., Oechel, W., Olefeldt, D., Parmentier, F.-J., Pirk, N., Poulter,  
3023 B., Quinton, W., Rezanezhad, F., Risk, D., Sachs, T., Schaefer, K., Schmidt, N. M., Schuur, E., Semenchuk,  
3024 P. R., Shaver, G., Sonnentag, O., Starr, G., Treat, C. C., Waldrop, M. P., Wang, Y., Welker, J., Wille, C., Xu,  
3025 X., Zhang, Z., Zhuang, Q., and Zona, D.: Large loss of CO<sub>2</sub> in winter observed across the northern  
3026 permafrost region, *Nat. Clim. Chang.*, 9, 852–857, doi:10.1038/s41558-019-0592-8, 2019.
- 3027 Nikandrova, A., Tabakova, K., Manninen, A., Väänänen, R., Petäjä, T., Kulmala, M., Kerminen, V.-M., and  
3028 O'Connor, E.: Combining airborne in situ and ground-based lidar measurements for attribution of aerosol  
3029 layers, *Atmos. Chem. Phys.*, 18, 10575–10591, doi:10.5194/acp-18-10575-2018, 2018.
- 3030 NILU, 2013: Sandanger, T.M., Anda, E., Berglen, T.F., Evenset, A., Christensen, G., and Heimstad, E.S.:  
3031 Health and environmental impacts in the Norwegian border area related to local Russian industrial emissions.  
3032 Knowledge status, 40/2013, 2013.
- 3033 Nissen, C., Munnich, M., Grube, M., and Haumann, N.: Factors controlling coccolithophore biogeography in  
3034 the Southern Ocean, *Biogeosciences*, 15(22), 6997-7024, doi:10.5194/bg-15-6997-2018, 2018.
- 3035 Nitzbon, J., Langer, M., Westermann, S., Martina, L., Aas, K. S., and Boike, J.: Pathways of ice-wedge  
3036 degradation in polygonal tundra under different hydrological conditions, *Cryosphere*, 13(4), 1089-1123,  
3037 doi:10.5194/tc-13-1089-2019, 2019.

- 3038 Nygård, T., Graversen, R. G., Uotila, P., Naakka, T., and Vihma, T.: Strong dependence of wintertime Arctic  
 3039 moisture and cloud distributions on atmospheric large-scale circulation, *J. Climate*, 32, 8771-8790, doi:  
 3040 10.1175/JCLI-D-19-0242.1, 2019.
- 3041 Overland, J., Dunlea, E., Box, J. E., Corell, R., Forsius, M., Kattsov, V., Olsen, M. S., Pawlak, J., Reiersen,  
 3042 L. O., and Wang, M.: The urgency of Arctic change, *Polar Science*, 21, 6-13,  
 3043 doi:10.1016/j.polar.2018.11.008, 2019.
- 3044 Paasonen, P., Peltola, M., Kontkanen, J., Junninen, H., Kerminen, V.-M., and Kulmala, M.: Comprehensive  
 3045 analysis of particle growth rates from nucleation mode to cloud condensation nuclei in boreal forest, *Atmos.*  
 3046 *Chem. Phys.*, 18, 12085–12103, doi:10.5194/acp-18-12085-2018, 2018.
- 3047 Palo, T., Vihma, T., Jaagus, J., and Jakobson, E.: Observations on temperature inversion over central Arctic  
 3048 sea ice in summer, *Q. J. R. Meteorol. Soc.*, 143(708), 2741-2754, doi:10.1002/qj.3123, 2017.
- 3049 Panov, A. V., Prokushkin, A. S., Bryukhanov, A. V., Korets, M. A., Ponomarev, E. I., Sidenko, N. V.,  
 3050 Zrazhevskaya, G. K., Timokhina, A. V., and Andreae, M. O.: A complex approach for the estimation of  
 3051 carbonaceous emissions from wildfires in Siberia, *Russian Meteorol, Hydrol.*, 43(5), 295-301, 2018.
- 3052 Parmentier, F. W., Christensen, T. R., Rysgaard, S. Bendtsen, J., Glud, R. N., Else, B., van Huissteden, J.,  
 3053 Sachs, T., Vonk, J. E., and Sejr, M. K.: A synthesis of the arctic terrestrial and marine carbon cycles under  
 3054 pressure from a dwindling cryosphere, *Ambio*, 46, 53–69, doi:10.1007/s13280-016-0872-8, 2017.
- 3055 Parshintsev, J., Vaikkinen, A., Lipponen, K., Vrkoslav, V., Cvačka, J., et al. : Desorption atmospheric  
 3056 pressure photoionization high-resolution mass spectrometry: a complementary approach for the chemical  
 3057 analysis of atmospheric aerosols, *Rapid Commun. Mass Spectrom.*, 29, 1233–1241, 2015.
- 3058 Passananti, M., Zapadinsky, E., Zanca, T., Kangasluoma, J., Myllys, N., Rissanen, M.P., Kurtén, T., Ehn,  
 3059 M., Attoui, M., and Vehkamäki, H.: How well can we predict cluster fragmentation inside a mass  
 3060 spectrometer? *Chem. Commun.*, 55, 5946-5949, 2019.
- 3061 Payne, R. J., Creevy, A., Malysheva, E., Ratcliffe, J., Andersen, R., Tsyganov, A. N., Rowson, J., Marcisz,  
 3062 K., Zielinska, M., Lamentowicz, M., Lapshina, E. D., and Mazei, Y.: Tree encroachment may lead to  
 3063 functionally-significant changes in peatland testate amoeba communities. *Soil Biology & Biochemistry*, 98,  
 3064 18-21. doi:10.1016/j.soilbio.2016.04.002, 2016.
- 3065 Peltola, O., Vesala, T., Gao, Y.; Rätty, O. et al. : Monthly gridded data product of northern wetland methane  
 3066 emissions based on upscaling eddy covariance observations, *Earth System Science Data*, 11, 1263-1289,  
 3067 doi:10.5194/essd-11-1263-2019, 2019.
- 3068 Peltoniemi, J. I., Gritsevich, M., Hakala, T., Dagsson-Waldhauserová, P., Arnalds, Ó., Anttila, K., Hannula,  
 3069 H.-R., Kivekäs, N., Lihavainen, H., Meinander, O., Svensson, J., Virkkula, A., and de Leeuw, G.: Soot on

- 3070 Snow experiment: bidirectional reflectance factor measurements of contaminated snow, *The Cryosphere*, 9,  
3071 2323–2337, doi:10.5194/tc-9-2323-2015, 2015.
- 3072 Peterson, B. J., Holmes, R. M., McClelland, J. W., Vörösmarty, C. J., Lammers, R. B., Shiklomanov, A. I.,  
3073 Shiklomanov, I. A., and Rahmstorf, S.: Increasing river discharge to the Arctic Ocean, *Science*, 80, 298,  
3074 2171–2173, doi: 10.1126/science.1077445, 2002.
- 3075 Petäjä, T., Järvi, L., Kerminen, V.-M., Ding, A. J., Sun, J. N., Nie, W., Kujansuu, J., Virkkula, A., Yang, X.-  
3076 Q., Fu, C. B., Zilitinkevich, S., and Kulmala M.: Enhanced air pollution via aerosol-boundary layer feedback  
3077 in China, *Scientific Reports*, 6, 18998, doi:10.1038/srep18998, 2016.
- 3078 Petäjä, T., Duplissy, E.-M., Tabakova, K., Schmale, J., Altstädter, B., Ancellet, G., Arshinov, M., Balin, Y.,  
3079 Baltensperger, U., Bange, J., Beamish, A., Belan, B., Berchet, A., Bossi, R., Cairns, W. R. L., Ebinghaus, R.,  
3080 El Haddad, I., Ferreira-Araujo, B., Franck, A., Huang, L., Hyvärinen, A., Humbert, A., Kalogridis, A.-C.,  
3081 Konstantinov, P., Lampert, A., MacLeod, M., Magand, O., Mahura, A., Marelle, L., Masloboev, V.,  
3082 Moisseev, D., Moschos, V., Neckel, N., Onishi, T., Osterwalder, S., Ovaska, A., Paasonen, P., Panchenko,  
3083 M., Pankratov, F., Pernov, J. B., Platis, A., Popovicheva, O., Raut, J.-C., Riandet, A., Sachs, T., Salvatori, R.,  
3084 Salzano, R., Schröder, L., Schön, M., Shevchenko, V., Skov, H., Sonke, J. E., Spolaor, A., Stathopoulos, V.,  
3085 K., Strahlendorff, M., Thomas, J. L., Vitale, V., Vratolis, S., Barbante, C., Chabrillat, S., Dommergue, A.,  
3086 Eleftheriadis, K., Heilimo, J., Law, K. S., Massling, A., Noe, S. M., Paris, J.-D., Prévôt, A. S. H., Riipinen,  
3087 I., Wehner, B., Xie, Z., and Lappalainen, H. K.: Overview: Integrative and Comprehensive Understanding on  
3088 Polar Environments (iCUPE) – concept and initial results, *Atmos. Chem. Phys.*, 20, 8551–8592,  
3089 doi:10.5194/acp-20-8551-2020, 2020a.
- 3090 Petäjä, T., Ganzei, K. S., Lappalainen, H. K., Tabakova, K., Makkonen, R., Räisänen, J., Chalov, S.,  
3091 Kulmala, M., Zilitinkevich, S. S., Baklanov, P., Shakirov, R. B., Mishina, N.V., Egidarev, E.G., and  
3092 Kondrat'ev, I. I.: Research agenda for the Russian Far East and utilization of multi-platform comprehensive  
3093 environmental observations, *J. Big Data*, 5:3, 277-305, doi:10.1080/17538947.2020.1826589 , 2020b.
- 3094 Pietron, J., Jarsjo, J., Romanchenko, A. O., and Chalov, S. R.: Model analyses of the contribution of in-  
3095 channel processes to sediment concentration hysteresis loops, *Journal of Hydrology*, 527, 576-589.  
3096 doi:10.1016/j.jhydrol.2015.05.009, 2015.
- 3097 Pietroń, J., Nittrouer, J. A., Chalov, S. R., Dong, T. Y., Kasimov, N., Shinkareva, G., and Jarsjö, J.:  
3098 Sedimentation patterns in the Selenga River delta under changing hydroclimatic conditions, *Hydrological  
3099 Processes*, 32(2), 278-292, doi:10.1002/hyp.11414, 2018.
- 3100 Pirazzini, R., Leppanen, L., Picard, G., Lopez-Moreno, J. I., Marty, C., Macelloni, G., Kontu, A., Von  
3101 Lerber, A., Tanis, C.M., Schneebeli, M., De Rosnay, P., Arslan, A. N.: European in-situ snow measurements:  
3102 practices and purposes, *Sensors*, 18(7), 51, doi:10.3390/s18072016, 2018.
- 3103 Pisso, I., Myhre, C. L., Platt, S. M., Eckhardt, S., Hermansen, O., Schmidbauer, N., Mienert, J.,  
3104 Vadakkepuliambatta, S., Bauguitte, S., Pitt, J., Allen, G., Bower, K. N., O'Shea, S., Gallagher, M. W.,

- 3105 Percival, C. J., Pyle, J., Cain, M., and Stohl, A.: Constraints on oceanic methane emissions west of Svalbard  
 3106 from atmospheric in situ measurements and Lagrangian transport modeling, *J. Geophys. Res. Atmos.*,  
 3107 121(23), 14188-14200, doi:10.1002/2016jd025590, 2016.
- 3108 Platt, S. M., Eckhardt, S., Ferré, B., Fisher, R. E., Hermansen, O., Jansson, P., Lowry, D., Nisbet, E. G.,  
 3109 Pisso, I., Schmidbauer, N., Silyakova, A., Stohl, A., Svendby, T. M., Vadakkepuliambatta, S., Mienert, J.,  
 3110 and Lund Myhre, C.: Methane at Svalbard and over the European Arctic Ocean, *Atmos. Chem. Phys.*, 18,  
 3111 17207–17224, doi:10.5194/acp-18-17207-2018, 2018.
- 3112 Ponomarev, Evgenii I., Kharuk, Viacheslav I., and Ranson, Kenneth J.: Wildfires Dynamics in Siberian Larch  
 3113 Forests, *Forests*, 7(6), 125, 2016.
- 3114 Popovicheva O., Evangelidou N., Eleftheriadis K., Kalogridis A. C., Sitnikov V. N., Eckhardt S., Stohl A.:  
 3115 Black carbon sources constrained by observations and modeling in the Russian high Arctic, *Environmental  
 3116 Science Technology*, 51(7), 3871-3879, 2017.
- 3117 Popovicheva, O., Diapouli, E., Makshtas, A., Shonija, N., Manousakas, M., Saraga, D., Uttal, T., and  
 3118 Eleftheriadis, K.: East Siberian Arctic background and black carbon polluted aerosols at HMO Tiksi, *Science  
 3119 of the Total Environment*, 655, 924-938, doi:10.1016/j.scitotenv.2018.11.165, 2019a.
- 3120 Popovicheva, O. B., Engling, G., Ku, I. T., Timofeev, M. A., and Shonija, N. K.: Aerosol emissions from  
 3121 long-lasting smoldering of boreal peatlands: chemical composition, markers, and microstructure, *Aerosol  
 3122 and Air Quality Research*, 19(3), 484-503, doi:10.4209/aaqr.2018.08.0302, 2019b.
- 3123 Popovicheva, O. B., Padoan, S., Schnelle- Kreis, J., Nguyen, D. L., Adam, T.W., Kistler, M., Steinkogler, T.,  
 3124 Kasper-Giebl, A., Zimmermann, R., and Chubarova, N. E.: Spring aerosol in urban atmosphere of megacity:  
 3125 analytical and statistical assessment for source impacts, *Aerosol and Air Quality Research*, 20, 702–719,  
 3126 2020a.
- 3127 Popovicheva O., Ivanov A., and Vojtisek M.: Functional Factors of Biomass Burning Contribution to Spring  
 3128 Aerosol Composition in a Megacity: Combined FTIR-PCA Analyses, *Atmosphere*, 11, 319-339, 2019b.
- 3129 Popovicheva, O., Volpert, E., Sitnikov, N., Chichaeva, M., and Padoan, S.: Black carbon in spring aerosols  
 3130 of Moscow urban background, *Geography, Environment, Sustainability*, 13, 1, 233-243, 2020c
- 3131 Pozdnyakov D. V., Pettersson L. H., and Korosov A. A.: *Exploring the Marine Ecology from Space*.  
 3132 Springer, Switzerland, 2017.
- 3133 Pozdnyakov, D. V., Kondrik, D.V., Kazakov, E. E., and Chepikova, S.: Environmental conditions favoring  
 3134 coccolithophore blooms in subarctic and arctic seas: a 20-year satellite and multi-dimensional statistical  
 3135 study, *Proc. SPIE 11150, Remote Sensing of the Ocean, Sea Ice, Coastal Waters, and Large Water Regions*,  
 3136 111501W, 14 October 2019, doi: 10.1117/12.2547868, 2019.

- 3137 Pozdnyakov D., Kondrik D., and Chepikova S.: Origination of *E. huxleyi* extraordinary bloom outbursts in  
 3138 the Bering Sea between the late 1990s and early 2000s, and in 2018-2019: A hypothesis, *Fisheries*  
 3139 *Oceanography*, submitted, 2020.
- 3140 Preis, Y. I., Simonova, G. V., Voropay, N. N., and Dyukarev, E. A.: Estimation of the influence of  
 3141 hydrothermal conditions on the carbon isotope composition in *Sphagnum* mosses of bogs of Western Siberia,  
 3142 *IOP Conf. Series: Earth Environ. Sci.*, 211, doi:10.1088/1755-1315/211/1/012031, 2018.
- 3143 Pugac, S. P., Pipko I. I., Shakhova, N. E., Shirshin, E. A., Perminova, I. V., Gustafsson, O., Bondur, V. G.,  
 3144 Ruban, A. S., and Semiletov, I. P.: Dissolved organic matter and its optical characteristics in the Laptev and  
 3145 East Siberian seas: spatial distribution and interannual variability (2003–2011), *Ocean Sci.*, 14, 87–103,  
 3146 doi:10.5194/os-14-87-2018, 2018.
- 3147 Pulliainen, J., Aurela, M., Laurila, T., Aalto, T., Takala, M., Salminen, M., Kulmala, M., Barr, A., Heimann,  
 3148 M., Lindroth, A., Laaksonen, A., Derksen, C., Mäkelä, A., Markkanen, T., Lemmetyinen, J., Susiluoto, J.,  
 3149 Dengel, S., Mammarella, I., Tuovinen, J.-P., and Vesala, T.: Early snowmelt significantly enhances boreal  
 3150 springtime carbon uptake, *PNAS*, 114(42), 11081-11086, doi:10.1073/pnas.1707889114, 2017.
- 3151 Pulliainen, J., Luojus, K., Derksen, C., Mudryk, L., Lemmetyinen, J., Salminen, M., Ikonen, J., Takala, M.,  
 3152 Cohen, J., Smolander, T., and Norberg, J.: Patterns and trends of Northern Hemisphere snow mass from  
 3153 1980 to 2018, *Nature* 581, 294–298, doi:10.1038/s41586-020-2258-0, 2020.
- 3154 Pärn, J., Verhoeven, J.T., Butterbach-Bahl, K., Dise, N.B., Ullah, S., Aasa, A., Egorov, S., Espenberg, M.,  
 3155 Järveoja, J., Jauhiainen, J. and Kasak, K.: Nitrogen-rich organic soils under warm well-drained conditions  
 3156 are global nitrous oxide emission hotspots, *Nat. Commun.*, 9, 1135, doi:10.1038/s41467-018-03540-1, 2018.
- 3157 Qi, X. M., Ding, A. J., Nie, W., Petäjä, T., Kerminen, V.-M., Herrmann, E., Xie, Y. N., Zheng, L. F.,  
 3158 Manninen, H., Aalto, P., Sun, J. N., Xu, Z. N., Chi, X. G., Huang, X., Boy, M., Virkkula, A., Yang, X.-Q.,  
 3159 Fu, C. B., and Kulmala, M.: Aerosol size distribution and new particle formation in the western Yangtze  
 3160 River Delta of China: 2 years of measurements at the SORPES station, *Atmos. Chem. Phys.*, 15, 12445–  
 3161 12464, doi:10.5194/acp-15-12445-2015, 2015.
- 3162 Rakitin, V. S., Elansky, N. F., Wang, P., Wang, G., Pankratova, N. V., Shtabkin, Y. A., Skorokhod A.I.,  
 3163 Safronov A.N., Makarova M.V., and Grechko E.I.: Changes in trends of atmospheric composition over urban  
 3164 and background regions of Eurasia: estimates based on spectroscopic observations, *Geography,*  
 3165 *Environment, Sustainability*, 11(2), 84-96, doi:10.24057/2071-9388-2018-11-2-84-96, 2018.
- 3166 Rautiainen, K., Parkkinen, T., Lemmetyinen, J., Schwank, M., Wiesmann, A., Ikonen, J., Derksen, C.,  
 3167 Davydov, S., Davydova, A., Boike, J., Langer, M., Druschg, M., and Pulliainen, J.: SMOS prototype  
 3168 algorithm for detecting autumn soil freezing, *Remote Sensing of Environment*, 180, 346-360,  
 3169 doi:10.1016/j.rse.2016.01.012, 2016.



- 3170 Rinke, A., Segger, B., Crewell, S., Maturilli, M., Naakka, T., Nygård, T., Vihma, T., Alshawaf, F., Dick, G.,  
 3171 Wickert, J., and Keller, J.: Trends of vertically integrated water vapor over the Arctic during 1979-2016:  
 3172 Consistent moistening all over?, *J. Climate*, 32, 6097–6116, doi:10.1175/JCLI-D-19-0092.1, 2019.
- 3173 Ripple, W. J., Wolf, C., Newsome, T. M., Galetti, M., Alamgir, M., Crist, E., Mahmoud, M. I., Laurance, W.  
 3174 F., and 15,364 scientist signatories from 184 countries. World scientists' warning to humanity: A second  
 3175 notice, *BioScience*, 67(12), 1026-1028, 2017.
- 3176 Rivero-Calle, S., Gnanadesikan, A., Del Castillo, C., Balch, W., and Guikema, S.: Multidecadal increase in  
 3177 North Atlantic coccolithophores and the potential role of rising CO<sub>2</sub>, *Science*, 350 (6267), 1533-1537, doi:  
 3178 10.1126/science.aaa8026, 2015.
- 3179 Romanowsky, E., Handorf, D., Jaiser, R., Wohltmann, I., Dorn, W., Ukita, J., Cohen, J., Dethloff, K., and  
 3180 Rex, M.: The role of stratospheric ozone for Arctic-midlatitude linkages, *Sci. Rep.* 9, 7962,  
 3181 doi:10.1038/s41598-019-43823-1, 2019.
- 3182 Romanovsky, V. E., and Osterkamp, T. E.: Effects of unfrozen water on heat and mass transport processes in  
 3183 the active layer and permafrost, *Permafrost Periglac. Process*, 11, 219–39, 2000.
- 3184 Roshydromet & GGO (2019): The State of Atmospheric Pollution in Cities on the Territory of Russia for  
 3185 2018. Yearbook. Federal Service on Hydrometeorology and Monitoring Environment, Roshydromet & A.I.  
 3186 Voeikov Main Geophysical Observatory, ISBN 978-5-9500883-8-4, St.Petersburg, 250 p., In Russian  
 3187 ([http://voeikovmgo.ru/images/stories/publications/2019/ejegodnik\\_zagr\\_atm\\_2018+.pdf](http://voeikovmgo.ru/images/stories/publications/2019/ejegodnik_zagr_atm_2018+.pdf))  
 3188
- 3189 Rost, B., and Riebesell, U.: Coccolithophores and the biological pump: responses to environmental changes,  
 3190 in: *Coccolithophores, from molecular processes to global impact*, edited by: Thierstein, H. R., Young, J. R.,  
 3191 99–125, Springer, Heidelberg, Germany, 2004.
- 3192 Ryazanova, A., and Voropay, N. N.: Droughts and Excessive Moisture Events in Southern Siberia in the  
 3193 Late XXth - Early XXIst Centuries, *IOP Conf. Ser.: Earth Environ. Sci.*, 96, 012015, 2017.
- 3194 Räisänen, J.: Effect of atmospheric circulation on recent temperature changes in Finland, *Clim. Dyn.*, 53,  
 3195 5675–5687, doi:10.1007/s00382-019-04890-2, 2019.
- 3196 Räisänen, J.: Effect of atmospheric circulation on surface air temperature trends in years 1979–2018. *Clim.*  
 3197 *Dyn.*, 56, 2303–2320, doi:10.1007/s00382-020-05590-y, 2021.
- 3198 Saarela, T., Rissanen, A. J., Ojala, A. et al.: CH<sub>4</sub> oxidation in a boreal lake during the development of  
 3199 hypolimnetic hypoxia, *Aquat Sci*, 82, 19, /doi.org/10.1007/s00027-019-0690-8, 2020.
- 3200 Salmon, Y., Lintunen, A., Dayet, A., Chan, T., Dewar, R., Vesala, T. and Hölttä, T.: Leaf carbon and water  
 3201 status control stomatal and non-stomatal limitations of photosynthesis in trees, *New Phytologist* 226, 690-  
 3202 703. doi: 10.1111/nph.16436, 2020.

- 3203 Santalahti, M., Sun, H., Sietiö, O.M., Köster, K., Berninger, F., Laurila, T., Pumpanen, J., and Heinonsalo,  
 3204 J.: Reindeer grazing alter soil fungal community structure and litter decomposition related enzyme activities  
 3205 in boreal coniferous forests in Finnish Lapland, *App. Soil Ecol.*, 132, 74-82,  
 3206 doi:10.1016/j.apsoil.2018.08.013, 2018.
- 3207 Schallhart, S., Rantala, P., Kajos, M. K., Aalto, J., Mammarella, I., Ruuskanen, T. M., and Kulmala, M.:  
 3208 Temporal variation of VOC fluxes measured with PTR-TOF above a boreal forest, *Atmospheric Chemistry  
 3209 and Physics*, 18(2), 815-832. doi:10.5194/acp-18-815-2018, 2018.
- 3210 Schmale, J., Arnold, S. R., Law, K. S., Thorp, T., Anenberg, S., Simpson, W. R., Mao, J. and Pratt, K. A.:  
 3211 Local Arctic air pollution: a neglected but serious problem, *Earths Future*, 6(10), 1385-1412,  
 3212 doi:10.1029/2018ef000952, 2018a.
- 3213 Schmale, J., Henning, S., Decesari, S., Henzing, B., Keskinen, H., Sellegri, K., Ovadnevaite, J., Pöhlker, M.  
 3214 L., Brito, J., Bougiatioti, A., Kristensson, A., Kalivitis, N., Stavroulas, I., Carbone, S., Jefferson, A., Park,  
 3215 M., Schlag, P., Iwamoto, Y., Aalto, P., Äijälä, M., Bukowiecki, N., Ehn, M., Frank, G., Fröhlich, R.,  
 3216 Frumau, A., Herrmann, E., Herrmann, H., Holzinger, R., Kos, G., Kulmala, M., Mihalopoulos, N., Nenes,  
 3217 A., O'Dowd, C., Petäjä, T., Picard, D., Pöhlker, C., Pöschl, U., Poulain, L., Prévôt, A. S. H., Swietlicki, E.,  
 3218 Andreae, M. O., Artaxo, P., Wiedensohler, A., Ogren, J., Matsuki, A., Yum, S. S., Stratmann, F.,  
 3219 Baltensperger, U., and Gysel, M.: Long-term cloud condensation nuclei number concentration, particle  
 3220 number size distribution and chemical composition measurements at regionally representative observatories,  
 3221 *Atmos. Chem. Phys.*, 18, 2853–2881, doi:10.5194/acp-18-2853-2018, 2018b.
- 3222 Schmeisser, L., Backman, J., Ogren, J. A., Andrews, E., Asmi, E., Starkweather, S., Uttal, T., Fiebig, M.,  
 3223 Sharma, S., Eleftheriadis, K., Vratolis, S., Bergin, M., Tunved, P., and Jefferson, A.: Seasonality of aerosol  
 3224 optical properties in the Arctic, *Atmos. Chem. Phys.*, 18, 11599–11622, doi:10.5194/acp-18-11599-2018,  
 3225 2018.
- 3226 Schuur, E. A. G., Bockheim, J., Canadell, J. G., Euskirchen, E., Field, C. B., Goryachkin, S. V., Hagemann,  
 3227 S., Kuhry, P., Lafleur, P.M., Lee, H., Mazhitova, G., Nelson, F. E., Rinke, A., Romanovsky, V. E.,  
 3228 Shiklomanov, N., Tarnocai, C., Venevsky, S., Vogel, J. G., and Zimov, S. A.: Vulnerability of permafrost  
 3229 carbon to climate change: implications for the global carbon cycle, *BioScience*, 58(8), 701–714,  
 3230 doi:10.1641/B580807, 2008.
- 3231 Schuur, E. A. G., McGuire, A. D., Romanovsky, V., Schädel, C., and Mack, M.: Chapter 11: Arctic and  
 3232 boreal carbon, in: *Second State of the Carbon Cycle Report (SOCCR2): A Sustained Assessment Report*,  
 3233 edited by: Cavallaro, N., Shrestha, G., Birdsey, R., Mayes, M. A., Najjar, R. G., Reed, S. C., Romero-  
 3234 Lankao, P., and Zhu, Z., U.S. Global Change Research Program, Washington, DC, USA, 428-468,  
 3235 doi:10.7930/SOCCR2.2018.Ch11, 2018.
- 3236 Scott, C. E., Monks, S. A., Spracklen, D. V., Arnold, S. R., Forster, P. M., Rap, A., Äijälä, M., Artaxo, P.,  
 3237 Carslaw, K. S., Chipperfield, M. P., Ehn, M., Gilardoni, S., Heikkinen, L., Kulmala, M., Petäjä, T.,

- 3238 Reddington, C. L. S., Rizzo, L. V., Swietlicki, E., Vignati, E., and Wilson, C.: Impact on short-lived climate  
3239 forcers increases projected warming due to deforestation, *Nat. Commun.*, 9, 9, doi:10.1038/s41467-017-  
3240 02412-4, 2018.
- 3241 Shakhova, N., Semiletov, I., and Belcheva, N.: The great Siberian rivers as a source of methane on the  
3242 Russian Arctic shelf, *Dokl. Earth Sci.*, 415, 734–736, doi: 10.1134/S1028334X07050169, 2007.
- 3243 Shalina, E. V., and Sandven, S.: Snow depth on Arctic sea ice from historical in situ data, *Cryosphere*, 12(6),  
3244 1867-1886, doi:10.5194/tc-12-1867-2018, 2018.
- 3245 Shen, Y., Virkkula, A., Ding, A., Wang, J., Chi, X., Nie, W., Qi, X., Huang, X., Liu, Q., Zheng, L., Xu, Z.,  
3246 Petäjä, T., Aalto, P. P., Fu, C., and Kulmala, M.: Aerosol optical properties at SORPES in Nanjing, east  
3247 China, *Atmos. Chem. Phys.*, 18, 5265–5292, doi: 10.5194/acp-18-5265-2018, 2018.
- 3248 Shen, Y., Virkkula, A., Ding, A., Luoma, K., Keskinen, H., Aalto, P. P., Chi, X., Qi, X., Nie, W., Huang, X.,  
3249 Petäjä, T., Kulmala, M., and Kerminen, V.-M.: Estimating cloud condensation nuclei number concentrations  
3250 using aerosol optical properties: role of particle number size distribution and parameterization, *Atmos.*  
3251 *Chem. Phys.*, 19, 15483–15502, doi:10.5194/acp-19-15483-2019, 2019.
- 3252 Shestakova, T. A., Gutierrez, E., Valeriano, C., Lapshina, E., and Voltas, J.: Recent loss of sensitivity to  
3253 summer temperature constrains tree growth synchrony among boreal Eurasian forests, *Agr. Forest Meteorol.*,  
3254 268, 318-330, doi:10.1016/j.agrformet.2019.01.039, 2019.
- 3255 Shevchenko, V. P., Starodymova, D. P., Vinogradova, A. A., Lisitzin, A. P., Makarov, V. I., Popova, S. A.,  
3256 Sivonen, V. V., and Sivonen, V. P.: Elemental and organic carbon in atmospheric aerosols over the  
3257 northwestern coast of Kandalaksha Bay of the White Sea, *Dokl. Earth Sci.*, 461(1), 242-246,  
3258 doi:10.1134/s1028334x1503006x, 2015.
- 3259 Shevchenko, V. P., Maslov, A. V., and Stein, R.: Distribution of some rare and trace elements in ice-rafted  
3260 sediments in the Yermak Plateau area, the Arctic Ocean, *Oceanol.*, 57(6), 855-863,  
3261 doi:10.1134/s0001437017060157, 2017a.
- 3262 Shevchenko, V. P., Pokrovsky, O. S., Vorobyev, S. N., Krickov, I. V., Manasypov, R. M., Politova, N. V.,  
3263 Kopysov, S. G., Dara, O. M., Auda, Y., Shirokova, L. S., Kolesnichenko, L. G., Zemtsov, V. A., and  
3264 Kirpotin, S. N.: Impact of snow deposition on major and trace element concentrations and elementary fluxes  
3265 in surface waters of the Western Siberian Lowland across a 1700 km latitudinal gradient, *Hydrol. Earth Syst.*  
3266 *Sci.*, 21, 5725–5746, doi:10.5194/hess-21-5725-2017, 2017b.
- 3267 Shevchenko, V. P., Kopeikin, V. M., Novigatsky, A. N., and Malafeev, G. V.: Black carbon in the  
3268 atmospheric boundary layer over the North Atlantic and the Russian Arctic seas in June–September 2017,  
3269 *Oceanol.*, 59(5), doi:10.1134/S0001437019050199, 692–696, 2019.

- 3270 Shevnina, E., Kourzeneva, E., Kovalenko, V., and Vihma, T.: Assessment of extreme flood events in a  
 3271 changing climate for a long-term planning of socio-economic infrastructure in the Russian Arctic, *Hydrol.*  
 3272 *Earth Syst. Sci.*, 21(5), 2559-2578, doi:10.5194/hess-21-2559-2017, 2017.
- 3273 Shevnina, E., Silaev, A., and Vihma, T.: Probabilistic projections of annual runoff and potential hydropower  
 3274 production in Finland, *Universal Journal of Geoscience*, 7(2), 43-55, doi:10.13189/ujg.2019.070201, 2019.
- 3275 Shiklomanov, A.I., and Lammers, R.B.: Record Russian river discharge in 2007 and the limits of analysis,  
 3276 *Environ. Res. Lett.*, 4, doi: 10.1088/1748-9326/4/4/045015, 2009.
- 3277 Shinkareva G. L., Lychagin M. Y., Tarasov M. K., Pietronó J., Chichaeva M. A., and Chalov S. R.:  
 3278 Biogeochemical specialization of macrophytes and their role as a biofilter in the Selenga delta, *Geography,*  
 3279 *Environment, Sustainability*, 12(3), 240-263, 2019.
- 3280 Silkin, V. A., Pautova, L., Giordano, M., Chasovnikov, V., Vostokov, S., Podymov, O., Parkhomova, S., and  
 3281 Moskalenko, L.: Drivers of phytoplankton blooms in the northeastern Black Sea, *Mar. Pollution Bull.*, 138,  
 3282 274-284, doi:10.1016/j.marpolbul.2018.11.042, 2018.
- 3283 Sizov O. S., and Lobotrosova S. A.: Features of revegetation of drift sand sites in the northern taiga subzone  
 3284 of Western Siberia. *Earth Cryosphere*, (3), 3–13, doi:10.21782/kz1560-7496-2016-3(3-13), 2016.
- 3285 Skorokhod, A. I., Berezina, E. V., Moiseenko, K. B., Elansky, N. F., and Belikov, I. B.: Benzene and toluene  
 3286 in the surface air of northern Eurasia from TROICA-12 campaign along the Trans-Siberian Railway, *Atmos.*  
 3287 *Chem. Phys.*, 17(8), 5501-5514, doi:10.5194/acp-17-5501-2017, 2017.
- 3288 Slukovskaya, M. V., Vasenev, V. I., Ivashchenko, K. V., Morev, D. V., Drogobuzhskaya, S. V., Ivanova, L.  
 3289 A., and Kremenetskaya, I. P.: Technosols on mining wastes in the subarctic: Efficiency of remediation under  
 3290 Cu-Ni atmospheric pollution, *Int. Soil Water Conserv. Res.*, 7(3), 297-307, doi:10.1016/j.iswcr.2019.04.002,  
 3291 2019.
- 3292 Smith, L.: *The new north: The world in 2050*, Profile Books, London, UK, 2011.
- 3293 Song, S., Li, C., Shi, X., Zhao, S., Li, Z., Bai, Y., Cao, X., Wang, Q., Huotari, J., Tulonen, T., Uusheimo, S.,  
 3294 Leppäranta, M., and Arvola, L.: Under-ice metabolism in a shallow lake (Wuliangshuai) in Inner Mongolia,  
 3295 in cold and arid climate zone, *Freshw. Biol.*, 1–11, 2019.
- 3296 Spengler, T., Renfrew, I. A., Terpstra, A., Tjernström, M., Screen, J., Brooks, I. M., Andrew Carleton, A.,  
 3297 Chechin, D., Chen, L., Doyle, J., Esau, I., Hezel, P. J., Jung, T., Kohyama, T., Lüpkes, C., McCusker, C. E.,  
 3298 Nygård, T., Sergeev, D., Shupe, M. D., Sodemann, H., and Vihma, T.: High-latitude dynamics of  
 3299 atmosphere–ice–ocean interactions, *Bull. Am. Meteorol. Soc.*, 97(9), ES179-ES182, doi:10.1175/bams-d-15-  
 3300 00302.1, 2016.
- 3301 Sporre, M. K., Blichner, S. M., Karset, I. H. H., Makkonen, R., and Berntsen, T. K.: BVOC–aerosol–climate  
 3302 feedbacks investigated using NorESM, *Atmos. Chem. Phys.*, 19, 4763–4782, doi:10.5194/acp-19-4763-  
 3303 2019, 2019.

- 3304 Starodymova, D. P., Shevchenko, V. P., Sivonen, V. P., and Sivonen, V. V.: Material and elemental  
 3305 composition of surface aerosols on the north-western coast of the Kandalaksha Bay of the White Sea, *Atmos.*  
 3306 *Oceanic Opt.*, 29(6), 507-511, doi:10.1134/s1024856016060154, 2016.
- 3307 Sun, H., Santalahti, M., Pumpanen, J., Koster, K., Berninger, F., Raffaello, T., Asiegbu, F. O., and  
 3308 Heinonsalo, J.: Bacterial community structure and function shift across a northern boreal forest fire  
 3309 chronosequence, *Scientific Rep.*, 6, 12, doi:10.1038/srep32411, 2016.
- 3310 Sun, Y., Frankenberg C., Wood JD, Schimel DS., Jung, M., Guanter L., Drewry, DT., Verma, M., Porcar-  
 3311 Castell, A., Griffis, TJ., Gu, L., Magney, S., Köhler P., Evans B., and Yuen, K.: OCO-2 advances  
 3312 photosynthesis observation from space via solar-induced chlorophyll fluorescence, *Science* 358, 189,  
 3313 doi:10.1126/science.aam5747, 2017.
- 3314 Suomi, I., Gryning, S-E. , O'Connor E.J., and Vihma, T.: Methodology for obtaining wind gusts  
 3315 using Doppler lidar, *Quarterly Journal of the Royal Meteorological Society*, 143, 2061-2072,  
 3316 doi.org/10.1002/qj.3059, 2016.
- 3317 Svensson, J., Virkkula, A., Meinander, O., Kivekäs, N., Hannula, H.-R., Järvinen, O., Peltoniemi, J.I.,  
 3318 Gritsevich, M., Heikkilä, A., Kontu, A., Neitola, K., Brus, D., DagssonWaldhauserova, P., Anttila, K.,  
 3319 Vehkamäki, M., Hienola, A., de Leeuw, G., and Lihavainen, H.: Soot-doped natural snow and its albedo —  
 3320 results from field experiments, *Boreal Environment Research*, 21, 481-503, 2016.
- 3321 Svensson, J., Ström, J., Kivekäs, N., Dkhar, N. B., Tayal, S., Sharma, V. P., Jutila, A., Backman, J.,  
 3322 Virkkula, A., Ruppel, M., Hyvärinen, A., Kontu, A., Hannula, H.-R., Leppäranta, M., Hooda, R. K., Korhola,  
 3323 A., Asmi, E., and Lihavainen, H.: Light absorption of dust and elemental carbon in snow in the Indian  
 3324 Himalayas and the Finnish Arctic, *Atmos. Meas. Tech.*, 11, 1403-1416, doi:10.5194/amt-11-1403-2018,  
 3325 2018.
- 3326 Svensson, J., Ström, J., and Virkkula, A.: Multiple-scattering correction factor of quartz filters and the effect  
 3327 of filtering particles mixed in water: implications for analyses of light absorption in snow samples, *Atmos.*  
 3328 *Meas. Tech.*, 12, 5913-5925, doi:10.5194/amt-12-5913-2019, 2019.
- 3329 Taylor, K. E., Stouffer, R. J., and Meehl, G. A.: An overview of CMIP5 and the experiment design, *Bull.*  
 3330 *Am. Meteorol. Soc.*, 93, 485-498, doi: 10.1175/BAMS-D-11-00094.1, 2012.
- 3331 Taylor, A., Brownlee, C., and Wheeler, G.: Coccolithophore cell biology: chalking up progress, *Ann. Rev.*  
 3332 *Mar. Sci.*, 9, 283-310, doi:10.1146/annurev-marine-122414-034032, 2017.
- 3333 Terentieva, I. E., Glagolev, M. V., Lapshina, E. D., Sabrekov, A. F., and Maksyutov, S.: Mapping of West  
 3334 Siberian taiga wetland complexes using Landsat imagery: implications for methane emissions,  
 3335 *Biogeosciences*, 13, 4615–4626, doi:10.5194/bg-13-4615-2016, 2016.

- 3336 Thompson, R. L., Sasakawa, M., Machida, T., Aalto, T., Worthy, D., Lavric, J. V., Lund Myhre, C., and  
 3337 Stohl, A.: Methane fluxes in the high northern latitudes for 2005–2013 estimated using a Bayesian  
 3338 atmospheric inversion, *Atmos. Chem. Phys.*, 17, 3553–3572, doi:10.5194/acp-17-3553-2017, 2017.
- 3339 Thonat, T., Saunio, M., Bousquet, P., Pison, I., Tan, Z., Zhuang, Q., Crill, P. M., Thornton, B. F., Bastviken,  
 3340 D., Dlugokencky, E. J., Zimov, N., Laurila, T., Hatakka, J., Hermansen, O., and Worthy, D. E. J.:  
 3341 Detectability of Arctic methane sources at six sites performing continuous atmospheric measurements,  
 3342 *Atmos. Chem. Phys.*, 17, 8371–8394, doi:10.5194/acp-17-8371-2017, 2017.
- 3343 Thorslund, J., Jarsjo, J., Wallstedt, T., Morth, C. M., Lychagin, M. Y., and Chalov, S. R.: Speciation and  
 3344 hydrological transport of metals in non-acidic river systems of the Lake Baikal basin: Field data and model  
 3345 predictions, *Reg. Environ. Chang.*, 17(7), 2007-2021, doi:10.1007/s10113-016-0982-7, 2017.
- 3346 Tian, Z. X., Cheng, B., Zhao, J. C., Vihma, T., Zhang, W. L., Li, Z. J., and Zhang, Z. H.: Observed and  
 3347 modelled snow and ice thickness in the Arctic Ocean with CHINARE buoy data, *Acta Oceanologica Sinica*,  
 3348 36(8), 66-75, doi:10.1007/s13131-017-1020-4, 2017.
- 3349 Tillman, H., Yang, J. and Nielsson, E.: The Polar Silk Road: China's New Frontier of International  
 3350 Cooperation, *China Quarterly of International Strategic Studies*, 4. 10.1142/S2377740018500215, 2018.
- 3351 Timokhina, A. V., Prokushkin, A. S., Onuchin, A. A., Panov, A. V., Kofman, G. B., and Heimann, M.:  
 3352 Variability of ground CO<sub>2</sub> concentration in the middle taiga subzone of the Yenisei region of Siberia, *Russ.*  
 3353 *J. Ecol.*, 46, 143-151, doi:10.1134/s1067413615020125, 2015a.
- 3354 Timokhina, A. V., Prokushkin, A. S., Onuchin, A. A., Panov, A. V., Kofman, G. B., Verkhovets, S. V., and  
 3355 Heimann, M., Long-term trend in CO<sub>2</sub> concentration in the surface atmosphere over Central Siberia, *Russ.*  
 3356 *Meteorol. Hydrol.*, 40, 186-190, 2015b.
- 3357 Tsuruta, A., Aalto, T., Backman, L., Hakkarainen, J., ... and Peters, W.: Global methane emission estimates  
 3358 for 2000–2012 from CarbonTracker Europe-CH<sub>4</sub> v1.0. *Geosci. Model Dev.*, 10, 1261–1289, 2017.
- 3359 Tuovinen, J-P., Aurela, M., Hatakka, J., Räsänen, A., ... Laurila, T.: Interpreting eddy covariance data from  
 3360 heterogeneous Siberian tundra: land-cover-specific methane fluxes and spatial representativeness,  
 3361 *Biogeosciences*, 16, 255–274, 2019.
- 3362 Uotila, P., Vihma, T., and Haapala, J.: Atmospheric and oceanic conditions and the extremely low Bothnian  
 3363 Bay sea ice extent in 2014/2015, 42, 7740-7749, *Geophysical Research and Letters*, 2015.
- 3364 Uotila, P., Iovino, D., Vancoppenolle, M., Lensu, M., and Rousset, C., Comparing sea ice, hydrography and  
 3365 circulation between NEMO3.6 LIM3 and LIM2, *Geosci. Model Dev.*, 10, 1009–1031, doi:10.5194/gmd-10-  
 3366 1009-2017, 2017.
- 3367 Uotila, P., Goosse, H., Haines, K., Chevallier, M., Barthélemy, A., Bricaud, C., Carton, J., Fučkar, N.,  
 3368 Garric, G., Iovino, D., Kauker, F., Korhonen, M., Lien, V. S., Marnela, M., Massonnet, F., Mignac, D.,

- 3369 Peterson, K. A., Sadikni, R., Shi, L., Tietsche, S., Toyoda, T., Xie, J., and Zhang, A.: An assessment of ten  
3370 ocean reanalyses in the polar regions, *Clim Dyn* 52, 1613–1650, doi:10.1007/s00382-018-4242-z, 2019.
- 3371 Uttal, T., Starkweather, S., Drummond, J. R., Vihma, T., Makshtas, A. P., Darby, L. S., Burkhart, J. F., Cox,  
3372 C. J., Schmeisser, L. N., Haiden, T., Maturilli, M., Shupe, M. D., De Boer, G., Saha, A., Grachev, A. A.,  
3373 Crepinsek, S. M., Bruhwiler, L., Goodison, B., McArthur, B., Walden, V. P., Dlugokencky, E. J., P. Persson,  
3374 O., Lesins, G., Laurila, T., Ogren, J. A., Stone, R., Long, C. N., Sharma, S., Massling, A., Turner, D. D.,  
3375 Stanitski, D. M., Asmi, E., Aurela, M., Skov, H., Eleftheriadis, K., Virkkula, A., Platt, A., Førland, E. J.,  
3376 Iijima, Y., Nielsen, I. E., Bergin, M. H., Candlish, L., Zimov, N. S., Zimov, S. A., O'Neill, N. T., Fogal, P.  
3377 F., Kivi, R., Konopleva-Akish, E. A., Verlinde, J., Kustov, V. Y., Vassel, B., Ivakhov, V. M., Viisanen Y.,  
3378 and Intrieri, J. M.: International Arctic Systems for Observing the Atmosphere: An International Polar Year  
3379 Legacy Consortium, *Bull. Amer. Meteor. Soc.*, 97, 1033–1056, doi:10.1175/BAMS-D-14-00145.1, 2016.
- 3380 Vanhatalo, A., Ghirardo, A., Juurola, E., Schnitzler, J.-P., Zimmer, I., Hellén, H., Hakola, H., and Bäck, J.:  
3381 Long-term dynamics of monoterpene synthase activities, monoterpene storage pools and emissions in boreal  
3382 Scots pine, *Biogeosciences*, 15, 5047–5060, doi:10.5194/bg-15-5047-2018, 2018.
- 3383 Varentsov, M., Konstantinov, P., Baklanov, A., Esau, I., Miles, V., and Davy, R.: Anthropogenic and natural  
3384 drivers of a strong winter urban heat island in a typical Arctic city, *Atmos. Chem. Phys.*, 18(23), 17573-  
3385 17587, doi:10.5194/acp-18-17573-2018, 2018a.
- 3386 Varentsov, M., Wouters, H., Platonov, V., and Konstantinov, P.: Megacity-induced mesoclimatic effects in  
3387 the lower atmosphere: a modeling study for multiple summers over Moscow, Russia, *Atmos.*, 9(2), 24,  
3388 doi:10.3390/atmos9020050, 2018b.
- 3389 Vasileva, A., Moiseenko, K., Skorokhod, A., Belikov, I., Kopeikin, V., and Lavrova, O.: Emission ratios of  
3390 trace gases and particles for Siberian forest fires on the basis of mobile ground observations, *Atmos. Chem.*  
3391 *Phys.*, 17(20), 12303-12325, doi:10.5194/acp-17-12303-2017, 2017.
- 3392 Vestenius, M., Hellén, H., Levula, J., Kuronen, P., Helminen, K. J., Nieminen, T., Kulmala, M., and Hakola,  
3393 H.: Acidic reaction products of monoterpenes and sesquiterpenes in atmospheric fine particles in a boreal  
3394 forest, *Atmos. Chem. Phys.*, 14, 7883–7893, doi:10.5194/acp-14-7883-2014, 2014.
- 3395 Vihma, T., Uotila, P., Sandven, S., Pozdnyakov, D., Makshtas, A., Pelyasov, A., Pirazzini, R., Danielsen, F.,  
3396 Chalov, S., Lappalainen, H. K., Ivanov, V., Frolov, I., Albin, A., Cheng, B., Dobrolyubov, S., Arkhipkin, V.,  
3397 Myslenkov, S., Petäjä, T., and Kulmala, M.: Towards an advanced observation system for the marine Arctic  
3398 in the framework of the Pan-Eurasian Experiment (PEEX), *Atmos. Chem. Phys.*, 19, 1941-1970,  
3399 doi:10.5194/acp-19-1941-2019, 2019.
- 3400 Vihma, T., Graversen, R., Chen, L., Dörthe H., Skific, N., Francis, J.A., Tyrrell, N., Hall, R., Hanna, E.,  
3401 Uotila, P., Dethloff, K., Karpechko, A. Y., Björnsson, H. and Overland, J. E.: Effects of the tropospheric  
3402 large-scale circulation on European winter temperatures during the period of amplified Arctic warming, *Int J*  
3403 *Climatol.*, 40, 509– 529, doi:10.1002/joc.6225, 2020

- 3404 Virkkula, A., Chi, X., Ding, A., Shen, Y., Nie, W., Qi, X., Zheng, L., Huang, X., Xie, Y., Wang, J., Petäjä,  
 3405 T., and Kulmala, M.: On the interpretation of the loading correction of the aethalometer, *Atmos. Meas.*  
 3406 *Tech.*, 8, 4415-4427, doi:10.5194/amt-8-4415-2015, 2015.
- 3407 Voigt, C., Marushchak, M.E., Lamprecht, R.E., et al.: Nitrous oxide emissions from thawing permafrost,  
 3408 *PNAS* May 2017, 201702902; DOI: 10.1073/pnas.1702902114.
- 3409 Voigt, C., Lamprecht, R. E., Marushchak, M. E., Lind, S. E., Novakovskiy, A., Aurela, M., Martikainen, P. J.  
 3410 and Biasi, C.: Warming of subarctic tundra increases emissions of all three important greenhouse gases -  
 3411 carbon dioxide, methane, and nitrous oxide, *Glob. Change Biol.*, 23(8), 3121-3138, doi:10.1111/gcb.13563,  
 3412 2016.
- 3413 Voropay, N. N., Kichigina, N. V.: Long-term changes in the hydroclimatic characteristics in the Baikal  
 3414 region, *IOP Conf. Ser.: Earth Environ. Sci.*, 107, 012042, 2018.
- 3415 Voropay N.N., Ryazanova A.A., Dyukarev E.A. Variability of vegetation index NDVI during periods of  
 3416 drought in the Tomsk Region, *IOP Conf. Series: Earth Environ. Sci.*, 381, 012096, doi:10.1088/1755-  
 3417 1315/381/1/012096, 2019.
- 3418 Walker, X. J., Baltzer, J. L., Cumming, S. G., Day, N. J., Ebert, C., Goetz, S., Johnstone, J. F., Potter, S.,  
 3419 Rogers, B. M., Schuur, E. A. G., Turetsky, M. R., and Mack, M. C., Increasing wildfires threaten historic  
 3420 carbon sink of boreal forest soils, *Nature*, 572, 520-523, doi:10.1038/s41586-019-1474-y, 2019.
- 3421 Walsh, M. G., de Smalen, A. W., and Mor, S. M.: Climatic influence on anthrax suitability in warming  
 3422 northern latitudes, *Sci Rep*, 8(1), 9269, doi:10.1038/s41598-018-27604-w, 2018.
- 3423 van Vuuren, D. P., Edmonds, J., Kainuma, M., Riahi, K., Thomson, A., Hibbard, K., Hurtt, G. C., Kram, T.,  
 3424 Krey, V., Lamarque, J. F., Masui, T., Meinshausen, M., Nakicenovic, N., Smith, S. J., and Rose, S. K.: The  
 3425 representative concentration pathways: an overview, *Clim. Chang.*, 109, 5-31, doi:10.1007/s10584-011-  
 3426 0148-z, 2011.
- 3427 Wang, J., Ge, X., Chen, Y., Shen, Y., Zhang, Q., Sun, Y., Xu, J., Ge, S., Yu, H., and Chen, M.: Highly time-  
 3428 resolved urban aerosol characteristics during springtime in Yangtze River Delta, China: insights from soot  
 3429 particle aerosol mass spectrometry, *Atmos. Chem. Phys.*, 16, 9109–9127, doi:10.5194/acp-16-9109-2016,  
 3430 2016.
- 3431 Wang, J., Zhao, B., Wang, S., Yang, F., Xing, J., Morawska, L., Ding, A., Kulmala, M., Kerminen, V.-M.,  
 3432 Kujansuu, J., Wang, Z., Ding, D., Zhang, X., Wang, H., Tian, M., Petäjä, T., Jiang, J., and Hao J.: Particulate  
 3433 matter pollution over China and the effects of control policies, *Sci. Total Environ.*, 584-585, 426-447, 2017a.
- 3434 Wang, Z. B., Wu, Z. J., Yue, D. L., Shang, D. J., Guo, S., Sun, J. Y., Ding, A. J., Wang, L., Jiang, J. K., Guo,  
 3435 H., Gao, J., Cheung, H. C., Morawska, L., Keywood, M., and Hu, M.: New particle formation in China:  
 3436 Current knowledge and further directions, *Sci. Total Environ.*, 577, 258–266,  
 3437 doi:10.1016/j.scitotenv.2016.10.177, 2017b.



- 3438 Wang, Z., Huang, X., and Ding, A.: Dome effect of black carbon and its key influencing factors, *Atmos.*  
 3439 *Chem. Phys.*, 18, 2821-2834, 2018**b**.
- 3440 Wang, P. C., Elansky, N. F., Timofeev, Y. M., Wang, G. C., Golitsyn, G. S., Makarova, M. V., Rakitin, V.  
 3441 S., Shtabkin, Yu., Skorokhod, A. I., Grechko, E. I., Fokeeva, E. V., Safronov, A. N., Ran, L., and Wang, T.:  
 3442 Long-term trends of carbon monoxide total columnar amount in urban areas and background regions:  
 3443 ground- and satellite-based spectroscopic measurements, *Adv. Atmos. Sci.*, 35(7), 785-795,  
 3444 doi:10.1007/s00376-017-6327-8, 2018a.
- 3445 Wang, Y., Wang, Y., Wang, L., Petäjä, T., Zha, Q., Gong, C., Li, S., Pan, Y., Hu, B., Xin, J., and Kulmala,  
 3446 M.: Increased inorganic aerosol fraction contributes to air pollution and haze in China, *Atmos. Chem. Phys.*,  
 3447 19, 5881–5888, doi:10.5194/acp-19-5881-2019, 2019.
- 3448 Wang, Y.H., Yu, M., Wang, Y., Tang, G., Song, T., Zhou, P., Liu, Z., Hu, B., Ji, D.S., Wang, L., Zhu, X.,  
 3449 Yan, C., Ehn, M., Gao, W.K., Pan, Y.P., Xin, J.Y., Sung, Y., Kerminen, V.-M., Kulmala, M. and Petäjä, T.:  
 3450 Rapid formation of intense haze episode via aerosol-boundary layer feedback in Beijing, *Atmos. Chem.*  
 3451 *Phys.*, 10, 45-53, 2020.
- 3452 Wei, L. X., Deng, X. H., Cheng, B., Vihma, T., Hannula, H. R., Qin, T., and Pulliainen, J.: The impact of  
 3453 meteorological conditions on snow and ice thickness in an Arctic lake, *Tellus A: Dyn. Meteorol. Oceanogr.*,  
 3454 68, 12, doi:10.3402/tellusa.v68.31590, 2016.
- 3455 Wickström, S., Jonassen, M., Vihma, T., and Uotila, P.: Trends in cyclones in the high latitude North  
 3456 Atlantic during 1979-2016, *Q. J. R. Meteorol. Soc.*, 146, 762– 779, doi:10.1002/qj.3707, 2020.
- 3457 Wiedensohler, A., Ma, N., Birmili, W., Heintzenberg, J., Ditas, F., Andreae, M. O., and Panov, A.:  
 3458 Infrequent new particle formation over the remote boreal forest of Siberia, *Atmos. Environ.*, 200, 167-169,  
 3459 doi:10.1016/j.atmosenv.2018.12.013, 2019.
- 3460 Wild, B., Andersson, A., Bröder, L., Vonk, J., Hugelius, G., McClelland, J.W., Song, W., Raymond, P.A.,  
 3461 and Gustafsson, Ö.: Rivers across the Siberian Arctic unearth the patterns of carbon release from thawing  
 3462 permafrost *Proceedings of the National Academy of Sciences*, 116 (21) 10280-10285., 2019.
- 3463 Williams, P. J., and Smith, M. W.: *The Frozen Earth: Fundamentals of Geocryology*, Cambridge University  
 3464 Press, Cambridge, UK, 1989.
- 3465 WMO, 2019 Guidance on Integrated Urban Hydrometeorological, Climate and Environmental Services.  
 3466 Volume 1: Concept and Methodology, Grimmond, S., Bouchet, S., Molina, L., Baklanov, A., Joe, P. et al.,  
 3467 WMO-No. 1234, [https://library.wmo.int/doc\\_num.php?explnum\\_id=9903](https://library.wmo.int/doc_num.php?explnum_id=9903), 2019.
- 3468 Wolf-Grosse, T., Esau, I., and Reuder, J.: The large-scale circulation during air quality hazards in Bergen,  
 3469 Norway, *Tellus A: Dyn. Meteorol. Oceanogr.*, 69, 16, doi:10.1080/16000870.2017.1406265, 2017a.

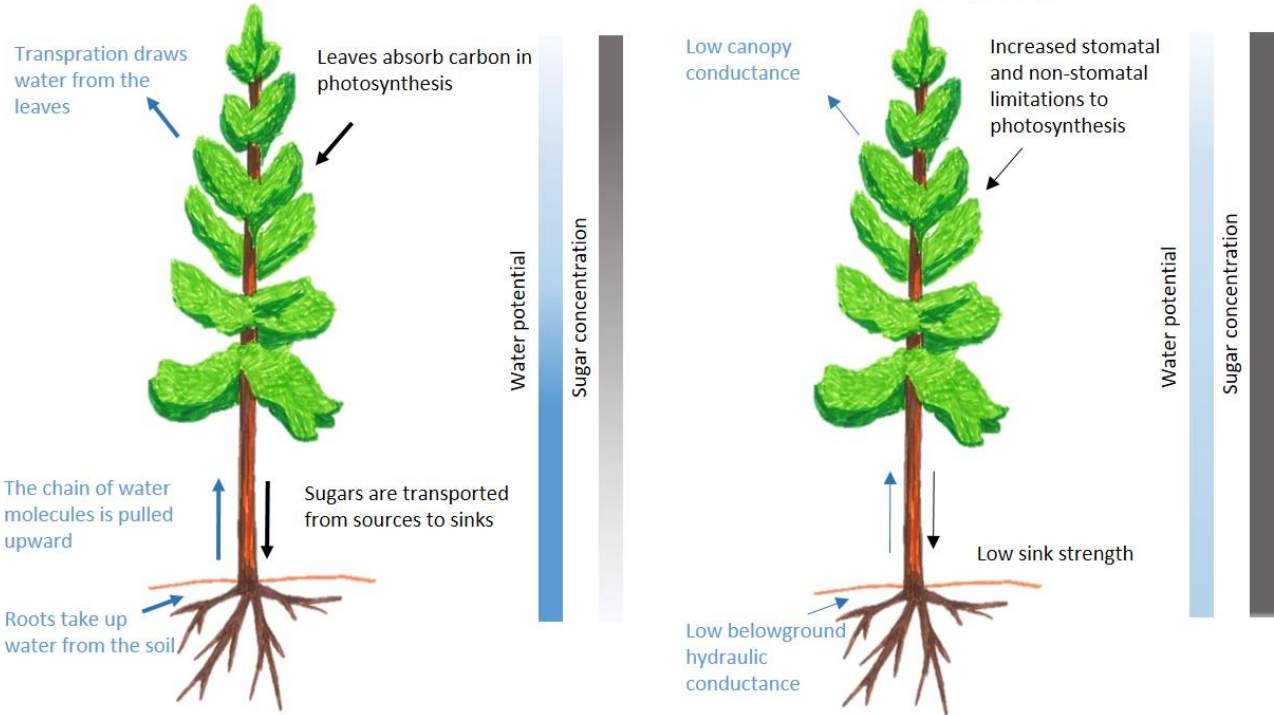
- 3470 Wolf-Grosse, T., Esau, I., and Reuder, J.: Sensitivity of local air quality to the interplay between small- and  
 3471 large-scale circulations: a large-eddy simulation study, *Atmos. Chem. Phys.*, 17(11), 7261-7276,  
 3472 doi:10.5194/acp-17-7261-2017, 2017b.
- 3473 Xausa, F., Paasonen, P., Makkonen, R., Arshinov, M., Ding, A., Denier Van Der Gon, H., Kerminen, V.-M.,  
 3474 and Kulmala, M.: Advancing global aerosol simulations with size-segregated anthropogenic particle number  
 3475 emissions, *Atmos. Chem. Phys.*, 18, 10039–10054, doi:10.5194/acp-18-10039-2018, 2018.
- 3476 Xiao, S., Wang, M. Y., Yao, L., Zhou, B., Yang, X., Chen, J. M., Wang, D. F., Fu, Q. Y., Worsnop, D. R.  
 3477 and Wang, L.: Strong atmospheric new particle formation in winter in urban Shanghai, China, *Atmos. Chem.*  
 3478 *Phys.*, 15, 1769-1781, 2015.
- 3479 Xie, Y. N., Ding, A. J., Nie, W., Mao, H. T., Qi, X. M., Huang, X., Xu, Z., Kerminen, V. K., Petäjä, T., Chi,  
 3480 X., Virkkula, A., Boy, M., Xue, L., Guo, J., Sun, J., Yang, X., Kulmala, M., and Fu, C. B.: Enhanced sulfate  
 3481 formation by nitrogen dioxide: Implications from in situ observations at the SORPES station, *J Geophys.*  
 3482 *Res.: Atmos.*, 120(24), 12679-12694, doi:10.1002/2015jd023607, 2015.
- 3483 Yan, C., Yin, R., Lu, Y., Dada, L., Yang, D., Fu, Y., Kontkanen, J., Deng, C., Garmash, O., Ruan, J.,  
 3484 Baalbaki, R., Schervish, M., Cai, R., Bloss, M., Chan, T., Chen, T., Chen, Q., Chen, X., Chen, Y., Chu, B.,  
 3485 Dällenbach, K., Foreback, B., He, X., Heikkinen, L., Jokinen, T., Junninen, H., Kangasluoma, J., Kokkonen,  
 3486 T., Kurppa, M., Lehtipalo, K., Li, H., Li, H., Li, X., Liu, Y. Ma, Q., Paasonen, P., Rantala, P., Pileci, R. E.,  
 3487 Rusanen, A., Sarnela, N., Simonen, P., Wang, S., Wang, W., Wang, Y. Xue, M., Yang, G., Yao, L., Zhou,  
 3488 Y., Kujansuu, J., Petäjä, T., Nie, W., Ma, N., Ge, M., He, H., Donahue, N. M., Worsnop, D. R., Kerminen,  
 3489 V.-M., Wang, L., Liu, Y., Zheng, J., Kulmala, M., Jiang, J. and Bianchi, F. (2021) The synergistic role of  
 3490 sulfuric acid, bases, and oxidized organics governing new-particle formation in Beijing. *Geophys. Res. Lett.*  
 3491 (in press).
- 3492 Yang, F., Li, C., Leppäranta, M., Shi, X., Zhao, S. and Zhang, C.: Notable increases in nutrient  
 3493 concentrations in a shallow lake during seasonal ice growth, *Water Sci. Technol.*, 74(12), 2773–2883, 2016.
- 3494 Yang, Y., Leppäranta, M. J., Ki, Z., Cheng, B., Zhai, M., and Demchev, D.: Model simulations of the annual  
 3495 cycle of the landfast ice thickness in the East Siberian Sea, *Advances in Polar Sciences*, 26(2), 168-178,  
 3496 doi:10.13679/j.advps.2015.2.00168, 2015.
- 3497 Yao, L., Garmash, O., Bianchi, F., Zheng, J., Yan, C., Kontkanen, J., Junninen, H., Mazon, S.B., Ehn, M.,  
 3498 Paasonen, P., Sipilä, M., Wang, M.Y., Wang, X.K., Xiao, S., Chen, H.F., Lu, Y.Q., Zhang, B.W., Wang,  
 3499 D.F., Fu, Q.Y., Geng, F.H., Li, L., Wang, H.L., Qiao, L.P., Yang, X., Chen, J.M., Kerminen, V.-M., Petäjä,  
 3500 T., Worsnop, D.R., Kulmala, M. and Wang, L.: Atmospheric new particle formation from sulfuric acid and  
 3501 amines in a Chinese megacity, *Science*, 361, 278-281, 2018.
- 3502 Yasunaka, S., Siswanto, E., Olsen, A., Hoppema, M., Watanabe, E., Fransson, A., Chierici, M., Murata, A.,  
 3503 Lauvset, S. K., Wanninkhof, R., Takahashi, T., Kosugi, N., Omar, A. M., van Heuven, S., and Mathis, J. T.:

- 3504 Arctic Ocean CO<sub>2</sub> uptake: an improved multiyear estimate of the air–sea CO<sub>2</sub> flux incorporating chlorophyll  
3505 a concentrations, *Biogeosciences*, 15, 1643–1661, doi:10.5194/bg-15-1643-2018, 2018.
- 3506 Ye, Z., Liu, J., Gu, A., Feng, F., Liu, Y., Bi, C., Xu, J., Li, L., Chen, H., Chen, Y., Dai, L., Zhou, Q., and Ge,  
3507 X.: Chemical characterization of fine particulate matter in Changzhou, China, and source apportionment with  
3508 offline aerosol mass spectrometry, *Atmos. Chem. Phys.*, 17, 2573–2592, doi:10.5194/acp-17-2573-2017,  
3509 2017.
- 3510 Ylivinkka, I., Kaupinmäki, S., Virman, M., Peltola, M., Taipale, D., Petäjä, T., Kerminen, V.-M., Kulmala,  
3511 M., and Ezhova, E.: Clouds over Hyytiälä, Finland: an algorithm to classify clouds based on solar radiation  
3512 and cloud base height measurements, *Atmos. Meas. Tech.*, 13, 5595–5619, 2020.
- 3513 He, Y., Chen, F., Jia, H., and Valery, G.: Bondur: Different Drought Legacies between Rain-fed and  
3514 Irrigated Croplands in a Typical Russian Agricultural Region, *Remote Sens.*, 12(11), 1700,  
3515 doi:10.3390/rs12111700, 2020
- 3516 Zaidan, M. A., Haapasilta, V., Relan, R., Junninen, H., Aalto, P. P., Kulmala, M., Laurson, L., and Foster, A.  
3517 S.: Predicting atmospheric particle formation days by Bayesian classification of the time series features,  
3518 *Tellus B: Chem. Phys. Meteorol.*, 70, 10, doi:10.1080/16000889.2018.1530031, 2018a.
- 3519 Zaidan, M. A., Haapasilta, V., Relan, R., Paasonen, P., Kerminen, V.-M., Junninen, H., Kulmala, M., and  
3520 Foster, A. S.: Exploring non-linear associations between atmospheric new-particle formation and ambient  
3521 variables: a mutual information approach, *Atmos. Chem. Phys.*, 18, 12699–12714, doi:10.5194/acp-18-  
3522 12699-2018, 2018b.
- 3523 Zanatta, M., Laj, P., Gysel, M., Baltensperger, U., Vratolis, S., Eleftheriadis, K., Kondo, Y., Dubuisson, P.,  
3524 Winiarek, V., Kazadzis, S., Tunved, P., and Jacobi, H.-W.: Effects of mixing state on optical and radiative  
3525 properties of black carbon in the European Arctic, *Atmos. Chem. Phys.*, 18, 14037–14057, doi:10.5194/acp-  
3526 18-14037-2018, 2018.
- 3527 Zapadinsky, E., Passananti, M., Myllyls, N., Kurten, T., and Vehkamäki, H.: Modeling on Fragmentation of  
3528 Clusters inside a Mass Spectrometer, *Journal of Physical Chemistry, A* 123 (2), 611–624,  
3529 <https://doi.org/10.1021/acs.jpca.8b10744>, 2019.
- 3530 Zha, Q., Yan, C., Junninen, H., Riva, M., Sarnela, N., Aalto, J., Quéléver, L., Schallhart, S., Dada, L.,  
3531 Heikkinen, L., Peräkylä, O., Zou, J., Rose, C., Wang, Y., Mammarella, I., Katul, G., Vesala, T., Worsnop, D.  
3532 R., Kulmala, M., Petäjä, T., Bianchi, F., and Ehn, M.: Vertical characterization of highly oxygenated  
3533 molecules (HOMs) below and above a boreal forest canopy, *Atmos. Chem. Phys.*, 18, 17437–17450,  
3534 doi:10.5194/acp-18-17437-2018, 2018.
- 3535 Zhang, J., Liu, C., and Chen, H.: The modulation of Tibetan Plateau heating on the multi-scale northernmost  
3536 margin activity of East Asia summer monsoon in northern China, *Global Planet. Change*, 161, 149–161,  
3537 2018.

- 3538 Zhang, S., Zhang, J. H., Bai, Y., Koju, U. A., Igbawua, T., Chang, Q., Zhang, D., and Yao, F. M.: Evaluation  
3539 and improvement of the daily boreal ecosystem productivity simulator in simulating gross primary  
3540 productivity at 41 flux sites across Europe, *Ecol. Model.*, 368, 205-232,  
3541 doi:10.1016/j.ecolmodel.2017.11.023, 2018.
- 3542 Zhang-Turpeinen, H., Kivimäenpää, M., Aaltonen, H., Berninger, F., Köster, E., Köster, K., Menyailo, O.,  
3543 Prokushkin, A., and Pumpanen, J.: Wildfire effects on BVOC emissions from boreal forest floor on  
3544 permafrost soil in Siberia, *Science of the Total Environment*, 134851, doi:10.1016/j.scitotenv.2019.134851,  
3545 2020.
- 3546 Zhao, H., Li, X., Zhang, Q., Jiang, X., Lin, J., Peters, G. P., Li, M., Geng, G., Zheng, B., Huo, H., Zhang, L.,  
3547 Wang, H., Davis, S. J., and He, K.: Effects of atmospheric transport and trade on air pollution mortality in  
3548 China, *Atmos. Chem. Phys.*, 17, 10367–10381, doi:10.5194/acp-17-10367-2017, 2017.
- 3549 Zhdanova, E. Y., Chubarova, N. Y., and Lyapustin, A. I.: Assessment of urban aerosol pollution over the  
3550 Moscow megacity by the MAIAC aerosol product, *Atmos. Meas. Tech.*, 13, 877–891, doi:10.5194/amt-13-  
3551 877-2020, 2020.
- 3552 Zhou, Y., Dada, L., Liu, Y., Fu, Y., Kangasluoma, J., Chan, T., Yan, C., Chu, B., Daellenbach, K. R.,  
3553 Bianchi, F., Kokkonen, T. V., Liu, Y., Kujansuu, J., Kerminen, V.-M., Petäjä, T., Wang, L., Jiang, J., and  
3554 Kulmala, M.: Variation of size-segregated particle number concentrations in wintertime Beijing, *Atmos.*  
3555 *Chem. Phys.*, 20, 1201–1216, doi:10.5194/acp-20-1201-2020, 2020.
- 3556 Zilitinkevich, S., Druzhinin, O., Glazunov, A., Kadantsev, E., Mortikov, E., Repina, I., and Troitskaya, Y.:  
3557 Dissipation rate of turbulent kinetic energy in stably stratified sheared flows, *Atmos. Chem. Phys.*, 19, 2489–  
3558 2496, doi:10.5194/acp-19-2489-2019, 2019.
- 3559 Öström, E., Putian, Z., Schurgers, G., Mishurov, M., Kivekäs, N., Lihavainen, H., Ehn, M., Rissanen, M. P.,  
3560 Kurtén, T., Boy, M., Swietlicki, E., and Roldin, P.: Modeling the role of highly oxidized multifunctional  
3561 organic molecules for the growth of new particles over the boreal forest region, *Atmos. Chem. Phys.*, 17,  
3562 8887–8901, doi:10.5194/acp-17-8887-2017, 2017.
- 3563

Non-stressed conditions

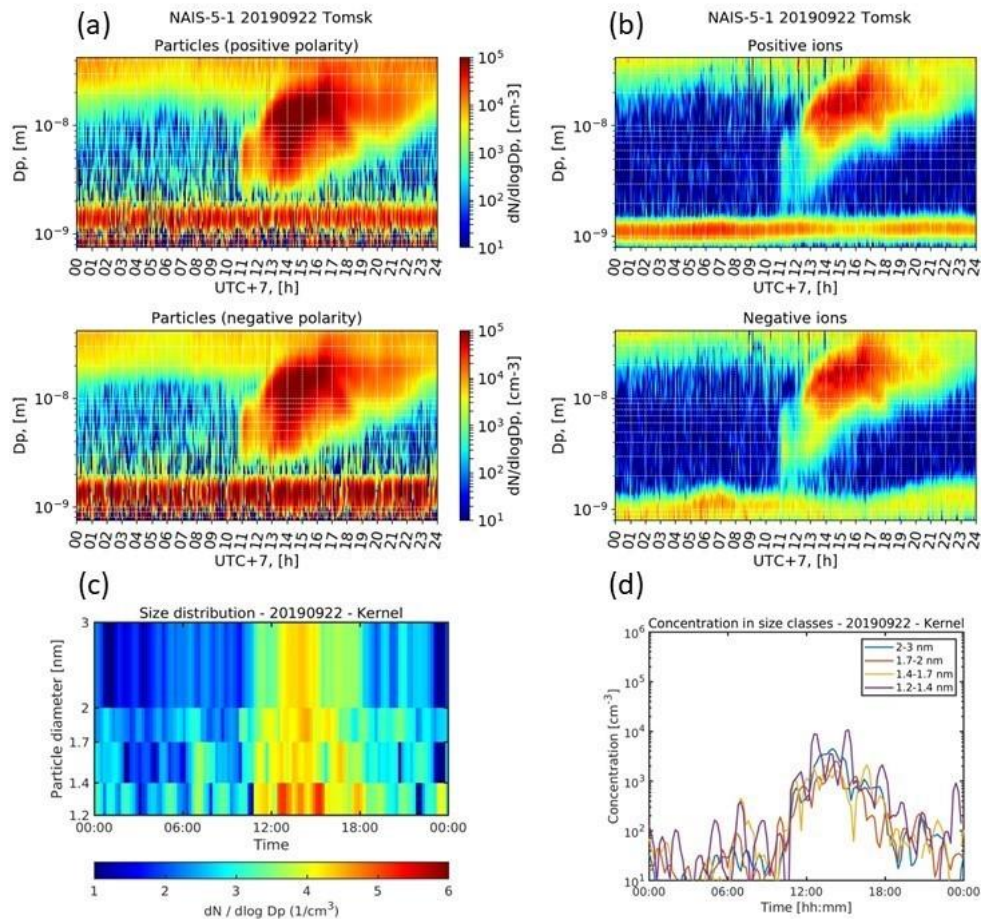
Cold soil in spring



3564

3565 Figure 1.

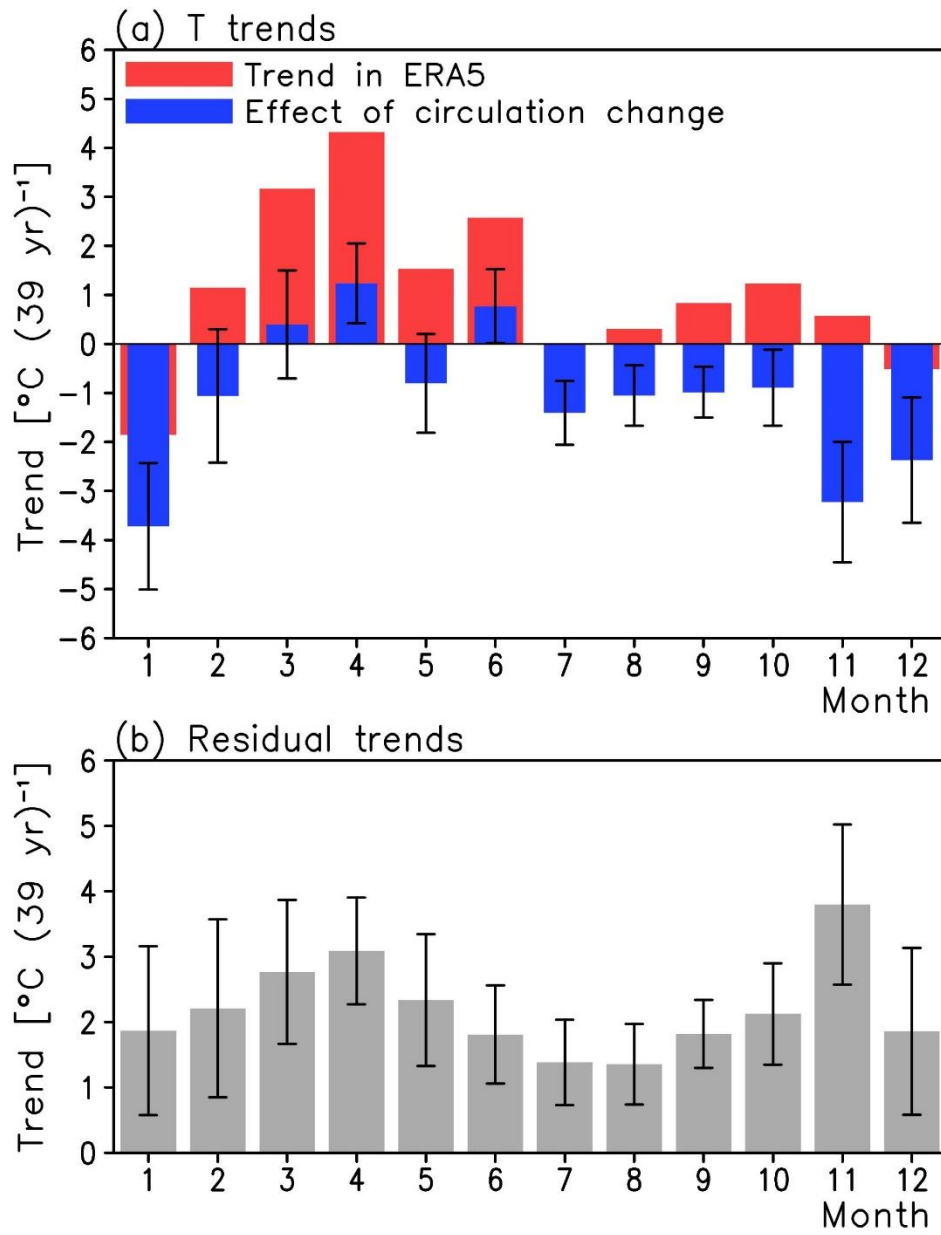
3566



3567

3568 Figure 2.

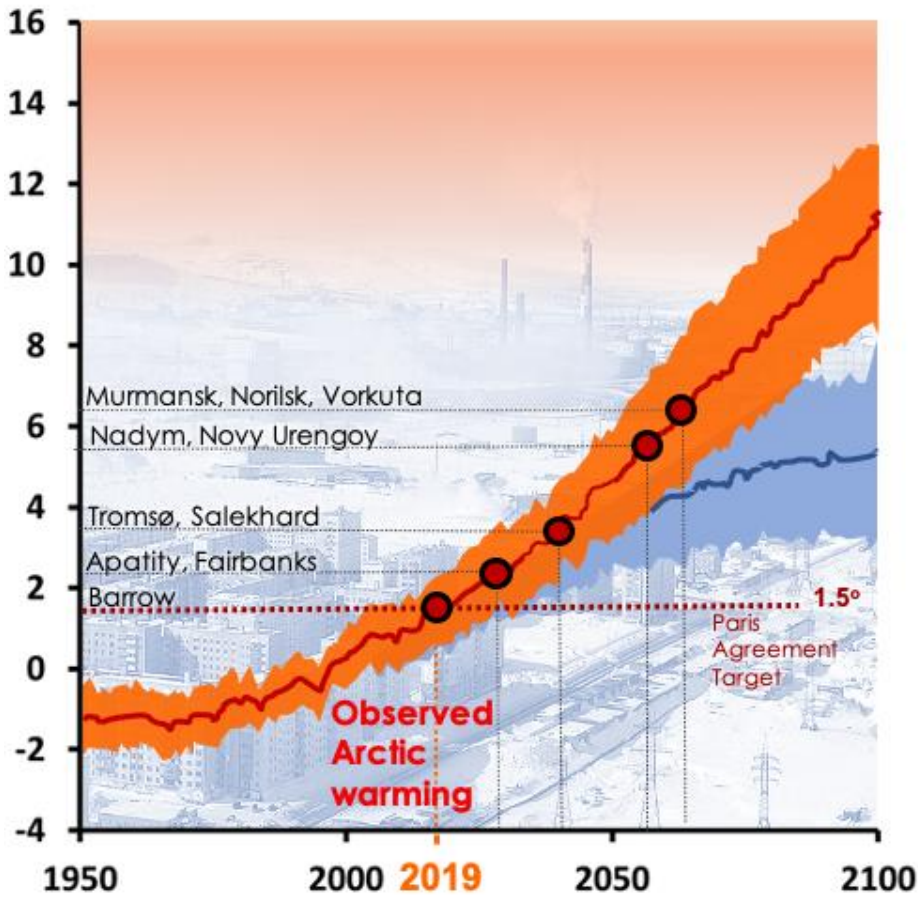
3569



3570

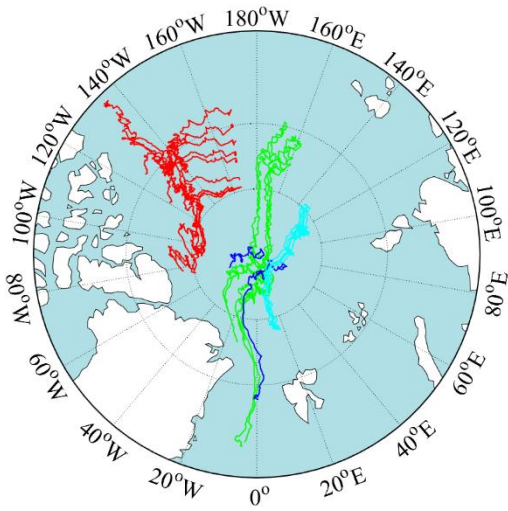
3571 Figure 3.

3572



3573

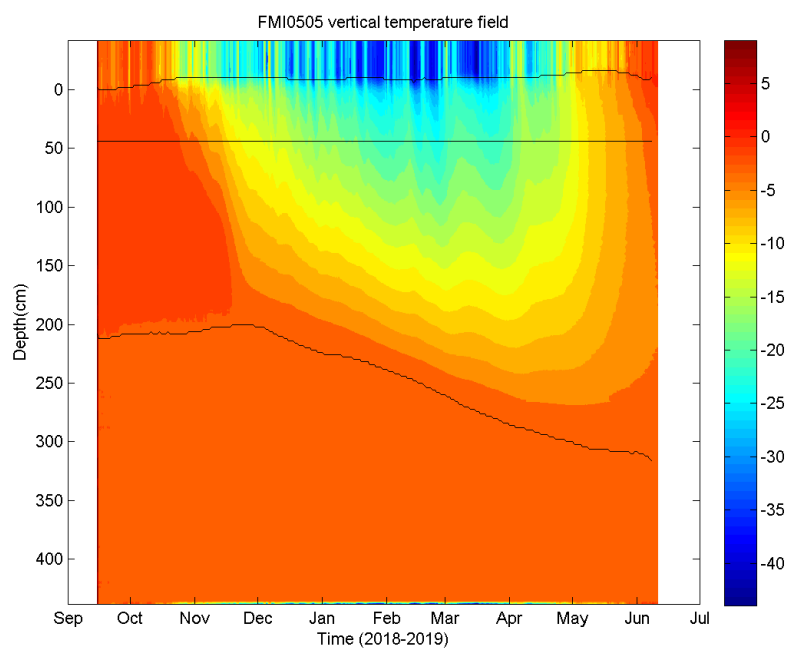
3574 Figure 4.



3575

3576 Figure 5.

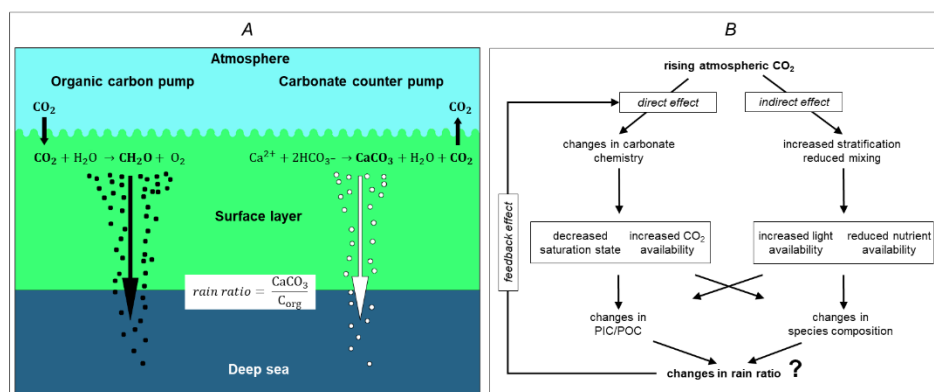
3577



3578

3579 Figure 6.

3580

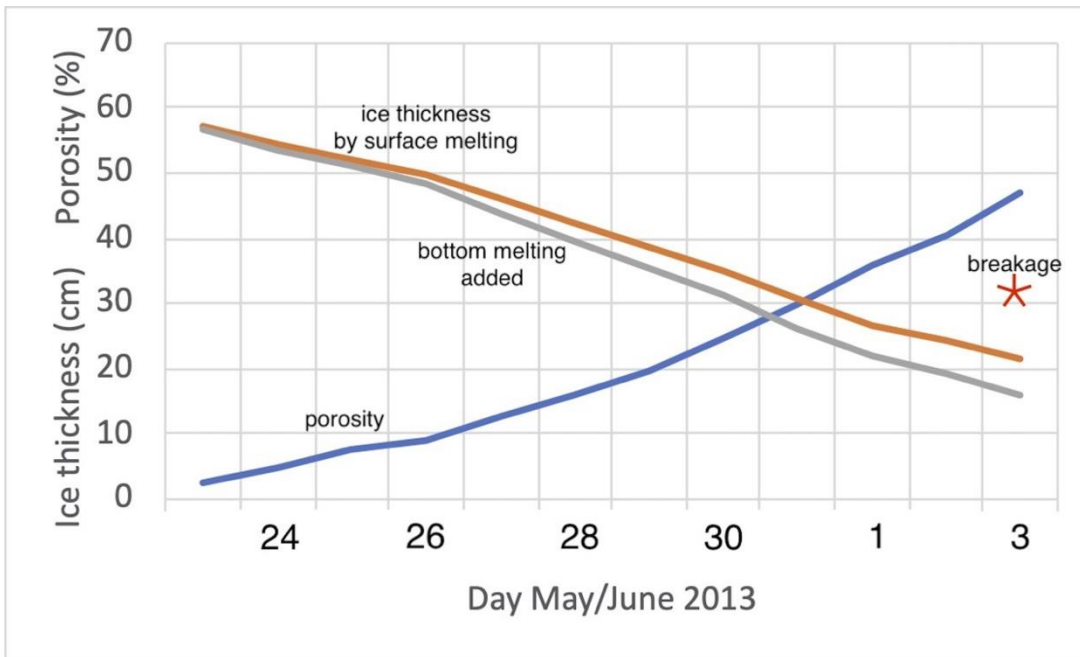


3581

3582 Figure 7.

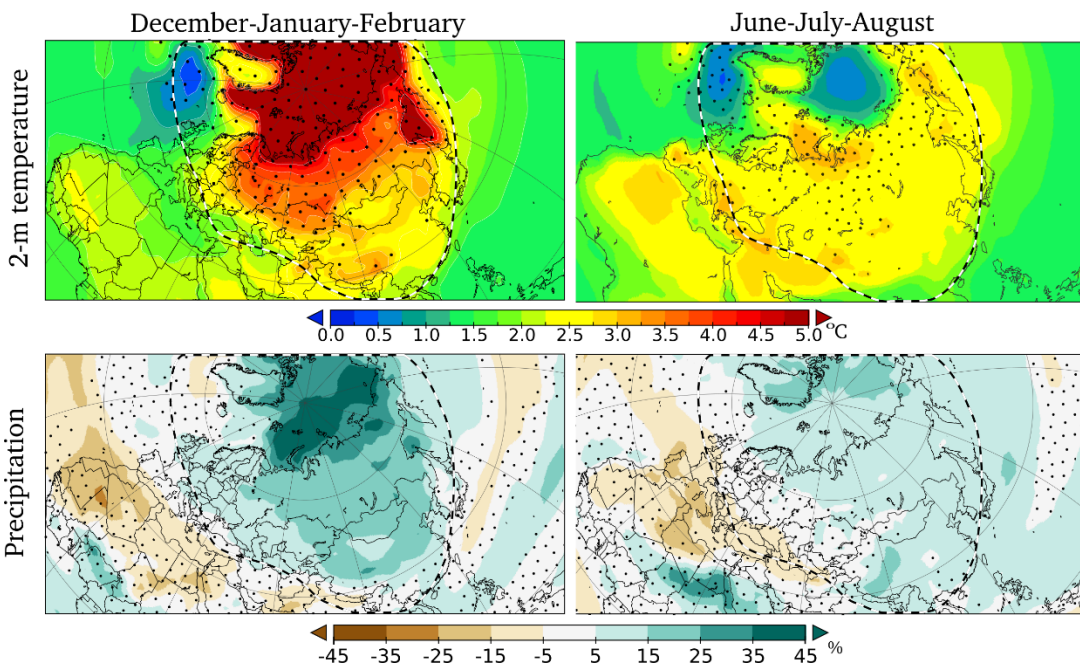
3583





3584

3585 Figure 8.



3586

3587 Figure 9.

3588

3589

3590

3591

3592 **Figure 1.** A recent field and modelling study shows that cold soil decreases belowground hydraulic  
 3593 conductance (i.e. less root water uptake), and further canopy conductance in mature, boreal trees in spring

3594 (Lintunen et al. 2020). Cold temperature also decreases sink strength (i.e. less sugars are needed for  
 3595 metabolism and growth). Low sink strength increases sugar concentration in leaves, which decreases  
 3596 photosynthesis due to increased stomatal and non-stomatal limitations for photosynthesis (Hölttä et al., 2017;  
 3597 Salmon et al., 2020).

3598 **Figure 2.** Example of results from the state-of-the-art aerosol instruments NAIS and PSM displaying NPF  
 3599 event at Fonovaya station, Siberia, on 22.09.2019. Particles of different polarity, NAIS (a), ions of different  
 3600 polarity, NAIS (b), particle number distribution at the smallest sizes, PSM (c), number concentration of the  
 3601 smallest particles in different size bins, PSM (d).

3602

3603 **Figure 3.** Linear trends of monthly mean temperature in Western Siberia (55°-65°N, 65°-90°E) in years  
 3604 1979-2018. In (a), the red bars show the trend in the ERA5 reanalysis and the blue bars the circulation-  
 3605 related trend. In (b), the residual trends are shown. The error bars indicate the 5-95% uncertainty range in the  
 3606 circulation-related trend and the residual trend based on interannual variability. Redrawn from Räisänen  
 3607 (2021).

3608

3609 **Figure 4.** The northern urban heat islands are forerunners of the global warming. Winter season future  
 3610 temperatures for the Arctic (60–90°N) averaged over 36 CMIP5 global climate models and expressed as  
 3611 departures from the means for the 1981–2005 period. The red line is the ensemble mean for RCP8.5, the blue  
 3612 line is for RCP4.5. Shaded areas denote  $\pm$  one standard deviation from the ensemble mean (Overland et al.,  
 3613 2014; and Fig. 2.15 of AMAP, 2017). The observed surface UHIs are shown as red dots collocated with the  
 3614 expected future Arctic temperature anomalies, e.g., the observed wintertime urban temperature anomaly in  
 3615 Nadyim corresponds to the regional warming as expected to be reached by 2060. Observe that the present  
 3616 Arctic climate is already 1.5°C warmer than the historical normals 1960-1990.

3617

3618 **Figure 5.** Trajectories of SIMBA buoys deployed in the Arctic in the period 2018-2019. Red: CHINARE (10  
 3619 buoys), green: NABOS (5 buoys), dark blue: CAATEX (2 buoys), and light blue: MOSAiC (15 buoys).  
 3620 SIMBA is a thermistor string-based ice mass balance (IMB) buoy. It measures high-resolution (2 cm)  
 3621 vertical environment temperature (ET) profiles (4 times a day) through the air-snow-sea ice-ocean column.  
 3622 The heating temperature (HT) measured by the thermistor string once per day is based on the use of a small  
 3623 identical heater on each sensor. The ET and HT data are used to derive snow depth and ice thickness.  
 3624 SIMBA uses GPS module to track the buoy location. The Iridium satellite is used for data transmission. A  
 3625 total 15 SIMBA buoys have been deployed in the Arctic Ocean during the Chinese National Arctic Research  
 3626 Expedition (CHINARE) 2018 and the Nansen and Amundsen Basins Observational System (NABOS) 2018  
 3627 field expeditions in late autumn. In 2019 17 SIMBA buoys were deployed during the CAATEX (2) and  
 3628 MOSAIC expeditions (15, leg 1).

3629

3630 **Figure 6.** SIMBA observations on the temporal evolution of the snow depth, ice thickness, and the  
 3631 temperature profile from the ocean through snow and sea ice to air. The results were obtained applying the  
 3632 algorithm by Liao et al. (2018). The black lines are snow surface (top), Initial freeboard (middle) and ice  
 3633 base (bottom). 0 level refers to snow/ice interface. The colors indicate the temperature in °C.

3634 **Figure 7. A:** Biological pumps resulting in (i) atmospheric CO<sub>2</sub> sink and(ii) calcium carbonate transport  
 3635 from surface to deep ocean; **B:** anticipated forward and feedback alterations in ocean ecology driven by  
 3636 atmospheric CO<sub>2</sub> increase. PIC=particulate inorganic carbon; POC=particulate organic carbon (modified  
 3637 after Rost & Riebesell, 2004).

3638 **Figure 8.** Field data for ice decay in Lake Kilpisjärvi in 2013 showing decrease of ice thickness by surface  
 3639 melting and bottom melting and increase of porosity until breakage of ice cover.

3640  
 3641 **Figure 9.** Changes in 2-meter temperature (°C, upper panels) and precipitation (% , lower panels) during the  
 3642 21st century. Present-day climatology is averaged over years 1981-2010 and end-of-century climatology  
 3643 over 2070-2099. Winter (left) and summer (right) are shown separately. Dotted areas indicate high  
 3644 variability in model ensemble (for temperature: standard deviation of 21st century change exceeds 1°C; for  
 3645 precipitation: standard deviation of 21st century change exceeds 100% or present-day precipitation). The  
 3646 model results are from IPCC AR5, based on 42 individual models in CMIP5 experiments under the RCP4.5  
 3647 scenario.

3648

3649 **Table 1.** Systems, key topical areas, research question introduced in the PEEEX Science Plan (SP) (Kulmala  
 3650 et al. 2015; 2016a, Lappalainen et al. 2018) connected to the addressed research themes over last 5 years by  
 3651 the PEEEX questionnaire (APPENDIX 1). The addressed research themes and the results are overviewed in  
 3652 section 3.

3653

3654

PEEX – SP System	PEEX - SP key topical area	PEEX - SP research question (Q-No)	Addressed research themes during the last 5 years
Land	Changing land ecosystem processes	<b>How could the land regions and processes that are especially sensitive to climate change be identified, and what are the best methods to analyze their responses? (Q-1)</b>	<ul style="list-style-type: none"> <li>• high-latitude photosynthetic productivity and vegetation changes (greening, browning)</li> <li>• new methodologies determining Earth surface characteristics</li> </ul>
Land	Risk areas of permafrost thawing	<b>How fast will permafrost thaw proceed, and how will it affect ecosystem processes and ecosystem-atmosphere feedbacks, including hydrology and greenhouse gas fluxes ? (Q-2)</b>	<ul style="list-style-type: none"> <li>• soil temperature evolution</li> <li>• changing GHG fluxes, carbon sink-source dynamics due to permafrost thawing</li> </ul>

Land	Ecosystem structural changes	<b>What are the structural ecosystem changes and tipping points in the future evolution of the Pan-Eurasian ecosystem? (Q-3)</b>	<ul style="list-style-type: none"> <li>• changes in soil microbial activity e.g. effect of forest fires</li> <li>• changes of the Northern soils and functioning of the Arctic tundra in global carbon cycling context</li> </ul>
Atmosphere	Atmospheric composition and chemistry	<b>What are the critical atmospheric physical and chemical processes with large-scale climate implications in a northern context? (Q4)</b>	<ul style="list-style-type: none"> <li>• carbon (C) balance in the boreal forests; methane (CH<sub>4</sub>) balance at the Arctic; carbon monoxide (CO), ozone (O<sub>3</sub>) at the Northern Eurasian region</li> <li>• Sources and properties of atmospheric aerosols in boreal and Arctic environments</li> <li>• black carbon and dust in the atmosphere and on snow at the Northern high latitudes</li> <li>• methodological and model developments related to atmospheric chemistry and physics</li> </ul>
Atmosphere	Urban air quality and megacities, ABL	<b>What are the key feedbacks between air quality and climate at northern high latitudes and in China? (Q5)</b>	<ul style="list-style-type: none"> <li>• recent observations on air quality in China</li> <li>• Anthropogenic emissions and environmental pollution in Russia</li> </ul>
Atmosphere	Weather and atmospheric circulation	<b>How will atmospheric dynamics (synoptic scale weather, boundary layer) change in the Arctic-boreal regions? (Q6)</b>	<ul style="list-style-type: none"> <li>• cold &amp; warm episodes</li> <li>• cyclone density dynamics</li> <li>• circulation effect on temperature and moisture</li> <li>• cloudiness in Arctic</li> <li>• atmospheric boundary layer (ABL) dynamics</li> </ul>
Water	The Arctic Ocean in the climate system	<b>How will the extent and thickness of the Arctic sea ice and terrestrial snow cover change? (Q-7)</b>	<ul style="list-style-type: none"> <li>• Sea ice dynamics and thermodynamics with atmospheric and ocean dynamics</li> <li>• Snow depth/mass and sea ice thickness</li> <li>• Sea ice research supporting navigation</li> <li>• Ocean floor, sediments: composition and fluxes</li> <li>• River runoff effecting the hydrological processes at coastal marine environments in Russia</li> </ul>
Water	Arctic marine ecosystem	<b>What is the joint effect of Arctic warming, ocean freshening, pollution load and acidification on the Arctic marine ecosystem, primary production and carbon cycle? (Q-8)</b>	<ul style="list-style-type: none"> <li>• Living marine organisms weaken or even subdue CO<sub>2</sub> accumulation</li> </ul>

Water	Lakes and large-scale river systems	<b>What is the future role of Arctic-boreal lakes, wetlands and large river systems, including thermokarst lakes and running waters of all size, in biogeochemical cycles, and how will these changes affect societies) ? (Q-9)</b>	<ul style="list-style-type: none"> <li>organic carbon, carbon balance, ice cover at lakes in the Northern high latitudes</li> <li>specific characteristics of the Lake Baikal and Selenga River delta in Russia</li> <li>specific characteristics of Asian water lakes</li> </ul>
Society	Anthropogenic impact	<b>How will human actions such as land-use changes, energy production, the use of natural resources, changes in energy efficiency and the use of renewable energy sources influence further environmental changes in the region? (Q-10)</b>	<ul style="list-style-type: none"> <li>Mitigation e.g method for the natural risk assessment in Russia and new clean energy technologies</li> </ul>
Society	Environmental impact	<b>How do the changes in the physical, chemical and biological state of the different ecosystems, and the inland, water and coastal areas affect the economies and societies in the region, and vice versa? (Q-11)</b>	<ul style="list-style-type: none"> <li>Reindeer grazing effects on the ground vegetation structure and biomass</li> </ul>
Society	Natural hazards	<b>In which ways are populated areas vulnerable to climate change? How can their vulnerability be reduced and their adaptive capacities improved? What responses can be identified to mitigate and adapt to climate change? (Q-12)</b>	<ul style="list-style-type: none"> <li>Emerging zoonotic diseases</li> <li>UV variation effects on health</li> <li>Air pollution in different scales and environments (street-level urban air pollution, transported air pollution in urban environments, air pollution at the Arctic) and related health effects;</li> </ul>
Feedbacks	Key topics: Atmospheric composition, biogeochemical cycles: water, C, N, P, S	<b>How will the changing cryospheric conditions and the consequent changes in ecosystems feed back to the Arctic climate system and weather, including the risk of natural hazards? (Q-13)</b>	<ul style="list-style-type: none"> <li><i>Research needs:</i> quantification of the COntinental Biosphere-Aerosol-Cloud-Climate (COBACC) feedback loop at different Northern boreal environments</li> <li>Gold &amp; high region quantification of BVOC – aerosols feedback loop at the Tibetan /Himalayan Plateau:..</li> </ul>
Feedbacks	Key topics: Atmospheric composition, biogeochemical cycles: water, C, N, P, S	<b>What are the net effects of various feedback mechanisms on (i) land cover changes, (ii) photosynthetic activity, (iii) GHG exchange and BVOC emissions (iv) aerosol and cloud formation and radiative forcing ? How do these vary with climate change on regional and global scales? (Q-14)</b>	<ul style="list-style-type: none"> <li><i>Research needs:</i> The Arctic greening and browning calls for a multi-disciplinary scientific approach together, improved modelling tools and new data in order to solve scientific questions related to the net effects of various feedback mechanisms connecting the biosphere-atmosphere - human activities</li> </ul>

Feedbacks	Key topics: Atmospheric composition, biogeochemical cycles: water, C, N, P, S	<b>How are intensive urbanization processes changing the local and regional climate and environment? (Q-15)</b>	<ul style="list-style-type: none"> <li>• <i>Research needs:</i> accelerating urbanization calls for studies on the effects of on air pollution, local climate and the effects these changes have on global climate. Integrated studies should lead to services for society, cities helping to mitigate hazards storms, flooding, heat waves, and air pollution episodes (see also 3.2.1)</li> </ul>
-----------	--	---	---

3655

3656 **Table 2.** Hydrogeochemical signature of large river system –Selenga River case study. The figure represent  
3657 metal(loid)s partitioning (Median values) in the Selenga river basin in the upper (Mongolian) and  
3658 downstream (Russian) part between 20 July -10 August 2011 under dominant high water (A) and 07 June -10  
3659 July 2012 under dominant low water conditions. Dark orange fill corresponds to the share of suspended  
3660 forms of elements > 75% (green), light orange – 75-50%, light blue – 50-25%, dark blue – < 25%. The  
3661 figure indicate that in the large river system some metals are mostly found in the dissolved form (84–96% of  
3662 Mo, U, B, and Sb on an average), whereas many others predominantly existed in suspension (66–87% of Al,  
3663 Fe, Mn, Pb, Co, and Bi). A consistently increasing share of metals in suspended particulate modes (about 2–  
3664 6 times) is observed under high discharge conditions For details and other hydrological seasons refer to  
3665 (Kasimov et al., 2020b).

		A																				
		Fe	Al	Mn	Pb	Bi	Co	Be	V	Ni	Cr	Cd	Cu	Zn	As	B	U	Mo	Sb	Ca	Sr	Sn
Russian part of the catchment		65	69	56	46	77	59	71	65	48	29	49	41	25	22	11	5	2	1	2	3	34
Mongolian part of the catchment		98	96	100	95	87	89	71	57	56	55	71	70	86	10	19	4	2	0	11	9	58

		B																				
		Fe	Al	Mn	Pb	Bi	Co	Be	V	Ni	Cr	Cd	Cu	Zn	As	B	U	Mo	Sb	Ca	Sr	Sn
Russian part of the catchment		60	70	52	45	75	57	41	56	40	47	19	42	26	39	18	6	4	41	2	3	15
Mongolian part of the catchment		78	83	59	72	76	59	49	43	35	49	13	62	23	12	10	1	1	42	2	2	11

3666

3667 **Code/Data availability:** This is an review paper and the data availability is introduced in the original articles.

3668 **Author contribution:** Co-authors have provided text and/or relevant references. Some of them have been  
3669 editors of the specific chapters of the manuscript.

3670 **Competing interests:** no spesific competing interests